5-2011

Molecular organic geochemistry of the oil and source rocks in Railroad Valley, eastern Great Basin, Nevada, United States

LaOde Ahdyar
University of Nevada, Las Vegas

MOLECULAR ORGANIC GEOCHEMISTRY OF THE OIL AND SOURCE ROCKS IN RAILROAD VALLEY, EASTERN GREAT BASIN, NEVADA, UNITED STATES

by

LaOde Ahdyar

Bachelor of Science
Padjadjaran University, Indonesia
2008

A thesis submitted in partial fulfillment
of the requirement for the

Master of Science in Geoscience
Department of Geoscience
College of Science

Graduate College
University of Nevada, Las Vegas
May 2011

UNLV
UNIVERSITY OF NEVADA LAS VEGAS

THE GRADUATE COLLEGE

We recommend the thesis prepared under our supervision by

LaOde Ahdyar

entitled

Molecular Organic Geochemistry of the Oil and Source Rocks in Railroad Valley, Eastern Great Basin, Nevada, United States

be accepted in partial fulfillment of the requirements for the degree of

Master of Science in Geoscience

Andrew D. Hanson, Committee Chair

Rodney V. Metcalf, Committee Member

Stephen M. Rowland, Committee Member

Daniel B. Thompson, Graduate Faculty Representative

Ronald Smith, Ph. D., Vice President for Research and Graduate Studies
and Dean of the Graduate College

May 2011

ABSTRACT

Molecular Organic Geochemistry of the Oil and Source Rock in Railroad Valley Eastern Great Basin, Nevada, United States

by

LaOde Ahdyar

Dr. Andrew Hanson, Examination Committee Chair
Associate Professor of Geology
University of Nevada, Las Vegas

A comprehensive geochemical study of oils from Railroad Valley, Nevada and two candidate source rock intervals from the nearby Egan Range, was conducted in order to establish oil-oil and oil-source rock correlations. Analyses consisted of total organic carbon, Rock-Eval pyrolysis, and vitrinite reflectance for source rock samples, as well as biomarker, diamondoids, and stable carbon isotope analyses on source rock extracts and oil samples.

Total organic carbon analyses showed high organic content in the Mississippian Chainman Shale. However, outcrop samples of the Paleogene Sheep Pass Formation Member B are organically lean. Strata in both of these units are immature to mature, and tend to be oil-gas prone.

Biomarker analysis of oil samples revealed that two different oil groups exist. Group 1 oils (Trap Spring and Grant Canyon oils) appear to originate from marine shale source rocks that were deposited under normal marine salinity and dysoxic conditions, as shown by high Pr/Ph ratios, low homohopane index, and high diasterane/steranes ratios. In addition, age related biomarker parameters showed this oil group to be derived from a source rock that is older than Cretaceous. Group 1 oil correlates with Chainman Shale

source rock extracts. Group 2 oils (Eagle Spring, Kate Spring, and Ghost Ranch oils) are lacustrine-derived and have low Pr/Ph, high gammacerane, good preservation of homohopane, and low diasterane/sterane ratios. High gammacerane and high C_{24} tetracyclic suggest that the oil in this group was derived from a source rock deposited under hypersaline conditions. The abundance of oleonane and dinosterane provides good evidence that oils belonging to this group are derived from source rocks younger than the Cretaceous, which points to the Sheep Pass Formation Member B. My comprehensive geochemical study of oil also suggests that the oils from Kate Spring and Ghost Ranch are different from oils from Eagle Spring but they are still closely related. I hypothesize that a difference in source rock facies and source rock depositional conditions in the lacustrine system serves as a key control that resulted in those differences.

Stable carbon isotope data clearly showed two different groups, which supports my biomarker data. Group 1 oils have low $\delta^{13}C_{SAT}$ and high $\delta^{13}C_{AROM}$, which is indicative of a marine source rock. On the other hand, Group 2 oils appear to have high $\delta^{13}C_{SAT}$ and high $\delta^{13}C_{AROM}$, which suggests a lacustrine-derived oil. Additionally, diamondoid analyses showed most of my oil and source rock extracts have low abundances of diamondoids, which suggest that intense oil cracking has not yet occurred.

The results of this research shows that two different intervals (the Chainman Shale and the Sheep Pass Formation Member B) serve as effective source rocks in this basin. Specifically, oil fields in the western and southern part of the basin (Trap Spring and Grant Canyon) were charged by the Chainman Shale source rock, whereas the Sheep Pass Formation member B was the main contributor of the reservoired oils in the eastern part of the basin (Eagle Spring, Kate Spring, and Ghost Ranch). This new understanding

of effective source rock(s) in this basin will significantly improve the hydrocarbon play concept as well as open the new perspective of hydrocarbon exploration within the Basin and Range area.

ACKNOWLEDGMENTS

I would like to thank all the people who have helped and inspired me during my master study. First and foremost I would like to express my ultimate gratitude to my advisor Dr. Andrew D. Hanson, under his guidance, critical review, motivation, sincerity and encouragement I can finish my thesis and gain my knowledge in geology. My special thanks go to my committee members, Dr. Stephen M. Rowland, Dr. Rodney V. Metcalf and Dr. Daniel B. Thompson for their constructive comments.

I would like to thank to all the faculty members, department staff, and graduate students at Department of Geoscience UNLV who always support me, open my mind and making my study and stay in UNLV a great experience. I would also like to thank Nick and Yuki for assisting me during the fieldwork. I was delighted to interact with Stanford Organic Geochemistry laboratory staff, especially J. Michael Moldowan and David Zinniker. Thank you for providing excellent support and helpful discussions during my organic geochemistry analysis. The generous support from ExxonMobil Oil Indonesia is greatly appreciated. Thank you for giving me the scholarship and opportunity to take an outstanding education journey in the United States.

I am grateful to have Indonesian friends in Las Vegas: Adam, Leon, Mas Pongky, Mas Nur, Redha, George, Ynnez, Sari, Yuki, Wiwid, and Mba Myta. Thank you for the unforgettable moment and continuous support. My sincerest thanks also go to my parents, Yuni Fitria and family in Indonesia for their prayer, support, and patience. Finally, I would like to dedicate this thesis to all my friends, colleagues, and family who have supported me. Thank you.

TABLE OF CONTENT

LIST OF FIGURES

LIST OF TABLES

CHAPTER 1

INTRODUCTION

Railroad Valley (RRV), the most prolific oil-producing basin in Nevada, is situated in the center of the Basin and Range province, in Nye County, east-central Nevada (Figure 1 and 2). Petroleum exploration in RRV began in 1950, and first met success with the discovery of the Eagle Spring field by Shell Oil Company (Bortz and Murray, 1979). Since 1954, numerous wells (Figure 3) have been drilled with varying degrees of success, and total production to date is approximately 44 million barrels of oil (MMBO). The oil in RRV is primarily trapped in Paleogene volcanic units, i.e., the Pritchards Station and Garret Ranch Fm (Duey, 1979; French and Freeman, 1979; Dolly, 1979), Paleogene lacustrine limestone of the Sheep Pass Fm (Bortz and Murray, 1979), and Paleozoic carbonate reservoirs, such as the Devonian Simonson and Guilmette Formations (Bortz and Murray, 1979; Garside et al., 1988). Traps are a combination of structural and stratigraphic traps (Foster, 1979; Dolly, 1979). The reservoir top seals include Neogene basin fill overlying an unconformity (Bortz and Murray, 1979; Dolly, 1978; Walker et al., 1992) and alteration zones within the Paleogene volcanic units. Although some aspects of the petroleum system are fairly well constrained, other components and processes, such as potential source rock, are loosely constrained.

Several researchers (Bortz and Murray, 1979; Duey, 1979; French, 1983; Poole and Claypool, 1984; Conlan, 1995) have suggested that there may be more than one source rock that generated oil in this region. They have speculated on the origin of oils in RRV but no consensus occurs amongst them, and no detailed and comprehensive molecular organic geochemistry studies have been published on oils in RRV or on the

most likely source rock intervals, the Mississippian Chainman Shale and the Paleogene Sheep Pass Formation. Consequently, the source of oil in this basin remains controversial.

To address the problem regarding the origin of the oil, I performed comprehensive geochemical analyses including total organic carbon, Rock-Eval pyrolysis, vitrinite reflectance, thermal alteration index analyses, and detailed modern molecular organic geochemistry as well as stable carbon isotope and diamondoids analyses on nineteen oil samples from Railroad Valley and on source rock samples from two stratigraphic units (the Mississippian Chainman Shale and Paleogene Sheep Pass Formation Member B). As a result, I successfully developed oil-oil and oil-source rock correlation, which allowed me to determine how many oil families exist in the basin and correlate each of them with the presumptive source rocks (the Chainman Shale and Sheep Pass Formation Member B). This oil source rock correlation study using organic geochemistry analysis is routinely conducted in order to constrain how many oil families are present in a particular basin as well as to constrain which source rock generated the different oil families.

CHAPTER 2

GEOLOGICAL FRAMEWORK

Regional Geology

RRV is located in the Basin and Range province, within the southwestern part of the eastern Great Basin physiographic province. This region is geologically complex, having experienced major episodes of tectonism and volcanic activity. The tectonic events that impacted the study area include the Antler Orogeny, Sonoma Orogeny, Sevier thrust faulting, synconvergent mid-crustal and upper-crustal extension within the Sevier hinterland, and Basin and Range extension. All of these events produced a great diversity of sedimentary facies (Figure 4) and major structural features.

After the supercontinent Rodinia broke up in the late Neoproterozoic, a passive continental margin developed on top of the rift sequences deposited during the late Proterozoic - Cambrian in the western United States, which produced a thick and widespread carbonate succession (Levy and Christie-Blick, 1991; Dickinson, 2006). The region accumulated passive margin sediments until the late Devonian when the Antler orogeny caused east-vergent thrusting, which created a progressive eastward-migrating foredeep adjacent to the main frontal thrust with a forebulge and back-bulge to the east (Poole and Claypool, 1984). The Sonoma orogeny happened in the Permian and Triassic and transported the Golconda allochthon eastward and thrust rocks onto the Antler highland, west of the Antler orogenic belt (Silberling, 1991). The central Nevada thrust belt (CNTB) formed in the earlier part of the development of Cordilleran foreland fold-thrust belt and is located in the Sevier hinterland. The CNTB is characterized by narrow ~400 km north-south-trending compressional structures whose maximum total shortening

is 10 – 15 kilometers (Taylor et al., 2000). The Sevier thrust system formed during the late Jurassic - Eocene and consisted of northeast-trending, east-vergent large-scale thrust faults (DeCelles, 2004). Widespread synconvergent mid-crustal extension occurred within the Sevier hinterland during the Late Cretaceous. In addition, contemporaneous upper-crustal synconvergent extension occurred in the Sevier Hinterland between ca 81.3 ± 3.7 Ma and 66.1 ± 5.4 Ma (Druschke et al., 2009), which created a series of normal fault systems and initiated the deposition of the Sheep Pass Fm. During the Cenozoic, large-magnitude extensional tectonism occurred in the Basin and Range province, which extended the crust by a factor of 2-4 and resulted in approximately 247 km net extension (Wernicke et al., 1988). The aforementioned paleotectonic events have greatly influenced petroleum generation, migration, accumulation, and preservation.

A wide range of depositional environments (non-marine to marine) in the eastern Great Basin resulted in deposition of various types of sediments. Several units are purported source rocks and several are reservoirs where hydrocarbons have accumulated, as shown in Figure 4. Specifically, suggested potential source rocks include the western assemblage (rocks of the Roberts Mountain Allochthon, such as the Woodruff Fm and Slaven Chert), Pilot Shale, Joana Limestone, Chainman Shale, Ely Limestone, Newark Canyon Fm, Sheep Pass Fm Member B, and Elko Fm (Poole and Claypool, 1984; Sandberg and Poole, 1975; Gilmore, 1990; Mullarkey et al., 1991; Palmer, 1984; Anna et al., 2007).

The western assemblage, which is a part of the Roberts Mountain allochthon, is a group of Cambrian to Devonian base-of-slope to deep basin strata that consist of chert, shale, siltstone, limestone, and sandstone. These are the Preble, Vinini, Comus, Valmy,

Woodruff, and Slaven formations (Poole and Claypool, 1984). The quantity of organic carbon in these source rocks is excellent (based on the classification of Peters and Cassa, 1994) with mean TOC 4.35 ± 5.13 wt %. Their kerogen type can be classified as a type III kerogen (gas prone) (Anna et al., 2007). In terms of maturity, these source rocks range from immature to overmature. Despite encouraging data, no oils are known to have been generated from these source rocks (Anna et al., 2007).

The Pilot Shale unconformably overlies the thick sequence of the Cambrian-Devonian western assemblage. The Pilot Shale was deposited in the Antler foreland basin during the latest Devonian – Kinderhookian time and is dominated by shale, mudstone, siltstone, and thin-bedded limestone (Sandberg and Poole, 1975). This formation is considered a poor to good source rock with TOC values of 0.2 – 1.7 wt % (Sandberg and Poole, 1975). The quality is poorly constrained, and the maturity is overmature with mean vitrinite reflectance (Ro) values of 1.37 % (Anna et al., 2007).

The Joanna Limestone is dominated by carbonate with minor siliciclastic material and was deposited on top of the Pilot Shale during the early Mississippian (Gutschick et al., 1980). This unit is a good source rock with a mean TOC value of 1.21 wt % (standard deviation 1.30 wt %) but it is thermally overmature with an Ro value of 2.8 % and a thermal alteration index (TAI) value of 3.35 (Gilmore, 1990).

The Lower Cretaceous Newark Canyon Formation, which was deposited unconformably on top of Permian rocks and is a freshwater lacustrine deposit consisting of limestone, shale, siltstone, sandstone and conglomerate (Nolan et al., 1956). Based on reported values of TOC ranging from 2.5 to 8 wt % (Anna et al., 2007) this interval has the potential to be a very good to excellent source rock. This interval has type II/III

kerogen (mixed oil and gas prone) and is thermally mature with a Tmax value of 440^{o} C (Mullarkey et al., 1991). However, this interval is thin in the subsurface due to attenuation faulting and subsequent erosion during the Neogene (Nolan et al., 1956).

The Elko Formation consists of Late Eocene to early Oligocene lacustrine strata and is dominated by black shale, thin-bedded limestone, chert, tuffaceous material, and conglomerate (Smith and Ketner, 1976). This interval has TOC values ranging from 1.58 – 3.4 wt % and kerogen type I and II, but it is still immature (Palmer, 1984).

Previous research (Claypool et al., 1979; French, 1983; Poole and Claypool, 1984; Conlan, 1995) has shown that two other source rock intervals, the Mississippian Chainman Shale and Paleogene Sheep Pass Fm Member B, appear to be very good - excellent source rocks in this region and were thus the main focus of this study.

The Mississippian Chainman Shale was deposited during the Antler orogeny and is widely considered to be a very good to excellent source rock in the eastern Great Basin because of its thickness, widespread distribution, its organic-rich content, and maturity (Poole and Claypool, 1984; French, 1995). The Chainman Shale was deposited after the Pilot Shale and Joanna Limestone in the Antler foreland basin and before the Pennsylvanian Ely Limestone. The approximately 1,000 m thick Chainman Shale consists of black to dark-gray organic-rich shale, deep flysch deposits, and mudstone-siltstone farther to the west (Poole and Claypool, 1984). Initially, the Chainman Shale was deposited in a deep marine setting, but as the foredeep gradually filled, the depositional environment changed to a shallow marine environment as indicated by cross-bedded sandstone in the upper part of the Chainman. This facies change influenced the quality and type of organic matter. French (1995) revealed that the lower member of

the Chainman Shale has more generative potential than the upper member, based on geochemical logs at the Illipah-1 well. The Chainman Shale contains a mixture of sapropelic and terrestrial kerogen, and TOC ranges from 0.1 to 10 wt % (Poole and Claypool, 1984), is thermally mature and can be categorized as a type II (oil-prone) source rock (Poole and Claypool, 1984).

The Sheep Pass Fm is also known as a fair to excellent source rock, which is generally assumed to serve as a main source rock in RRV (French, 1983; Poole and Claypool, 1984). The Sheep Pass Fm was deposited from the Late Cretaceous to Eocene (81.3 ± 3.7 Ma and 66.1 ± 5.4 Ma) in extensional basins within the Sevier hinterland (Druschke et al., 2009). The Sheep Pass Fm contains facies deposited in various depositional environments (alluvial fan, lacustrine, fluvial) (Winfrey, 1960), consequently the lithologies vary (sandstone, limestone, shale, conglomerate) and the facies change both laterally and vertically (Newman, 1979; Druschke et al., 2009). The Sheep Pass Fm consists of six members and has a maximum thickness in excess of 1000 m and a minimum thickness of 121 m (Winfrey, 1960). A basal conglomerate was deposited initially and is named Sheep Pass Member A. Stratigraphically above Member A is Member B, which contains freshwater lacustrine mud-supported carbonate. Member C is dominated by thin alluvial conglomerates, fluvial sandstone and claystone, and lacustrine carbonate. Member D is mainly a product of a saline lacustrine depositional environment; this member consists of a thin sequence of dolomitic, chert, and mud-supported carbonate. Members E and F are dominated by mud-supported carbonate and calcareous claystone. Among the different members within the Sheep Pass Fm, only Member B contains freshwater lacustrine deposits of mud-supported carbonate (Winfrey,

1960) and is known as a fair to excellent source rock. Total organic carbon of Sheep Pass Fm Member B ranges from 0.6 to 7.4 wt % (Poole and Claypool, 1984). Thermal maturity data are inconsistent; in some places it is in the early mature stage, but in other places it is overmature (Poole et al., 1983). The Sheep Pass Fm is widely accepted as having type III kerogen, although Claypool and others (1979) suggested it contains a mixture of oil-prone algal and sapropelic type II kerogen.

Previous Work

Oil-source rock correlation studies in RRV have been conducted by several researchers (Picard, 1960; Bortz and Murray, 1979; Claypool et al., 1979; Duey, 1979; French, 1983; Poole and Claypool, 1984; and Conlan, 1995). Previous geochemical analyses of oils from the five oil fields in RRV, including the Eagle Spring, Trap Spring, Bacon Flat, Grant Canyon, and Currant fields suggested that oils were generated from the Chainman Shale, the Sheep Pass Formation Member B, or a mixture of those two source rocks (Picard, 1960; Bortz and Murray, 1979; Claypool et al., 1979; Duey, 1979; French, 1983; Poole and Claypool, 1984; and Conlan, 1995). Surprisingly, researchers have reached different conclusions regarding oil-source rock correlations in RRV. Most notably, Picard (1960) suggested that oil in the Eagle Spring field was derived from the Sheep Pass Fm Member B while others suggest it was generated by a mixture of Paleogene Sheep Pass Fm Member B and the Mississippian Chainman Shale (Bortz and Murray, 1979; Duey, 1979; French, 1983).

CHAPTER 3

METHODS

Fieldwork

Fieldwork consisted of collecting rock samples and oil samples. A total of 15 rock samples were collected from several outcrops in the Egan Range, east of Railroad Valley (see Figure 2). These consist of samples from the Sheep Pass Member B (n = 11) and the Chainman Shale (n = 4) (Figure 6 and 7). I sampled from different stratigraphic intervals because I knew that the quality of rocks might be different from one location to another. For example, I collected samples both from the lower and upper members of the Chainman shale, because they had different characteristics (French, 1995). Additionally, the effect of weathering of the source rock samples collected from outcrop was a concern. Therefore, to reduce the weathering effect I dug into the selected outcrop and collected the rock samples from the freshest layer possible.

Whole crude oil samples from Railroad Valley were collected from the Trap Spring, Eagle Spring, Kate Spring, Ghost Ranch, and Grant Canyon oil fields (see Figure 3). Sample vials with a Teflon cap were used to store the oil samples collected from wellhead and battery tank. In addition, David Zinniker of Stanford University donated oil samples from Eagle Spring-1, Grant Canyon-6, and Tomaro Ranch (oilfield outside RRV). All the oil samples are listed in Table 1.

Laboratory Work

Source rock screening

Source rock screening was performed on all rock samples in order to assess their organic richness, quality, and maturity. Total organic carbon (TOC) measurements and Rock-Eval pyrolysis of all samples were performed at Weatherford Laboratories, while four selected samples from those two formations were sent to Egsploration Company for vitrinite reflectance analysis and thermal alteration analysis. Based on the results of the initial screening, the best source rocks were selected for further geochemical analyses, including molecular organic geochemistry analysis (biomarker analysis) and stable carbon isotope analysis.

Molecular organic geochemistry

A total of 16 oil samples and two source rocks extracts from the Chainman Shale were analyzed in this study. Geochemical analyses consisted of normal alkane analysis using gas chromatogaphy (GC), diamondoid analysis on gas chromatography–mass selective detector (GC-MSD), and biomarker analysis using gas chromatography–mass selective detector (GC-MSD) and metastable reaction monitoring GC–mass spectrometry (MRM-GCMS). In addition, stable carbon isotope analysis was conducted in order to support geochemical results. All of these analyses were done at the Molecular Organic Geochemistry Laboratory at Stanford University except for the stable isotopic analyses, which were performed in the Stable Isotope Biogeochemistry Laboratory at Stanford University.

Prior to the molecular geochemical analysis, the best source rocks were crushed using mortar and pestle, and a mechanized crushing tool. Approximately ninety grams of

rock powder from each sample was used. Soluble bitumen within those samples was extracted using a mixture of methanol (50%) and dichloromethane (50%). Whole oil samples and source rock extracts were diluted with solvent (pentane) to 1.5 ml and were analyzed using a Hewlett-Packard 5890 series Gas Chromatograph (GC) equipped with Flame Ion Detector (FID). Approximately 1 µl of each sample was auto-injected to the 60 m DB-1 long column GC with an internal diameter of 0.25 mm, 25 micron phase thickness, and hydrogen carrier gas. The initial temperature was 35^0 C for 0.5 minutes; the temperature then rose to 320^0C at 3^0 C/min and was held at 320^0C for 20 minutes. One sample (sample LA-04) contained high molecular weight *n*-alkanes, so it was run an extended period with a final temperature of 330^0C, which was held for 40 minutes while other parameters were the same.

Another portion of each whole oil sample was separated into saturate and aromatic fractions prior to biomarker analysis. The saturate/aromatic separation was done using glass columns filled with silica gel. Hexane flush was used to collect the saturate fraction and subsequently the remaining materials on the column were flushed with dichloromethane to obtain the aromatic fractions. Afterwards, the *n*-alkanes within the saturate fractions were removed using molecular sieves (high Si/Al ZSM-5 zeolite/"silicalite", pore size of 6 Å) with isooctane as a solvent. Silicalited saturate fractions and aromatic fractions were analyzed for biomarkers using a selected ion monitoring gas chromatography–mass selective detector (SIM GC-MSD). For silicalited saturate fractions, *m/z* 191, 217, 238, 218, 259, 177, 123, 205, and 231 were monitored, and *m/z* 253, 231, 245, 192, and 191 were monitored for the aromatic fractions. I utilized Hewlett-Packard 5973 series GC-MSD with a 60 m DB-1 long column, 0.25 mm i.d., 25-

micron phase thickness, and helium carrier gas. The GC-MSD program started at 140^0 C for 1 minute, then increased 2^0C/min to 320^0C and stayed at 320^0C for 20 minutes. In addition, silicalited saturate and aromatic fractions were further analyzed using metastable reaction monitoring (MRM-GCMS) Hewlett-Packard 5890 Series II Autospec.

Finally, one portion of each oil sample and source rock extract was allocated for diamondoid analysis. Diamondoids is a small, thermally stable, cage-like hydrocarbon, form as a result of carbonium ion arrangements of suitable organic precursors on a clay mineral (Peters et al., 2007). The purpose of the diamondoids analysis is to determine the degree of oil cracking in the oil because the high abundances of diamondoids within the oil samples represent the intense degree of oil cracking. In order to accurately measure the diamondoid concentrations, 20 µl of deuterated diamondoids internal standard (5β-cholane) with known quantity was added to 20 mg of each oil sample and source rock extract. The saturate aromatic separation was performed using the same procedure outlined above. The saturate fractions were analyzed using a Hewlett-Packard 5890 series II plus gas chromatography–mass selective detector (GC-MSD) with a 60 m long DB1 column, 0.25 mm internal diameters; the carrier gas was helium. The oven temperature started at 50^0 C for 1 minute, increased 15^0C/minute up to 80^0C, then programmed 3^0 C/minute to 320^0C, which was held for 15 minutes.

Statistical analysis

Statistical analysis was performed to help show the genetic relationship among oil samples in Railroad Valley and source rock extracts. The hierarchical cluster analysis using Ward's minimum variance method (JMP, 1995) was the primary statistical analysis

that I used. Basically, I entered the values of specific biomarker parameters to statistical software (JMP® v.8) and allowed the program to determine the similarity among samples based on those values. The end product of this statistical analysis is a dendrogram showing genetic relationships among the 19 oil samples and 2 source rock extracts.

CHAPTER 4

RESULTS AND DISCUSSIONS

Source Rock Screening

Results of total organic content (TOC) analysis, Rock-Eval pyrolysis, vitrinite reflectance (Ro), and thermal alteration index (TAI) are provided in Table 2. I classified the source rocks using the criteria of Peters and Cassa (1994). The results indicate that the Sheep Pass Formation Member B is a poor source rock and the highest TOC was 0.24 wt % (10SP09). On the other hand, the Chainman Shale has high TOC values ranging from 0.79 wt % to 4.31 wt %, which classifies it as a fair to excellent source rock.

Hydrogen Index (HI) and Oxygen Index (OI) values of the Sheep Pass Formation Member B plot between type II and III kerogen pathways. In contrast, Chainman Shale samples plot near the origin on the pseudo van Krevelen diagram (Figure 8).

In terms of maturity, the Sheep Pass Formation Member B has a vitrinite reflectance value of 0.46 %, a thermal alteration index value 2 to 2+, and Tmax values varying from 436 ^{0}C to 487 ^{0}C. The Chainman Shale has Ro values of 0.68 % to 1.01 %, TAI values of 2+ to 4, and Tmax ranging from 442 ^{0}C to 455 ^{0}C.

Based on the results of the initial source rock screening, two samples (10CH03 and 10CH04) of organic-rich and thermally mature Mississippian Chainman Shale were subjected to further molecular organic geochemistry analysis. However, due to insufficient TOC, none of Sheep Pass Formation Member B samples were included in further detailed geochemistry analyses.

Source Rock Geochemistry Results

Gas chromatography (GC) data were collected for two rock extracts of the Chainman Shale (10CH03 and 10CH04). GC traces are provided in Appendix 1. Gas chromatography-mass spectrometry results of these extracted whole-rock samples (10CH03 and 10CH04) reveal the presence of several important biomarker compounds including terpane and hopanes (*m/z* 191), steranes (*m/z* 217), and aromatic hydrocarbons (*m/z* 231, *m/z* 253, *m/z* 245) as shown in Appendix 2. Appendix 3 shows representative GCMS-MRM traces (*m/z* 358 → 217, *m/z* 372 → 217, 386 → 217, 400 → 217, 414 → 217, and 412 → 191). Additionally, the stable carbon isotope values of saturate and aromatic compounds in source rock extracts are listed in Table 3.

Oil Geochemistry Result

Geochemistry analyses of all oil samples in this study (n=19) included GC, GC-MSD, MRM-GCMS, diamondoids analysis using GC-MSD, and stable carbon isotopes analysis. Representative GC traces for oil samples from each field are shown in Appendix 4. My GC-MSD analysis of oil samples generated *m/z* 191, *m/z* 217, *m/z* 231, *m/z* 253, and *m/z* 245 chromatograms. Selected traces from each field are presented in Appendix 5. The MRM-GCMS analyses produced the following traces: *m/z* 358 → 217, *m/z* 372 → 217, 386 → 217, 400 → 217, 414 → 217, and 412 → 191. Representative traces from the GCMS-MRM results are shown in Appendix 6. All of the peak height and useful biomarker calculated ratios of oil and source rock samples that were derived from chromatograms are provided in Table 4 and 5. Finally, the stable carbon isotope and

diamondoids values of both saturate and aromatic compounds in oil samples are shown in Table 6 and 7.

Discussion

Geochemistry results of oils and source rocks reveal some important trends of biomarker signatures and are discussed in detail in this chapter. Most of the oil and source rock samples have similar GC patterns, except for LA-03 (Trap Spring), LA-09 (Grant Canyon), and LA-12A (Kate Spring), which show a small unresolved complex mixture (UCM). An important piece of information from GC data is the Pr/Ph ratio. Two general trends of Pr/Ph ratio are present in my data set. A high Pr/Ph ratio (>1) is present in the Chainman Shale extracts as well as in oil samples from Trap Spring, Grant Canyon, and Tomaro Ranch (group 1) and a low Pr/Ph ratio (<1) appears in oil samples from Eagle Spring, Kate Spring, and Ghost Ranch (group 2). The n-*alkane* distribution in the *n*-C_{25} to *n*-C_{27} range for group 1 and 2 show different odd/even preference (OEP) ratios (see Appendix 4). Group 1 oils and the Chainman Shale extracts have high OEP values, whereas group 2 oils have low OEP ratios. A cross plot of Pr/Ph ratios and OEP values are presented in Figure 9. None of the samples show any signature of β-carotane.

The relative abundance of a number of important peaks in the *m/z* 191 and *m/z* 217 chromatograms suggests two different trends. High tricyclic/hopane and Ts/(Ts+Tm) ratios (Figure 10) as well as C_{29} Ts/(C_{29}Ts+C_{29}), diahopane/(diahopane + C_{30} hopane) and moretane/hopane ratios consistently occur in the group 1 oils and the Chainman Shale extracts while low ratios of those compounds are mostly present in group 2 oils. Furthermore, high relative abundance of C_{24} tetracyclic, oleanane, gammacerane, and

homohopane are seen in group 2 oils, while those compounds have low relative abundances in group 1 oils and the Chainman Shale extracts (Figure 11). Group 1 oils tend to have poor homohopane preservations reflected by low concentration of $C_{30} - C_{35}$ 22S + 22R (homohopane index) and low C_{35}/C_{34} homohopane ratio (Figure 12). In contrast, group 2 oils have high C_{35} homohopane index and high C_{35}/C_{34} homohopane ratios, indicating good homohopane preservations.

Biomarker analyses of aromatic compounds reveal different trends. Triaromatic dinosterane relative peak heights (*m/z* 245 chromatograms) are high in all group 2 oil samples whereas triaromatic dinosterane relative peak heights for group 1 oils and the Chainman Shale extracts are all very low (see Appendix 2.E and 5.E). Furthermore, elevated $C_{21}+C_{22}$ triaromatic steroid (TA I) and C_{27} triaromatic steroid from *m/z* 231 chromatograms as well as $C_{20}+C_{21}$ monoaromatic steroid (MA I) ratios from *m/z* 253 chromatograms consistently occur in group 1 oils, whereas the ratios are low in group 2 (see Appendix 5.C and 5.D).

The analysis of sterane compounds suggests two trends in the sterane data. Group 2 oils, in contrast to group 1 oils and the Chainman Shale extracts, have high relative abundances of C_{26} 21-norcholestanes, C_{26} 24-norcholestanes, and C_{26} 27-norcholestanes as shown in *m/z* 358 →217 chromatograms (Figure 13). Most of the oils from group 2 have a higher tetracyclic polyprenoid (TPP) ratio compared to group 1 oils and the Chainman Shale extracts. Moreover, group 1 oils are distinguished by high relative abundances of C_{27} and C_{30} diasteranes in the *m/z* 372 → 217 and *m/z* 414 → 217 chromatograms. A cross plot of the TPP ratio versus C_{30} diasteranes is provided in Figure 14. Additionally, *m/z* 217 and *m/z* 386 → 217 chromatograms suggest that group 1 oils

and the Chainman Shale extracts have higher diasteranes/steranes ratio values than group 2 oils (see Appendix 3.B and 5.B).

Further investigation of the biomarker signatures reveals that there is some variability of the biomarker trends within the group 2 oil (Eagle Spring, Ghost Ranch, and Kate Spring). Based on the *m/z* 191 chromatograms, oil samples from Eagle Spring have a higher C_{24} tetracyclic / (C_{24} tetracyclic + C_{26} tricyclic) ratio, as well as higher oleanane, gammacerane, and homohopane index values than those from Ghost Ranch and Kate Spring. The relative abundance of C_{28} triaromatic steroids from Eagle Spring oil samples are higher than oils from Ghost Ranch and Kate Spring, as indicated by *m/z* 231 chromatograms. Additionally, oils from Eagle Spring, in contrast with those from Ghost Ranch and Kate Spring, have relative low abundances of C_{27} regular steranes derived from *m/z* 372 → 217 chromatograms. A cross plot of these parameters is provided in Figure 15.

Stable carbon isotope values of saturate and aromatic fractions from oil and source rock samples show two trends (Figure 16), which include isotopically heavy values that range from -29.5 ‰ to -28.5 ‰ and light carbon isotope values from -30 ‰ to -30.5 ‰.

Diamondoids analysis, which is useful to determine the degree of oil cracking, show that most of my oil samples have low values (0.74 ppm – 19.26 ppm) of methyldiamantane (Figure 17).

CHAPTER 5

INTERPRETATION

Geochemical Attributes of Source Rocks

Source rock assessment

Based on source rock screening (chapter 4), the geochemical characteristics of the Chainman Shale and the Sheep Pass Formation Member B were made. The Chainman Shale is a fair to excellent source rock (0.79 wt % to 4.31 wt %) based on the classification by Peters and Cassa (1994). Also, the Chainman Shale can be classified as a mature source rock as indicated by the Tmax (442 ^{0}C - 455 ^{0}C), Ro (0.68% – 1.01%), and TAI (2+ to 3-) values. In terms of quality of the source rock, the Chainman Shale samples plot near the origin on the pseudo-van Krevelen diagram (see Figure 8), which means that they do not contain sufficient kerogen to characterize their quality using the pseudo-van Krevelen diagram. The fact that all of the Chainman samples plot near the origin on the pseudo-van Krevelen diagram indicates that the HI and OI values have been affected by thermal maturity (Peters and Cassa, 1994).

The TOC analyses of the Sheep Pass Formation Member B samples show that most of the samples are poor source rocks; the highest TOC measurement was 0.24 wt %. This result most likely is due to the fact that rock samples were taken from outcrops, where oxidation probably reduced the organic content within the Sheep Pass Formation Member B interval. In terms of quality of source rock, the Sheep Pass samples appear to be mixed oil and gas prone (type 2 kerogen)(see Figure 8). Furthermore, the Sheep Pass Formation Member B is a thermally immature to early mature source rock. Even though Ro value of the Sheep Pass indicates immature source rocks (0.46 %), the other maturity

indicators, TAI (2 to 2+) and Tmax (436 ^{0}C – 487 ^{0}C) values, suggest that the Sheep Pass samples are in the early mature stage.

Source rock geochemistry

The high Pr/Ph, diasteranes/steranes, and Ts/(Ts+Tm) ratios as well as low C_{35} homohopane index (see Appendix 2.A-B and Figure 18) in my source rock extracts is a strong indication of a shale source rock (Peters et al., 2007). Low oleanane relative abundances and TPP ratios, as well as high C_{30} diasteranes, tricyclic/hopane and Pr/Ph ratios in my source rock samples all suggest marine-derived organic matter in the source rock (Peters et al., 2007; Holba et al., 2000). In terms of oxicity and salinity, the Chainman Shale source rock was deposited in relatively dysoxic conditions and has normal marine salinity, as indicated by consistently low gammacerrane and homohopane index, as well as low C_{24} tetracyclic/(C_{24} tetracyclic + C_{26} tricyclic) and high Pr/Ph ratios. Regionally, the Chainman Shale is widely known as a Mississippian source rock and my geochemical results agree with that interpretation. I found no evidence of oleanane (see Figure 11), C_{26} 21, 24, 27-norcholestanes (see Figure 13) and triaromatic dinosteranes in my samples. Maturity-related parameters, such as triaromatic steroids, C_{29}Ts/ (C_{29}Ts+C_{29} hopane), Ts/(Ts+Tm), diasterane/sterane ratios, and sterane isomerization ratios show the Chainman extracts are thermally mature.

Geochemical Attributes of Oils

Oil biodegradation

Most of my oil samples have not been biodegraded, which is indicated by an absence of unresolved complex mixture (UCM) in most of my oil samples. However,

three of the oil samples experienced moderate biodegradation. These are LA-03 (Trap Spring), LA-09 (Grant Canyon), and LA-12A (Kate Spring). The biodegradation of these three oil samples is attributed to the fact that they sat at the surface and were biodegraded there.

Oil geochemistry

Several biomarker parameters in crude oils are very powerful to effectively discriminate the oil group. For example, oleanane is highly specific for higher plant input of Cretaceous or younger age. Therefore, the cross plot of those highly specific biomarker parameter is used to further differentiate the oil group and to obtain the information about source rock age, organic matter type, depositional environment, and source rock facies. Critical information regarding their specificity and the means will be discussed more detail in this part.

Group 2 oils are characterized by low Pr/Ph, diahopane/diahopane + C_{29} hopane, and diahopane/diahopane + C_{30} hopane ratios as well as a high homohopane index (see Figure 18). These characteristics typify oils generated from lacustrine anoxic environments (Peters et al., 2007). In contrast, oils from group 1 differ from those in group 2 by having distinct high Pr/Ph, diahopane/diahopane + C_{29} hopane, diahopane/diahopane + C_{30} hopane ratios and a low homohopane index, which is indicative of oils that originated from a dysoxic marine environment (Peters et al., 2007).

I employed highly specific biomarker parameters, such as gammacerane, C_{24} tetracyclic, and homohopane index, in order to determine the environment and conditions during source rock deposition. Gammacerane is a highly specific biomarker of hypersaline lacustrine oil and bitumen (Peters et al., 2007). Gammacerane originates from

the reduction of tetrahymanol (produced by bacterivorous ciliates), which is present in the stratified water columns in lacustrine systems (Venkatesan and Dahl, 1989; Sinninghe Damste et al., 1995). Therefore, the existence of high relative abundances of gammacerrane in group 2 oils, and low relative abundance in group 1, is strongly linked to hypersaline lacustrine source rocks. This interpretation is also supported by a high C_{24} tetracyclic / (C_{24} tetracyclic + C_{26} tricyclic) ratio in group 2 oils, which is indicative of hypersaline condition during carbonate-rich source rock deposition (see Figure 11). Moreover, Peters and Moldowan (1993) suggest that high C_{35} homohopane preservation can be used as a general indicator of highly reducing conditions. Therefore, very well preserved homohopanes, specifically C_{34} and C_{35} homohopanes, in group 2 oils relative to those in group 1, suggest anoxic conditions during source rock deposition (see Appendix 5.A and Figure 12). All of the evidence described above strengthens the interpretation of strongly reducing and anoxic conditions in a lacustrine environment during source rock deposition for group 2 (Sheep Pass-derived). This is in contrast to group 1 oils, which originated from a source rock deposited in a marine setting under dysoxic condition (Chainman Shale-derived).

In terms of source rock facies, oils from group 2 can be interpreted as having been derived from a carbonate-dominated source rock as all the samples in group 2 consistently have low Ts/(Ts+Tm) as well as a high C_{35} homohopane index and C_{24} tetracyclic terpanes (Peters et al., 2007). This interpretation is also supported by low diasterane/sterane ratios in group 2 oils, which is indicative of clay-poor sediments during source rock deposition (Figure 19). As suggested by Peters et al. (2007), diasteranes and Ts/(Ts+Tm) could be affected by maturity (diasteranes/steranes and

Ts/(Ts+Tm) ratios increase as maturity increases). However, other maturity-related parameters show that group 2 oil is less mature than group 1. Therefore, maturity is not the main issue here, and the use of diasteranes and Ts/(Ts+Tm) as an indicator of lithology is reasonable. In contrast to group 2 oils, a clay-rich source rock is the main source of oils in group 1. This interpretation is based on elevated diasterane relative abundances, such as C_{27} and C_{30} diasteranes (see Figure 14). Diasteranes are moderately specific for source rock lithology because abundant clays can catalyze the conversion of sterols to diasteranes (Peters et al., 2007). High Ts/(Ts+Tm) accompanied by the low occurrence of C_{24} tetracyclic terpanes in my samples, also suggests a shale-dominated source rock for the origin of group 1 oils.

In terms of organic matter input, land-plant organic matter derived from a lacustrine environment is the main contributor to the source rock that generated group 2 oils. Numerous lines of evidence support this interpretation. Most notable is the high concentration of oleananes, a compound derived from betulins and taraxerene that are produced from land plant angiosperms (Peters et al., 2007). The high tetracyclic polyprenoid (TPP) ratio in the group 2 oils, which is highly specific for a lacustrine source rock (Holba et al., 2000), also shows that the source rock that generated group 2 oil was influenced by significant input of land-plant organic matter in a lacustrine setting. Additionally, the monoaromatic ternary diagram (Figure 20) shows that most of the oil samples in group 2 have high C_{29} monoaromatic steroids indicative of non-marine organic-matter-derived oil (Volkman, 1986; Peters et al., 2007). Group 1 oil is slightly different from group 2 oil in terms of the relative abundances of organic-matter-specific biomarkers. A significant lack of oleanane and low TPP ratio in most of the oil samples

are the supporting evidence that indicates that group 1 oil was not generated from a source rock rich in land plant input (Figure 21). Instead, group 1 oils originated from a source rock rich in algal input that was deposited in a marine setting, as suggested by a high tricyclic/hopane ratio (see Figure 10). It was proposed by Volkman et al. (1989) that the elevated concentrations of tricyclic terpanes is linked to primitive algae called *Tasmanites*. Further evidence shows that low TPP ratios and high relative abundances of C_{30} diasteranes in group 1 oils (see Figure 14), as well as where the samples plot on a sterane ternary diagram (Figure 22), strengthen my interpretation that group 1 oil is derived from a marine, algae-rich source rock.

In addition, stable carbon isotope analysis results support the depositional environment interpretation of the source rocks. Consistently heavy $\delta^{13}C$ values, ranging from -29.5 ‰ to -28.5 ‰, of saturate and aromatic fractions in group 2 oil are interpreted as typical of saline lake environments (Peters et al., 1993). Conversely, light $\delta^{13}C$ isotope values (-30 ‰ to -30.5 ‰) in both saturate and aromatic fractions within group 2 oil are indicative of marine-derived oil (see Figure 16).

Age-related biomarkers play an important role in differentiating oil families in Railroad Valley (Figure 23). Group 2 oil shows high proportions of oleanane, C_{26} 21-norcholestane, C_{26} 24-norcholestanes, C_{26} 27-norcholestanes and triaromatic dinosteranes, which are indicative of source rocks younger than Cretaceous (Moldowan et al., 1994; Holba et al., 1998). It is interesting to note that triaromatic dinosterane biomarkers exist in my lacustrine-derived oils. It is widely known that triaromatic dinosteroids are derived from dinoflagellates, one of the main producers in the modern ocean, which first occurred in the Triassic period (Moldowan et al., 1996). However,

Tasch (1980) proposed that dinoflagellates may occur in water bodies in non-marine settings, such as in the Great Salt Lake, and Hanson et al. (2001) provide a good example of the existence of triaromatic dinosterane in a hypersaline lacustrine source rock in Qaidam Basin, China. Therefore, I confidently interpret the relative abundance of triaromatic steroids in my group 2 samples to indicate a significant input of dinoflagellates in a post-Cretaceous lacustrine system. Furthermore, group 1 oils are remarkable by the absence of oleanane, C_{26} 21-norcholestane, C_{26} 24-norcholestanes, C_{26} 27-norcholestanes and triaromatic dinosteranes and appear to have high OEP (C_{25}-C_{27}) and tricyclic terpanes. Those characteristics suggest that group 1 were derived from source rocks older than the Mesozoic.

Maturity-related parameters, which include Ts/(Ts+Tm), C_{29} Ts / (C_{29}Ts + C_{29} hopane), moretane/hopane, diasteranes/steranes, C_{27} / C_{28}S triaromatic steroids, TA(I) / ((TA(I) + TA(II))), MA(I) / ((MA(I) + MA(II))), C_{29} sterane isomerization and C_{29} $\alpha\beta\beta/(\alpha\beta\beta+\alpha\alpha\alpha)$, consistently have higher concentrations in group 1 oil than in group 2 oil (Figure 24). The agreements between all maturity-related biomarker parameters indicate that group 1 oils are more thermally mature than group 2 oils. Additionally, diamondoids analyses show that most of the oil and source rock extracts have low concentrations of diamondoids (0.74 – 19.26 ppm), which suggests that intense oil cracking has not yet occurred (Dahl et al., 1999) (see Figure 17).

Hierarchical cluster analysis using Ward's method (Figure 25) strengthens the interpretation that two oil families are present in this basin. A dendrogram, which was generated by entering important biomarker parameters (Appendix 8) into the statistical software, suggests that Trap Spring, Grant Canyon, and Tomaro Ranch are genetically

related, whereas, oils from Eagle Spring, Ghost Ranch and Grant Canyon clustered in a second oil family. This fact further suggests that reservoirs in Railroad Valley basin have been charged by two source rock intervals. One source rock interval generated Trap Spring and Grant Canyon oils (Group 1) and another source rock interval generated Eagle Spring, Kate Spring, and Ghost Ranch oils (Group 2).

One interesting fact that can be seen in my dendrogram (see Figure 25) is the presence of a subgroup within the group 2 (lacustrine-derived) oils. Both Ghost Ranch and Kate Spring oils are slightly different from Eagle Spring oils but still closely related. I interpret this difference to be due to spatial variations in salinity, redox, depth, and organic matter input in the lacustrine system during source rock deposition (Figure 26). As suggested by Katz (1995), lacustrine systems commonly show more variability of specific conditions than marine settings. Greene et al. (2004) showed that the difference in source rock facies and source rock depositional conditions in a lacustrine system influence the oil characteristics in Turpan-Hami Basin, China. Therefore, I interpreted the oils from Eagle Spring to have been generated by lacustrine source rocks that were deposited in more anoxic and hypersaline conditions with high land plant contribution, as indicated by elevated oleanane, gammacerane, C_{24} tetracyclic, and homohopane, and C_{28} triaromatic steroid. Those conditions are indicative of a deep and stratified water column in a lacustrine system. In contrast, Ghost Ranch and Kate Spring oils originated from lacustrine source rock deposited in a lake with shallower water depths, lower salinity, and less anoxic conditions, as shown by relatively lower oleanane, gammacerane, C_{24} tetracyclic terpane, homohopane, and C_{28} triaromatic steroid compared to those exist in Eagle Spring oils (see Figure 15).

CHAPTER 6

CONCLUSION

I conclude that two genetically related groups of oils and one sub-group of oils occur in Railroad Valley and that they originated from two different source rock intervals. All of the geochemical evidence supports this interpretation.

Group 1 oils come from Trap Spring and Grant Canyon. Oils in this group have light $\delta^{13}C$ isotopic values (-30 ‰ to -30.5‰), low relative abundances of oleanane, C_{24} tetracyclic, gammacerane, homohopane index, triaromatic dinosteranes, C_{26} 21 norcholestanes, C_{26} 24 norcholestanes, C_{26} 27 norcholestanes and TPP ratios, and have high relative abundances of Pr/Ph, tricyclic/hopane ratio, Ts/(Ts+Tm), diasteranes/steranes ratio, and high C_{30} diasteranes. This geochemical evidence indicates that this oil family originated from a marine shale source rock older than the Cretaceous that was deposited in a dysoxic zone, under normal marine salinity conditions, with a lack of land plant input. These findings suggest that oils from Trap Spring and Grant Canyon originated from the Mississippian marine Chainman Shale.

Oils from Eagle Spring, Kate Spring, and Ghost Ranch are clustered in one oil family (group 2). This oil family has geochemical characteristics as follows: heavy $\delta^{13}C$ isotopic values (-29.5 ‰ to -28.5 ‰), high relative abundances of oleanane, C_{24} tetracyclic, gammacerane, homohopane index, triaromatic dinosteranes, C_{26} 21 norcholestanes, C_{26} 24 norcholestanes, C_{26} 27 norcholestanes and TPP ratios, and have low Pr/Ph, tricyclic/hopane, Ts/(Ts+Tm), diasterane/sterane ratios, and low C_{30} diasteranes. These characteristics typify oil generated from hypersaline and anoxic

lacustrine carbonate-rich source rock, which is post-Cretaceous in age. This points to the Sheep Pass Formation Member B as the source rock.

These comprehensive geochemical analyses also produce a new interesting result regarding the origin of oil in Railroad Valley that was previously unrecognized. Specifically, I suggest that one subgroup of oils are present within the main group of the Sheep Pass-derived oil. Oils from Kate Spring and Ghost Ranch are slightly different from Eagle Spring oils. My data indicate that the differences are primarily due to spatial/temporal variation in a lacustrine system, such as different depth of the water column, which affects the source rock facies and source rock depositional conditions. The Eagle Spring oils are derived from a source rock that was deposited under hypersaline and anoxic conditions. On the other hand, the source rock that generated Ghost Ranch and Kate Spring oils was deposited under less saline and less anoxic condition.

My results support the idea that two oil families from two different source rock intervals (Chainman Shale and Sheep Pass Formation Member B) are present in Railroad Valley area (Poole and Claypool, 1984; Conlan, 1995). Furthermore, I disagree with some workers who have proposed that oils in Railroad Valley basin were sourced from only one source rock (Picard, 1960; Poole et al., 1979), and with those who have proposed that the oils were produced by the mixing from 2 intervals (Bortz and Murray, 1979; Duey, 1979; French, 1983).

Additionally, from the diamondoids analyses I observe that all of my oil samples show low diamondoid concentrations. This result suggests that intense oil cracking has not yet occurred.

FIGURES

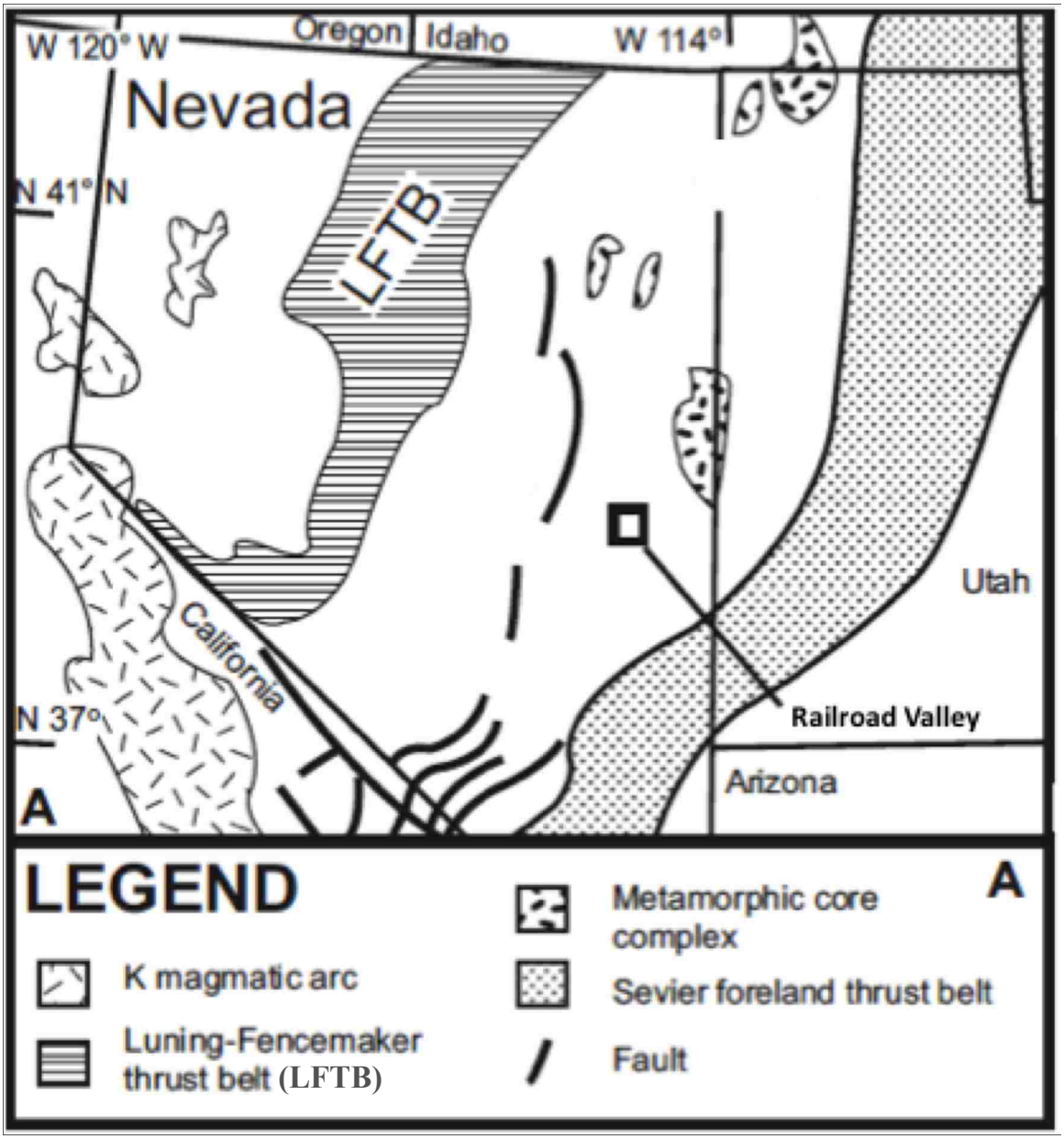

Figure 1. Map of Nevada with research area highlighted by box (modified from DeCelles, 2004)

Figure 2. Google Earth image of Railroad Valley and adjacent ranges, i.e. Egan Range, Grant Range, Pancake Range. A: Duckwater airport, Nye County.

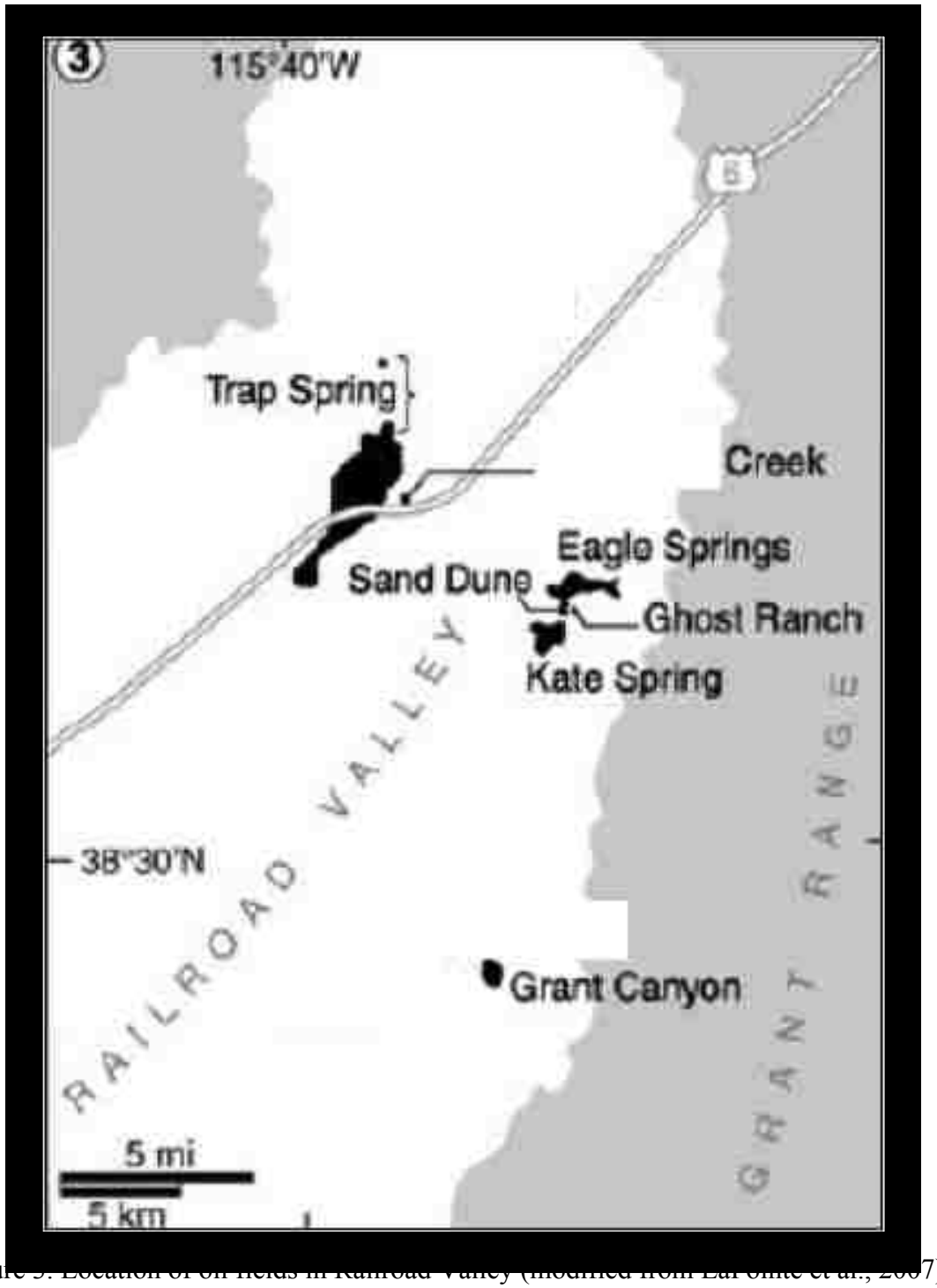

Figure 5. Location of oil fields in Railroad Valley (modified from LaFollette et al., 2007)

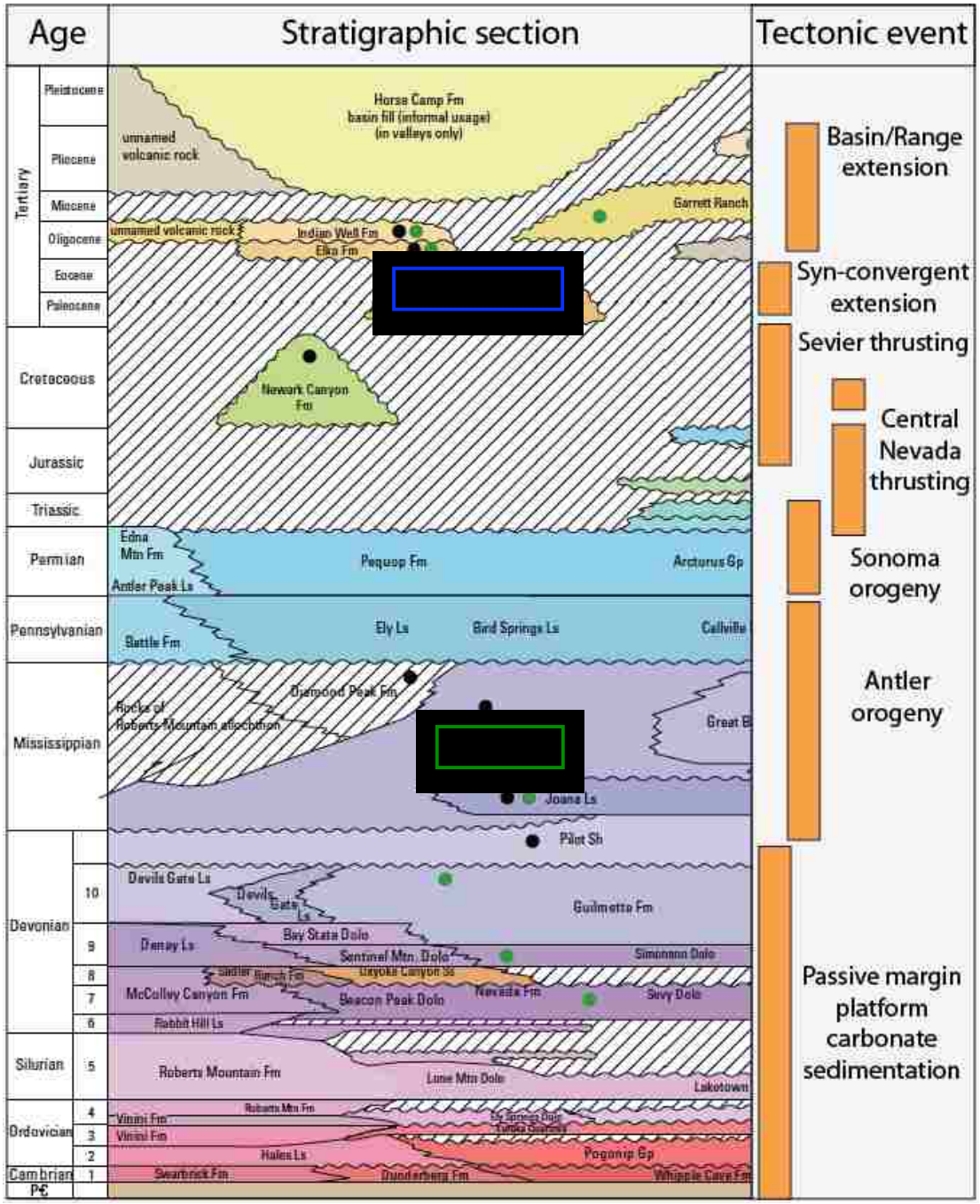

Figure 4. Generalized stratigraphic column of Phanerozoic strata in the eastern Great Basin showing intervals of petroleum production (green dots), source rocks (black dots), major sequence boundaries, hiatus intervals, and unconformities. Paleozoic section modified from Cook and Corboy, 2004. Ls: limestone; Dolo: dolomite; Fm: formation; Vol: volcanic ; Ss: sandstone. Two blue rectangles are the source rock intervals in RRV. Black dots are potential source rocks intervals and green dots are reservoir intervals.

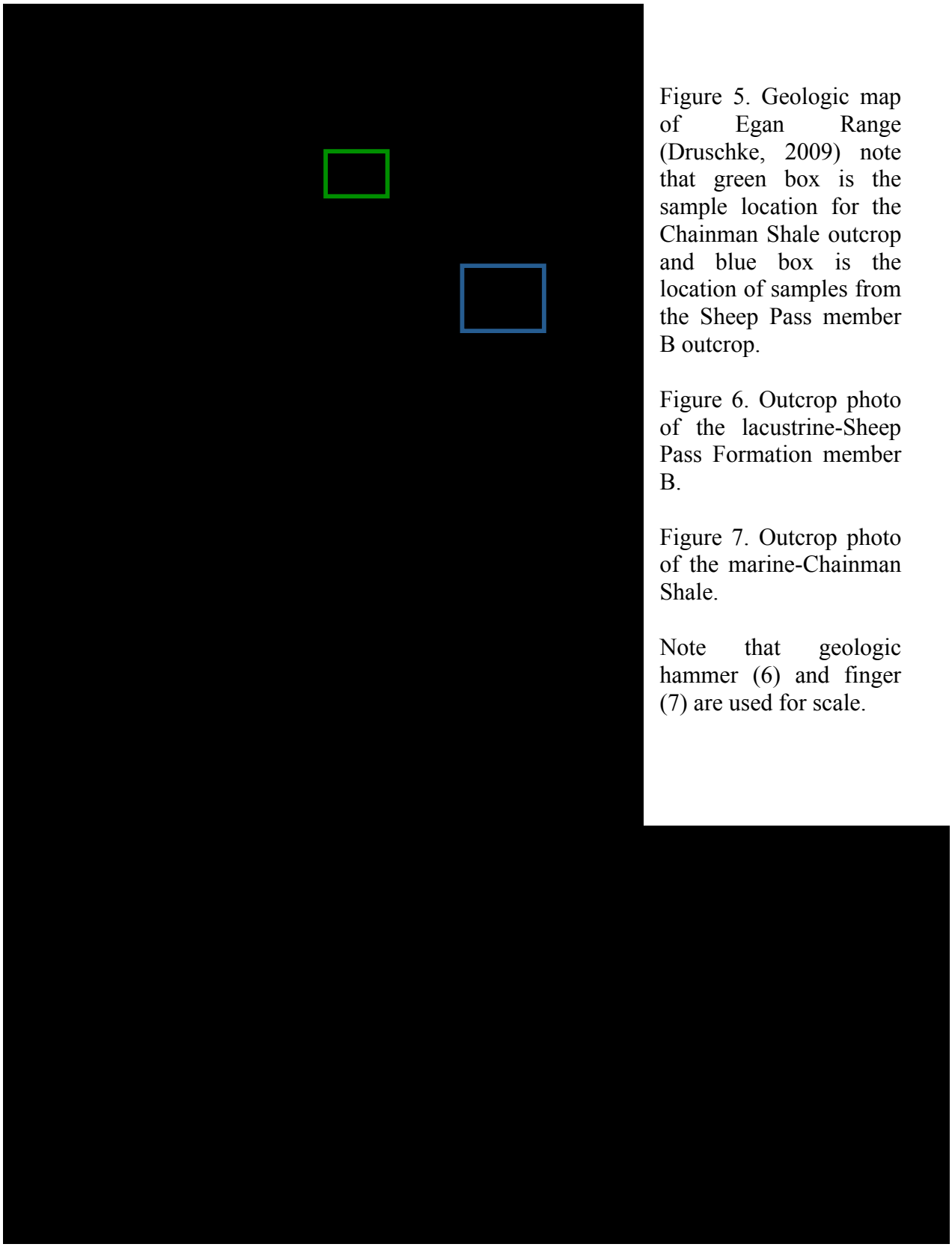

Figure 5. Geologic map of Egan Range (Druschke, 2009) note that green box is the sample location for the Chainman Shale outcrop and blue box is the location of samples from the Sheep Pass member B outcrop.

Figure 6. Outcrop photo of the lacustrine-Sheep Pass Formation member B.

Figure 7. Outcrop photo of the marine-Chainman Shale.

Note that geologic hammer (6) and finger (7) are used for scale.

Figure 8. Cross plot of the Chainman Shale and Sheep Pass samples on a modified pseudo van Krevelen diagram. Dashed line (A) is the limit of oxygen index values as described in Peters (1986). Oxygen Index (x-axis) was expanded due to elevated OI values on the Sheep Pass samples. Note that pseudo thermal maturation pathway (Peters, 1986) is added to this diagram because the high maturity is interpreted to have reduced the amount of organic matter in the Chainman Shale samples. Therefore, the observed HI and OI values of the Chainman samples do not reflect original kerogen amounts.

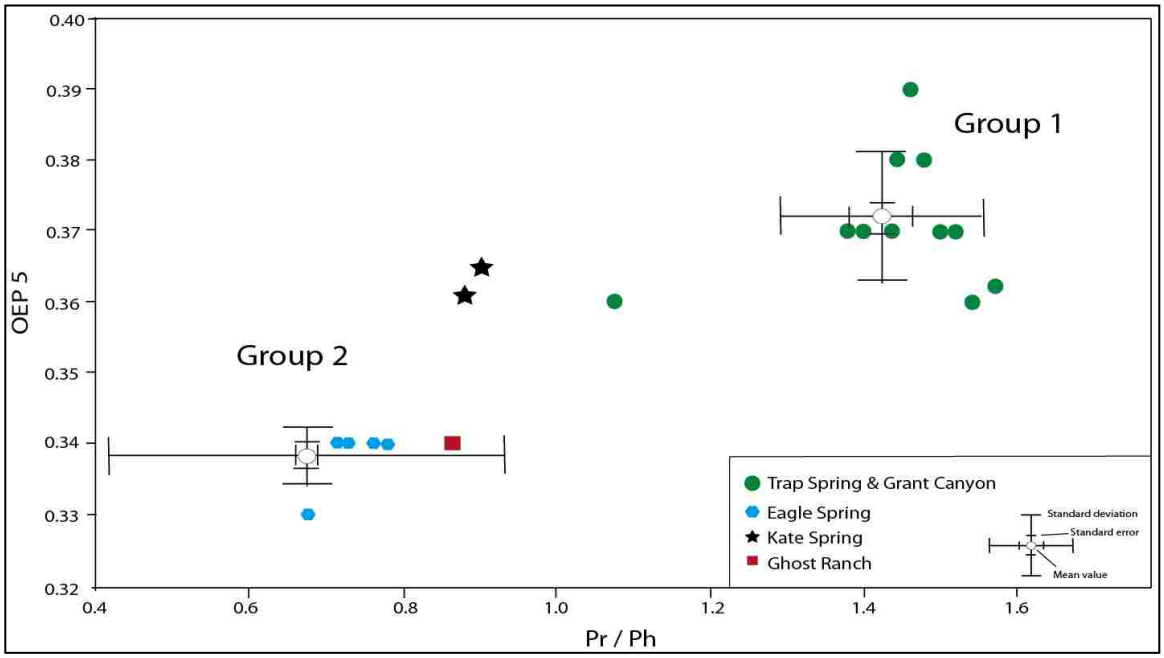

Figure 9. Cross plot of Pr/Ph ratios and OEP 5 ratios (as defined in Table 5)

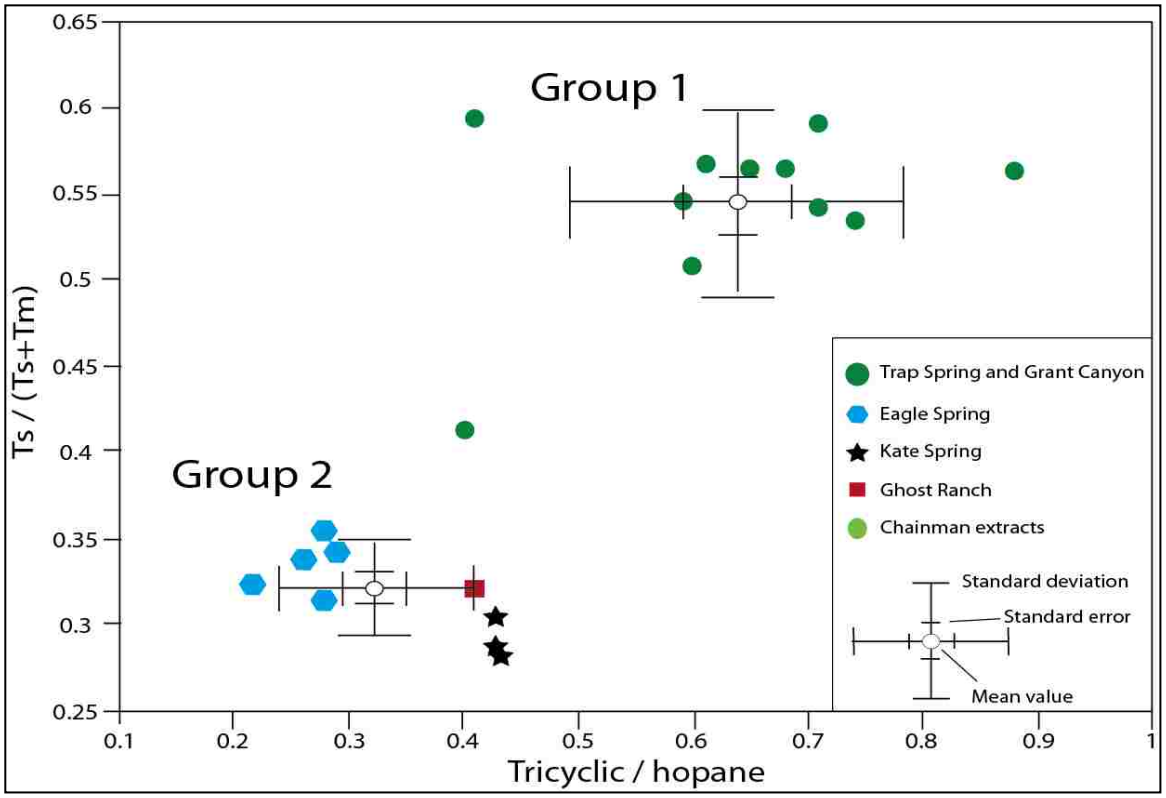

Figure 10. Cross plot of tricyclic/hopane vs Ts / (Ts+Tm) suggests group 1 oils, in contrast to group 2 oils, were derived from an algal-rich and clay-rich source rock.

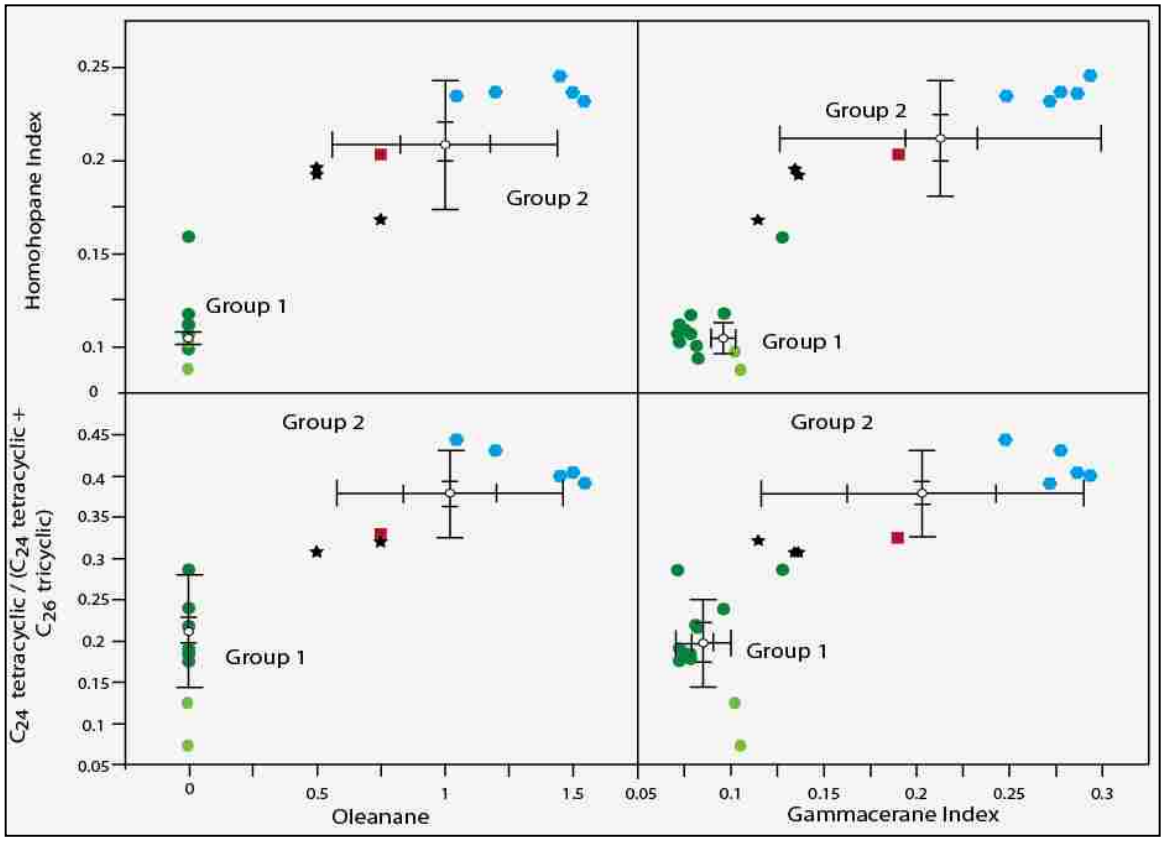

Figure 11. Cross plot of oleanane, gammacerane index, homohopane index, and C_{24} tetracyclic / (C_{24} tetracyclic + C_{26} tricyclic) suggests that group 2 oils are derived from a carbonate-rich lacustrine source rock (hypersaline and anoxic), whereas group 1 oils are marine-derived oil (normal marine salinity and dysoxic).

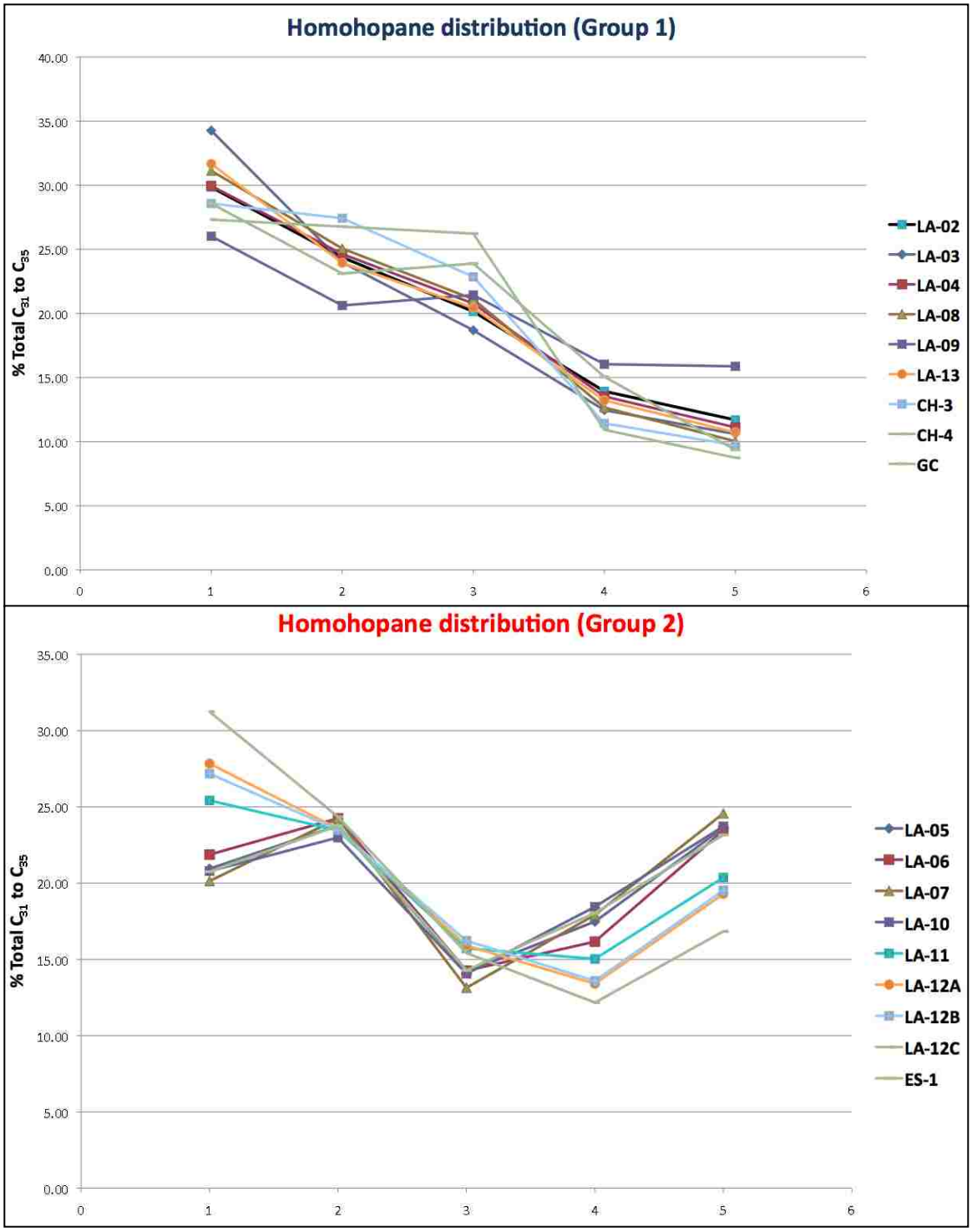

Figure 12. Homohopane distribution of group 1 (upper) and group 2 oils (lower). X-axis is homohopane homologs and y-axis is relative peak heights of homohopane. Note that group 2 oils have well-preserved and high C_{34} and C_{35} homohopane relative abundances suggesting highly reducing conditions during deposition (Peters and Moldowan, 1993). GC: Grant Canyon; ES: Eagle Spring.

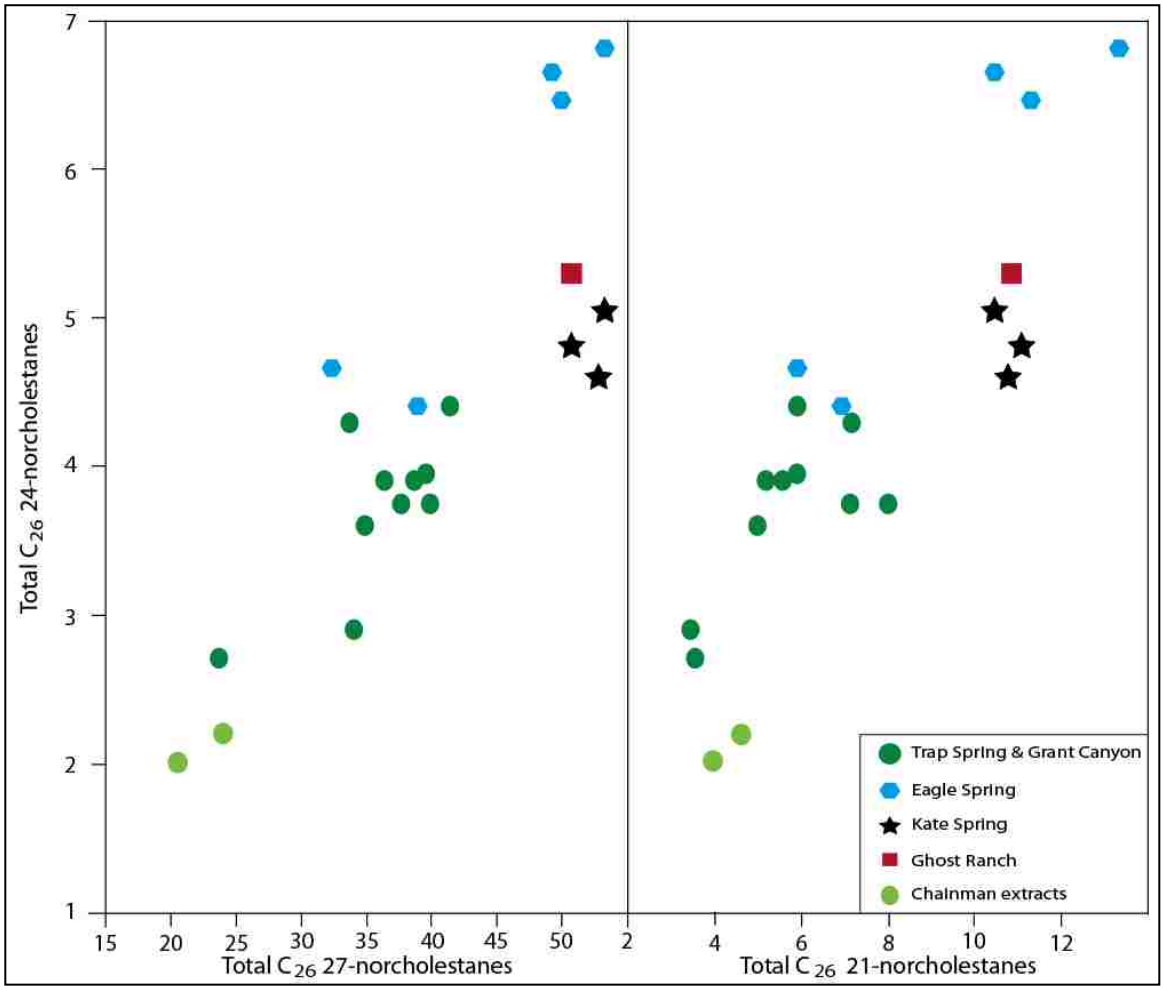

Figure 13. Cross plot of C_{26} 27-norcholestanes, C_{26} 24-norcholestanes, and C_{21} 27-norcholestanes. Note that group 2 oils have higher proportions of C_{26} 21, 24, 27 norcholestanes than group 1 oils, which indicates oils derived from a source rock younger than Cretaceous.

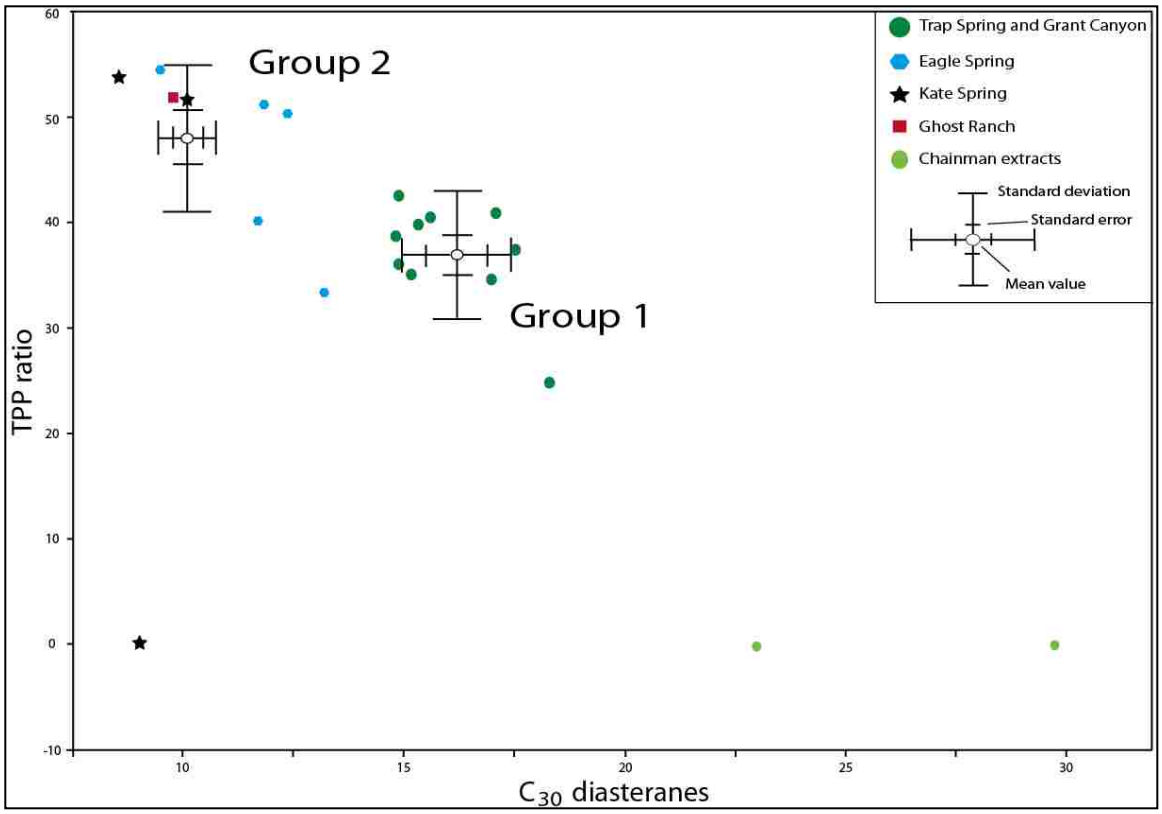

Figure 14. Cross plot of C_{30} diasteranes vs TPP ratio. This diagram illustrates the separation between the lacustrine Sheep Pass Fm and the marine Chainman Shale. Holba et al. (2000) suggested that lacustrine crude oils, as opposed to marine oils, have high tetracyclic polyprenoid (TPP) and low C_{30} diasteranes.

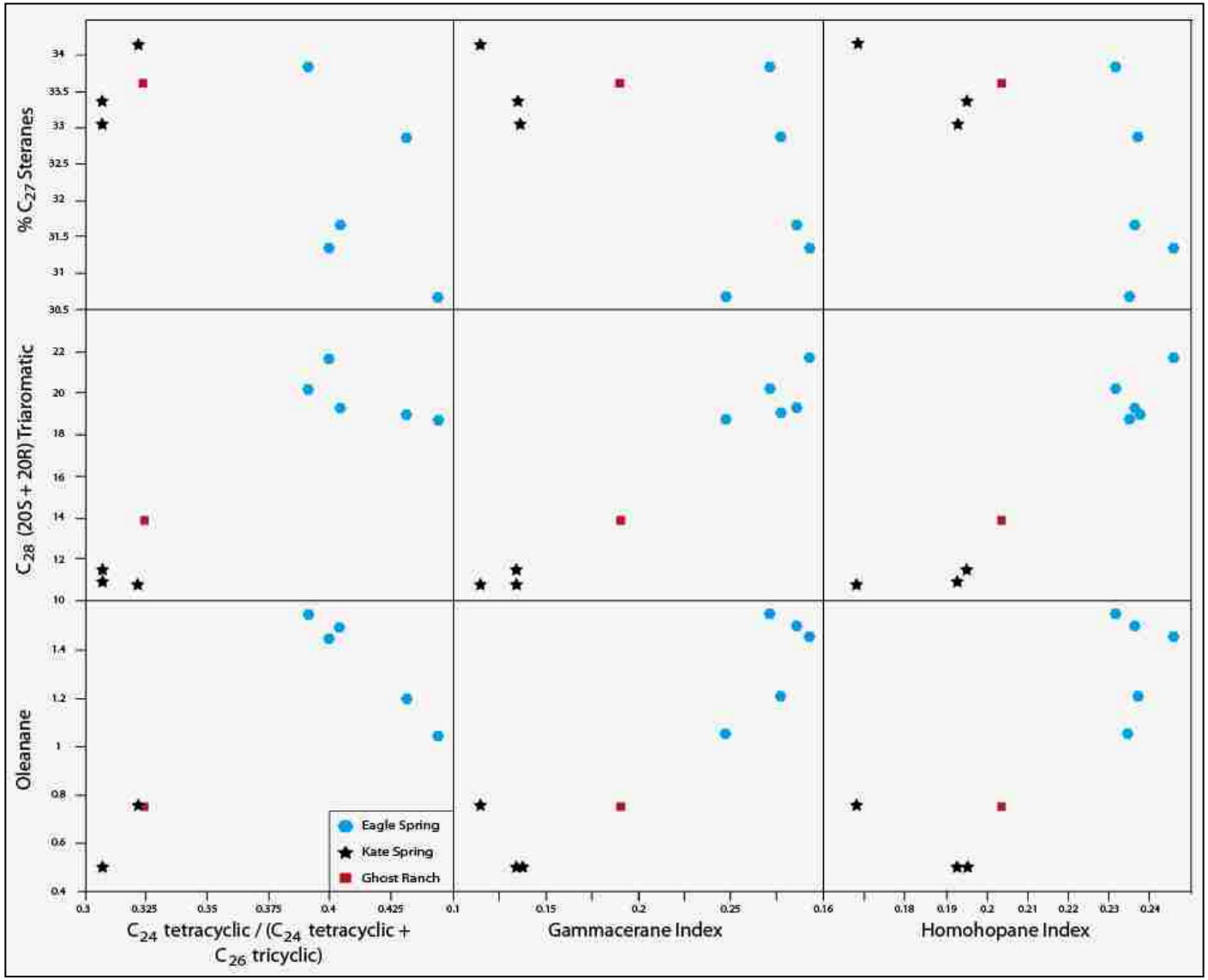

Figure 15. Cross plot to differentiate Sheep Pass-derived oils. Note that Eagle Spring oils plot differently from Kate Spring and Ghost Ranch oils. Based on these specific biomarker parameters, it is concluded that the Eagle Spring oils originated from a hypersaline-anoxic lacustrine source rock with significant land plant input, whereas Kate Spring and Ghost Ranch oils are derived from a shallower part of the lacustrine system in which relatively less saline and less anoxic conditions occurred.

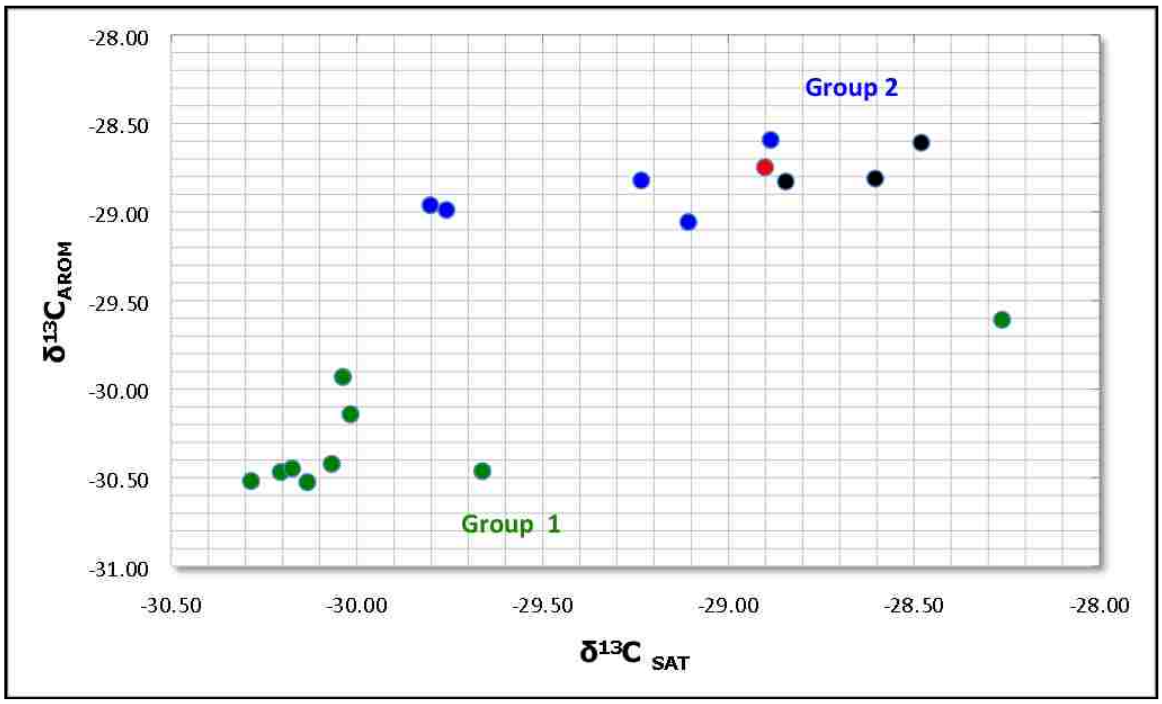

Figure 16. Cross plot of carbon isotope values of saturate and aromatic fractions. Note that Chainman Shale extract, Trap Spring and Grant Canyon oils (green) clustered in the same area, where Eagle Spring (blue), Kate Spring (black), and Ghost Ranch (red) oils are clustered in one group.

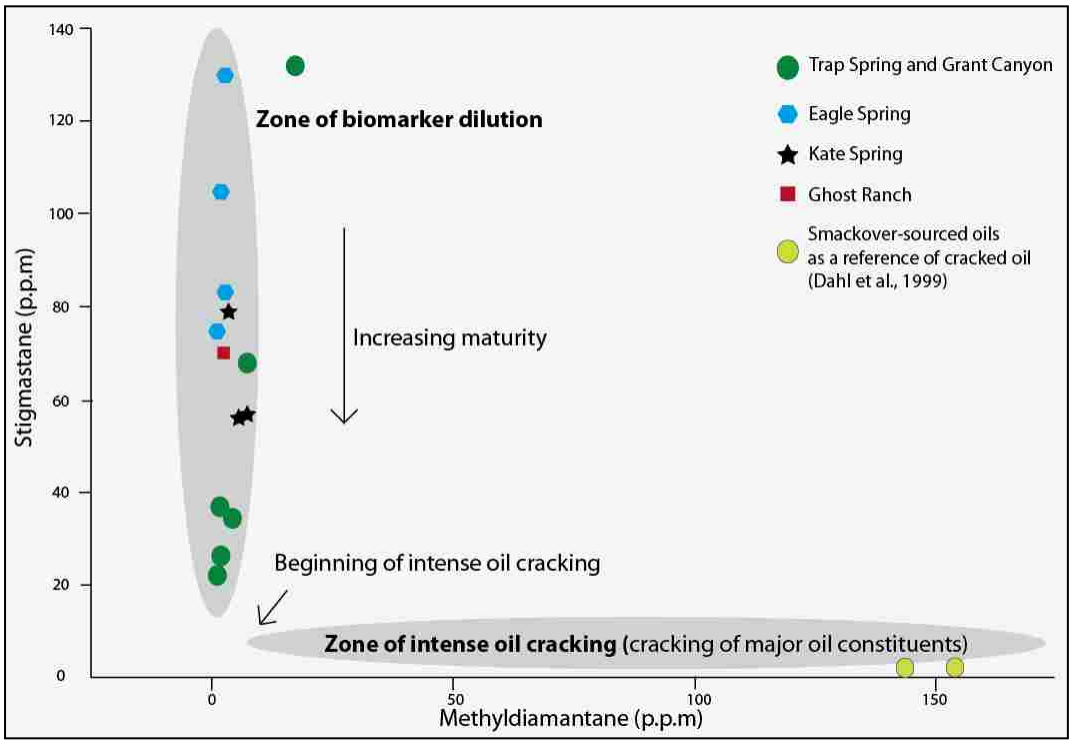

Figure 17. Cross plot of diamondoids (methyldiamantane) vs stigmastane indicating that Railroad Valley's oils have not been cracked (modified from Dahl et al., 1999)

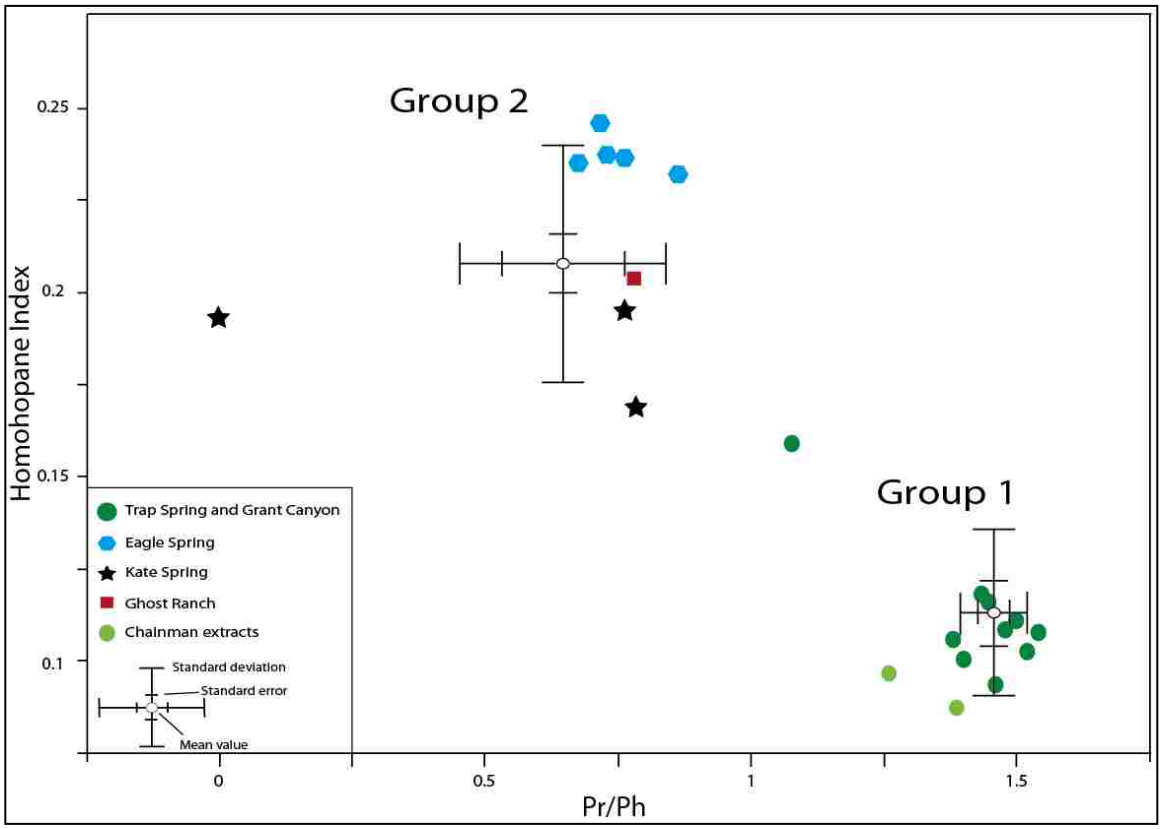

Figure 18. Cross plot of Pr/Ph vs homohopane index suggests anoxic conditions during Sheep Pass deposition and dysoxic conditions during the Chainman Shale deposition.

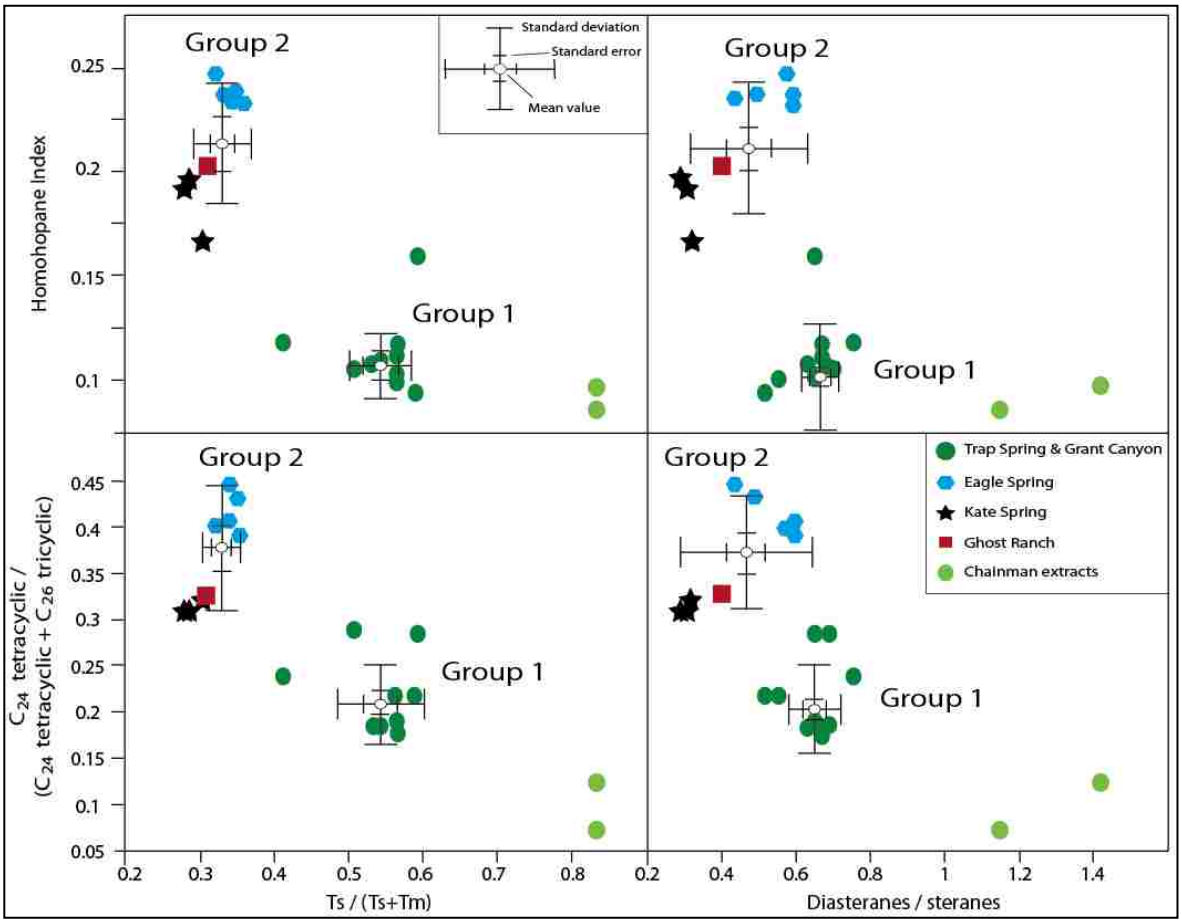

Figure 19. Cross plots of Ts/(Ts+Tm), diasteranes/steranes, C_{24} tetracyclic / (C_{24} tetracyclic + C_{26} tricyclic) ratios and homohopane index. The plots of group 2 oils indicate carbonate-derived oil, where the plots of group 1 oil suggest clay-rich derived oils. Note that group 1 oils always plot near the Chainman Shale extracts suggests that group 1 oils originated from the clay-rich Chainman Shale source rock.

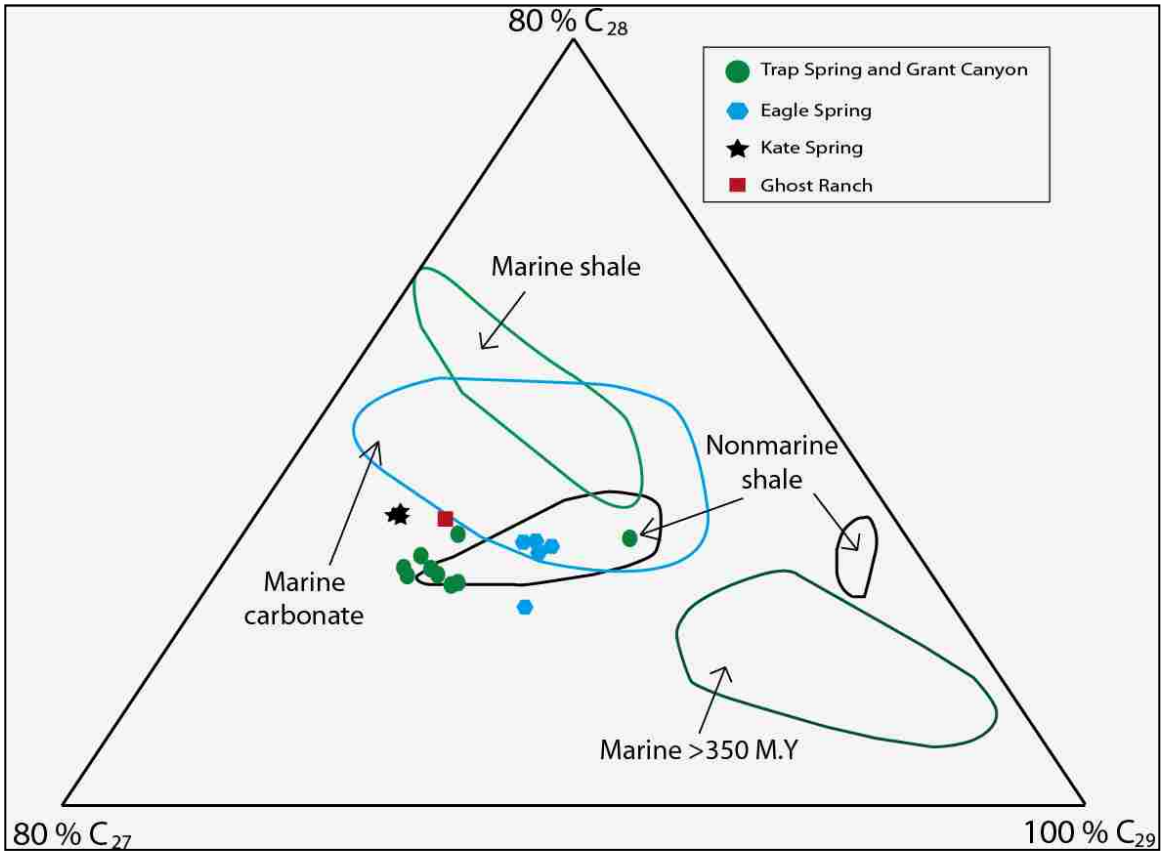

Figure 20. Monoaromatic steroid ternary diagram shows high concentrations of C_{29} monoaromatic steroids on most of the oil samples in group 2 oils. This suggests that these oils were derived from non-marine organic matter (Volkman, 1986; Peters et al., 2007).

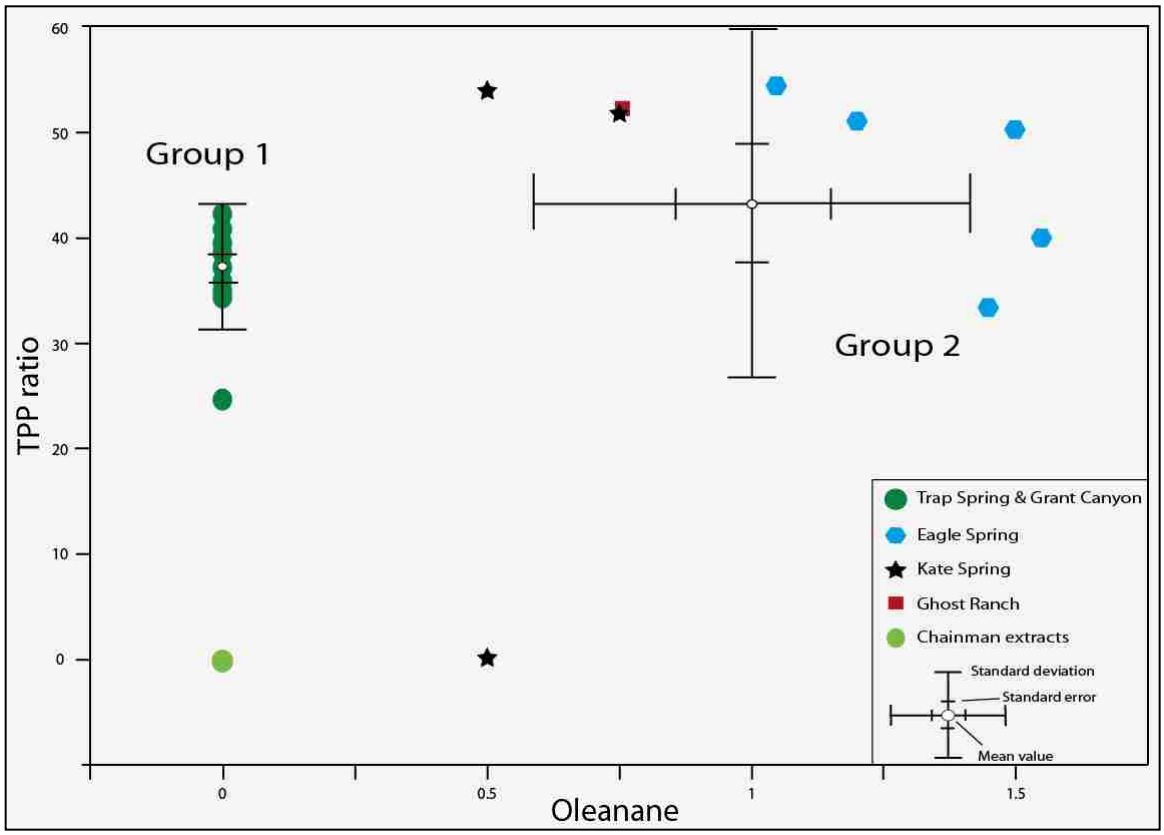

Figure 21. Cross plot of oleanane vs TPP ratio. This cross plot suggests that the Chainman Shale source rock is older than the Cretaceous because no oleanane is present in the samples.

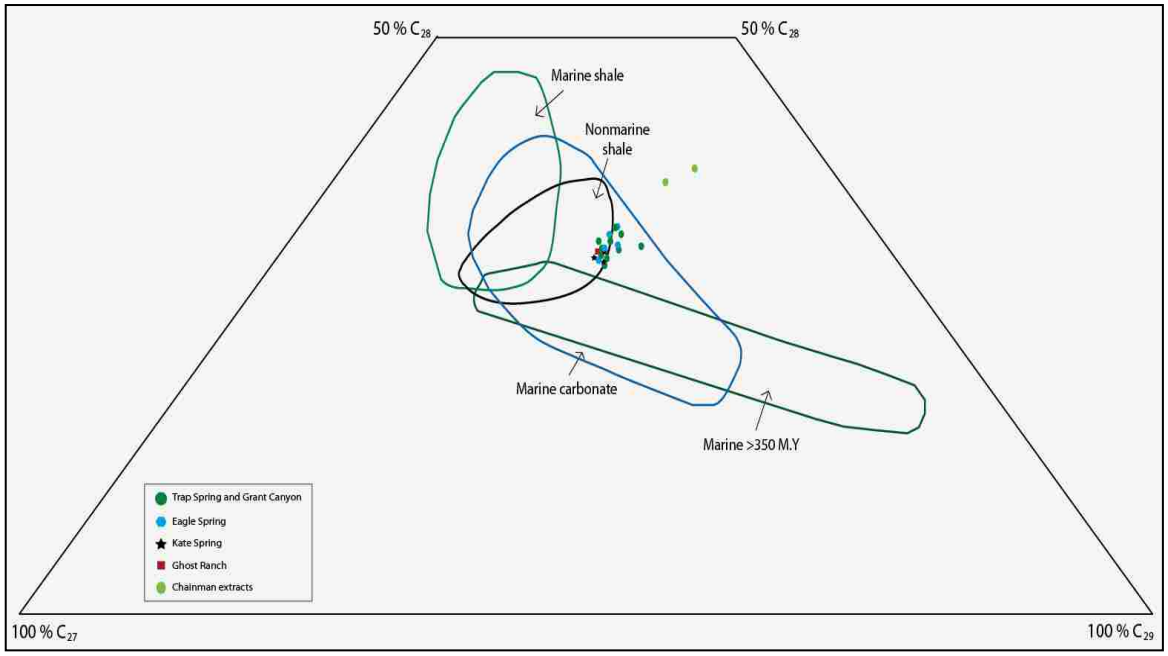

Figure 22. Ternary diagram showing the relative abundance of C_{27}, C_{28}, and C_{29} regular steranes (Moldowan et al., 1985). Overlap in a sterane ternary diagram limit the use of this diagram to describe the source-rock depositional environment. Although this figure does not show clear separation between group 1 and group 2 oils, the results of sterane ternary diagrams suggests that most group 2 oils are non marine-derived oil and most oils in group 1 are marine-derived oil.

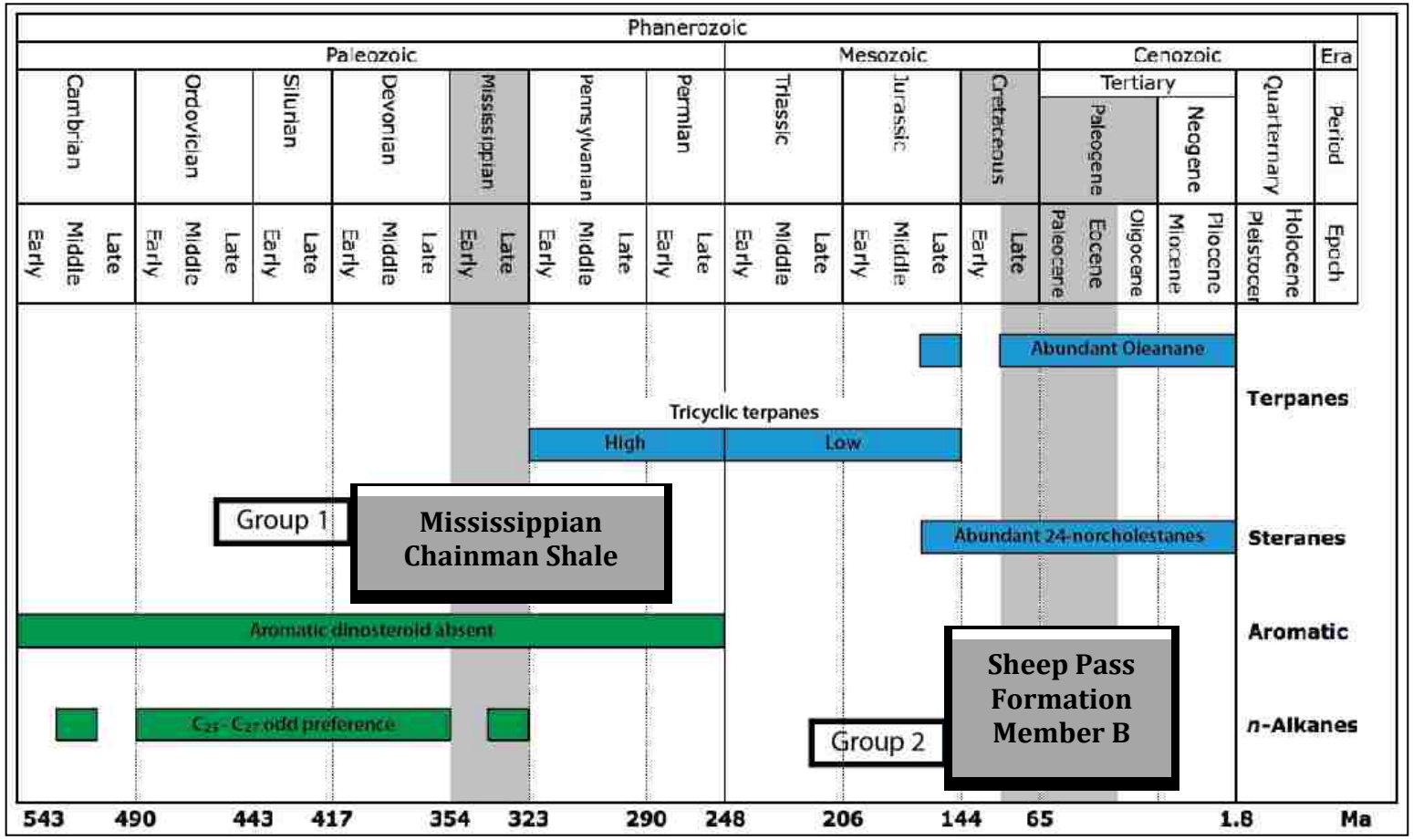

Figure 23. Age related biomarkers adapted from Peters et al. (2007). High tricyclic terpanes, C_{25}-C_{27} odd preference and low aromatic dinosteroid are present in group 1 oils. Those compounds occur earlier in geologic history. This fact indicates group 1 oils were derived from source rock that is older than the Mesozoic (Chainman Shale). Contrastingly, group 2 oils show low tricyclic terpanes and abundant oleanane, C_{26} 24-norcholestanes, and triaromatic dinosteranes. Those compounds show later in geologic history, which strongly suggest that group 2 oil originated from a source rock that is younger than the Cretaceous (Sheep Pass Formation Member B).

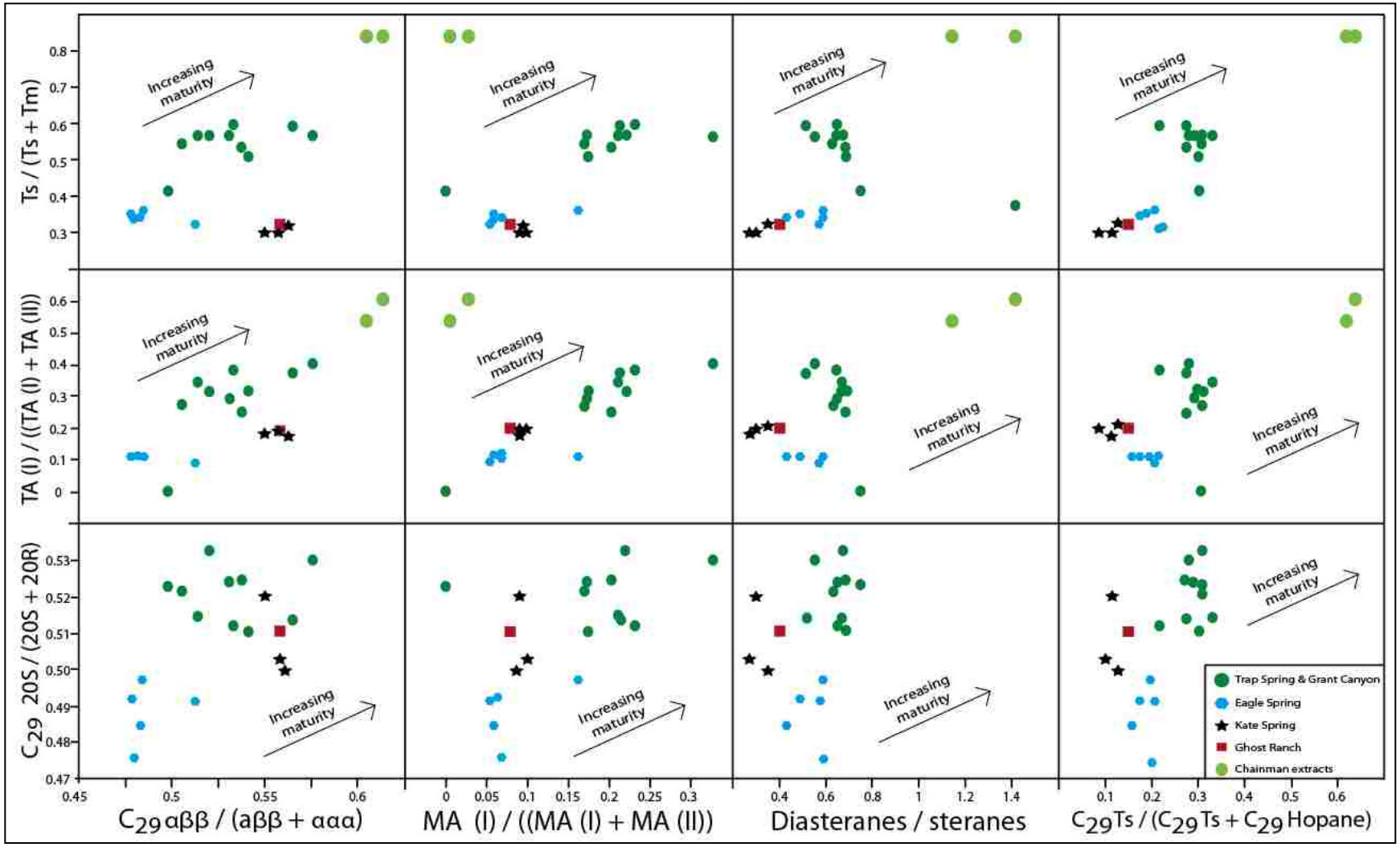

Figure 24. Cross plots of maturity related parameters. Note that all maturity related parameters show that oils from group 1 appeared to be more thermally mature than group 2 oil.

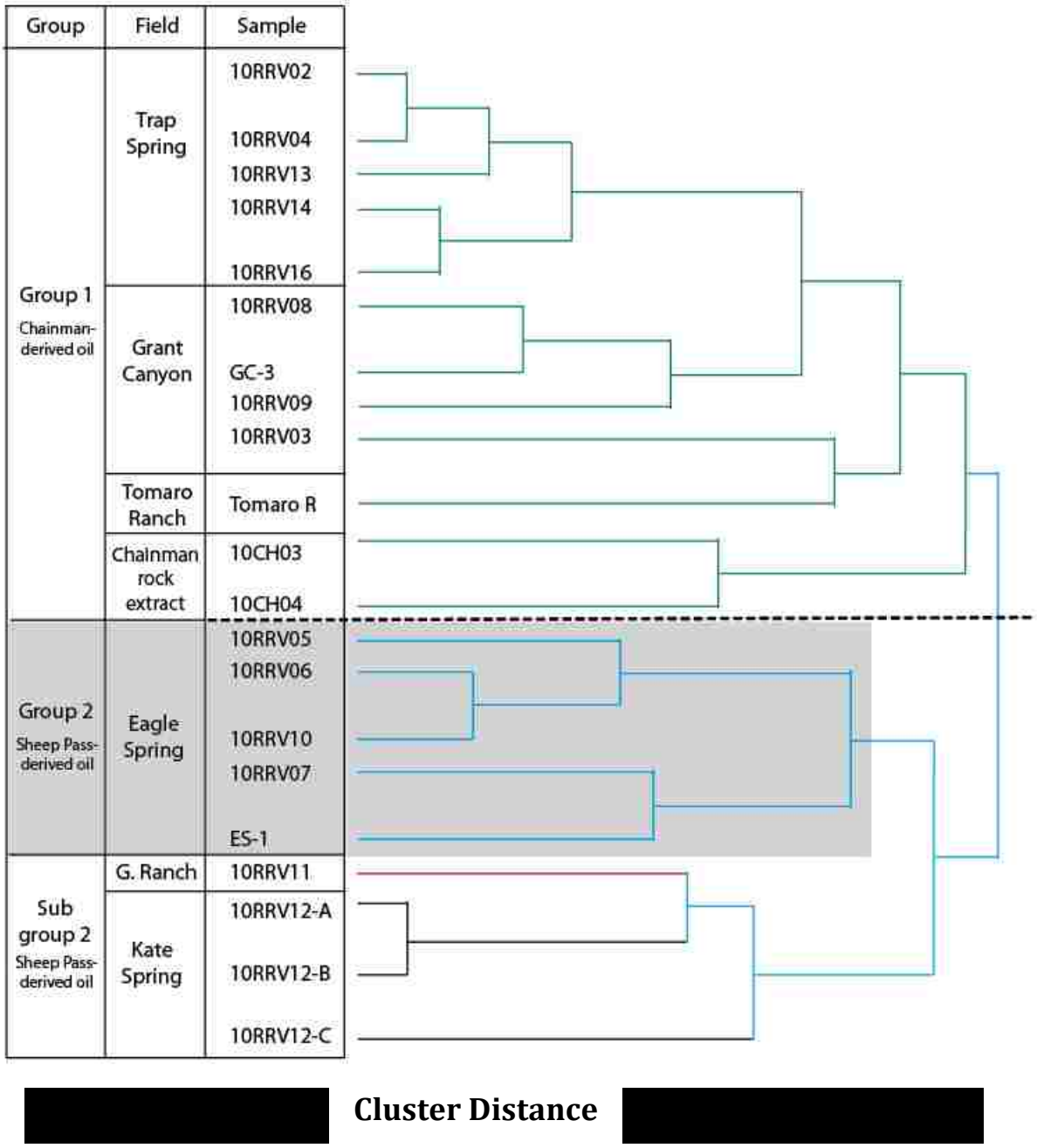

Figure 25. Dendrogram showing genetic relationship between 19 oil samples from Railroad Valley and two source rock extracts from the Chainman Shale. This dendrogram is based on statistical analysis using Ward's method. All input parameters for the cluster analysis are provided in Appendix 8. G. Ranch: Ghost Ranch.

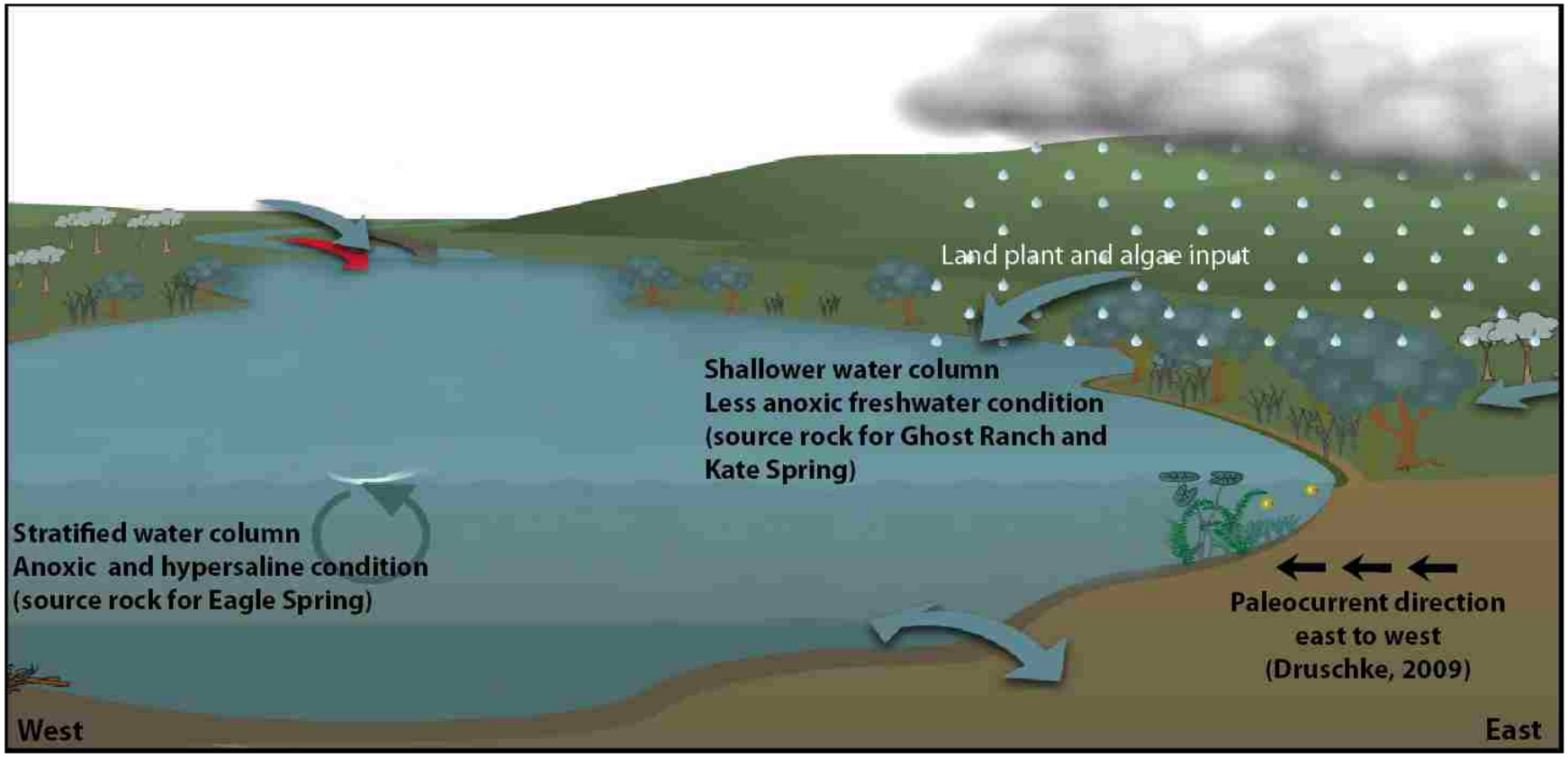

Figure 26. Depositional model of Paleogene-lacustrine Sheep Pass Formation member B source rock. This figure shows that spatial variations in lacustrine systems, such as salinity, redox, depth, temperature, and organic matter, influence the source rock facies, which in turn control the petroleum characteristics. Note that Eagle Spring oils were derived from a deeper lacustrine source facies (stratified, anoxic and hypersaline conditions) while the Kate Spring and Ghost Ranch oils originated from shallower lacustrine source facies (dysoxic and less reducing conditions). Arrows indicate land plant and algae input. Figure is modified after Department of Environment and Resource Management of Queensland (http://www.derm.qld.gov.au/).

APPENDIX 1

GC CHROMATOGRAM OF SOURCE ROCK EXTRACT

(All numbered peaks correlate to different biomarker compounds as listed in Appendix 7)

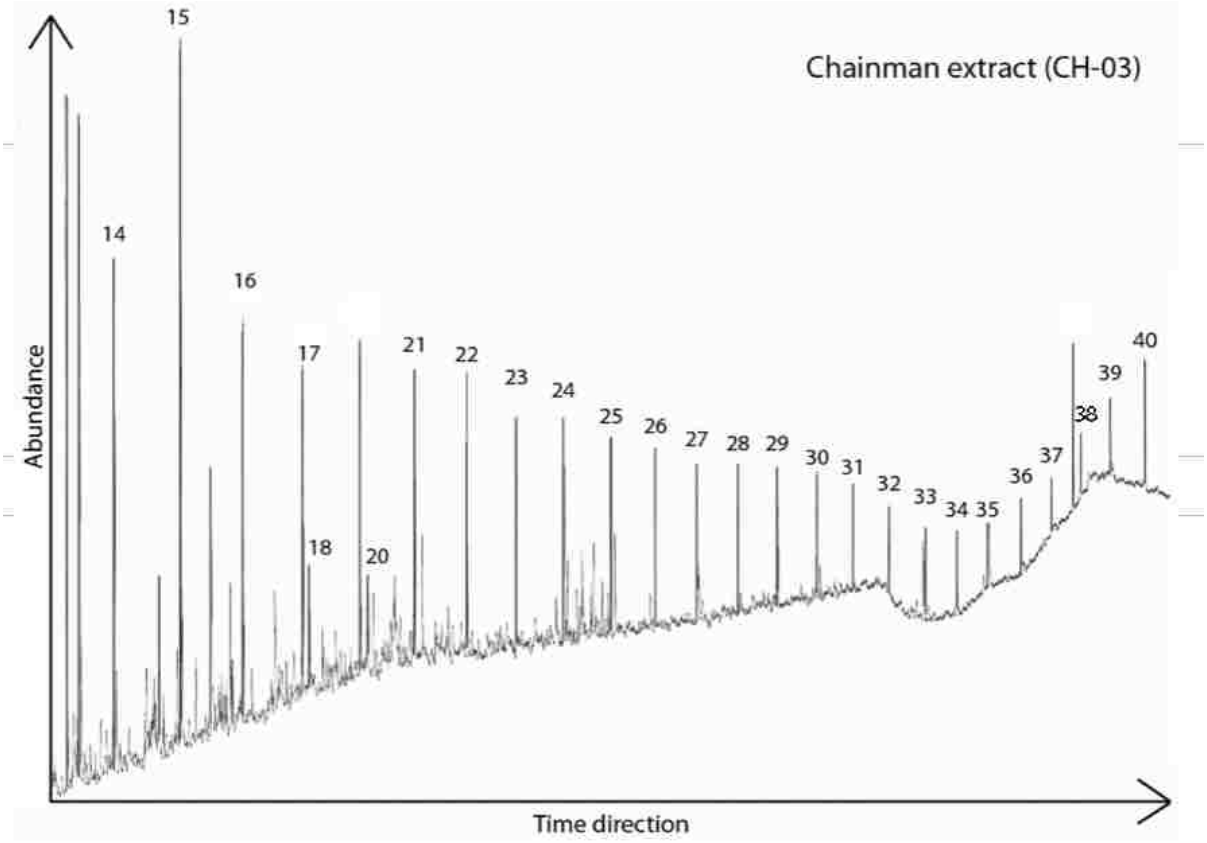

APPENDIX 2

GC-MSD CHROMATOGRAMS OF SOURCE ROCK EXTRACTS

(All numbered peaks correlate to different biomarker compounds as listed in Appendix 7)

A. m/z 191 chromatogram of CH-03

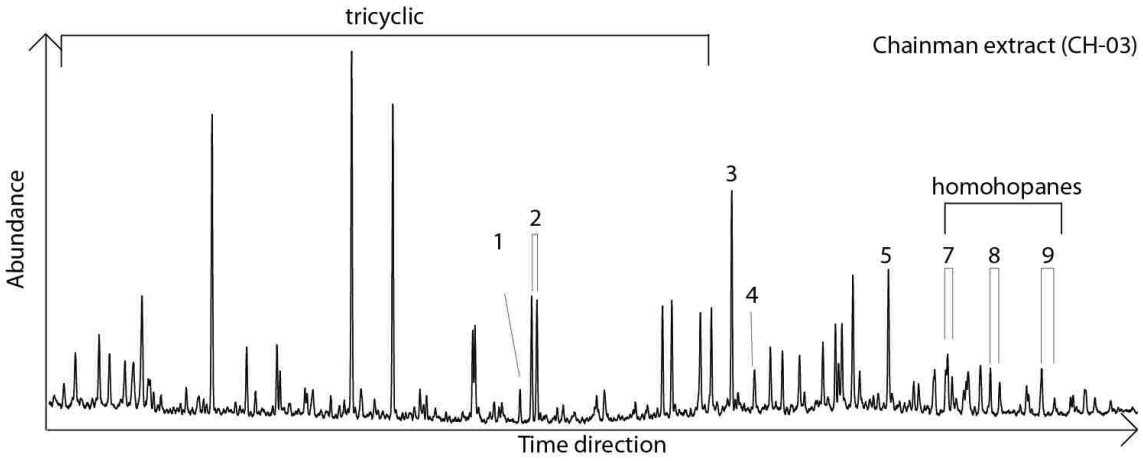

B. m/z 217 chromatogram of CH-03

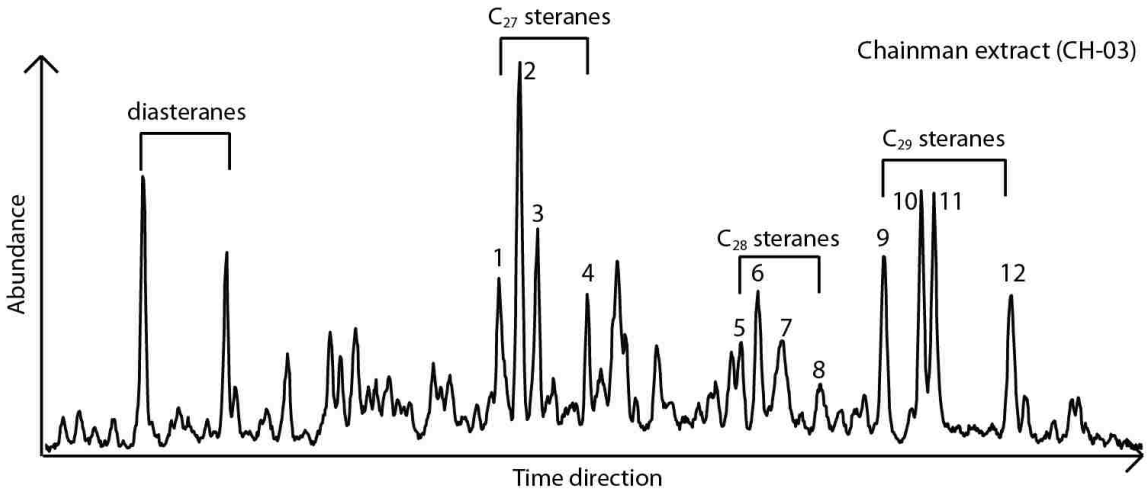

C. m/z 253 chromatogram of CH-03

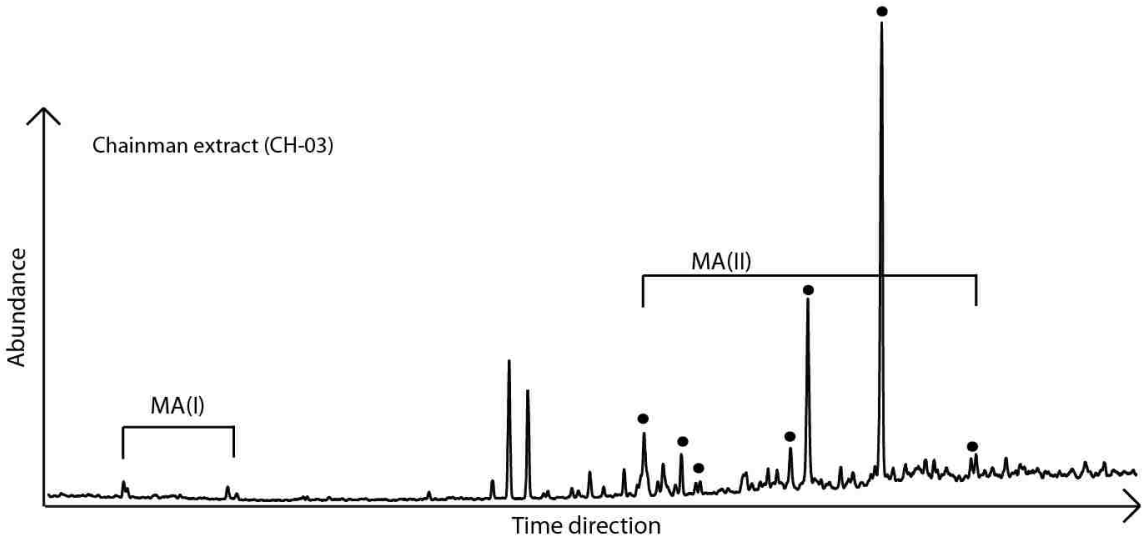

D. m/z 231 chromatogram of CH-03

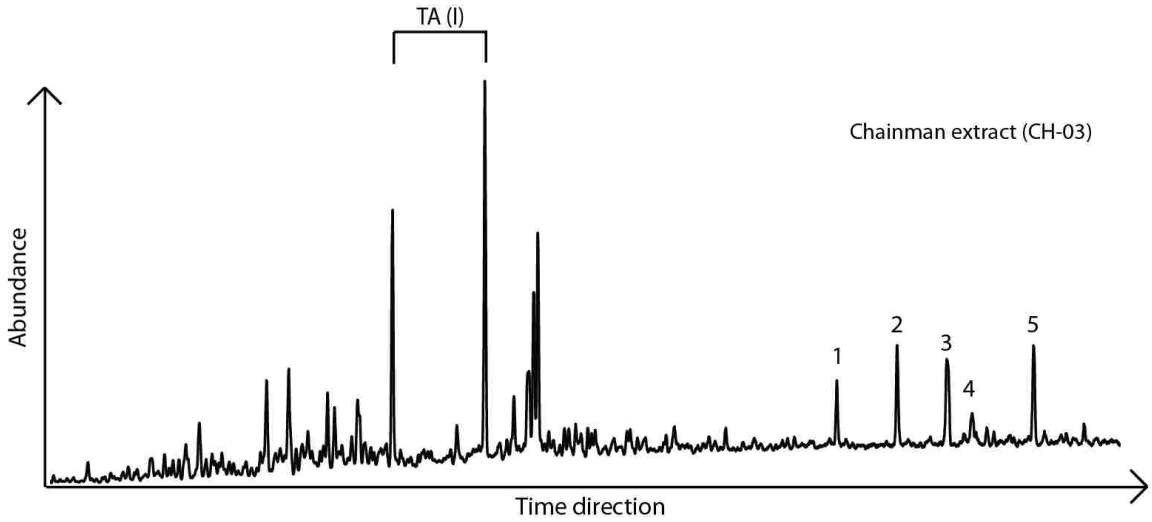

E. m/z 245 chromatogram of CH-03

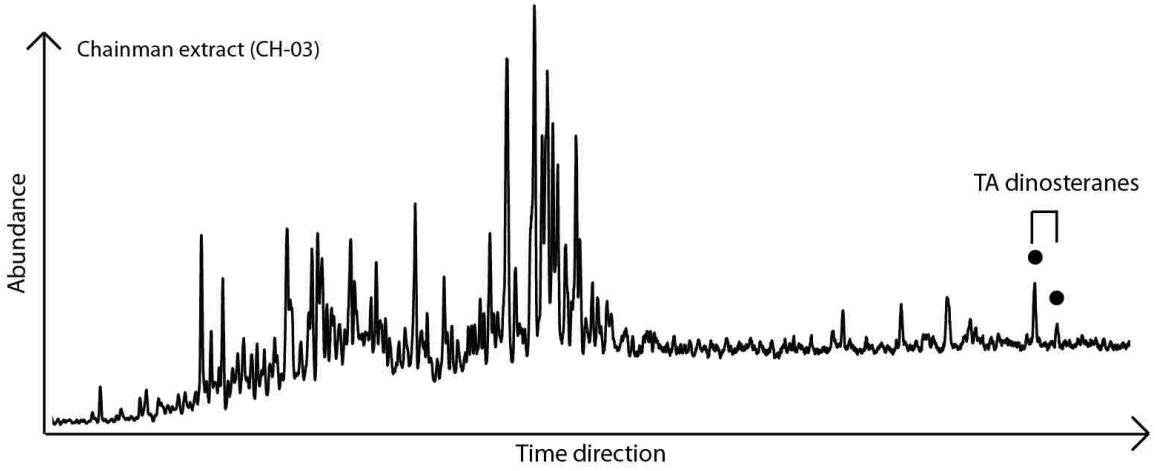

APPENDIX 3

GCMS-MRM CHROMATOGRAMS OF SOURCE ROCK EXTRACTS

(All numbered peaks correlate to different biomarker compounds as listed in Appendix 7)

F. m/z 358 → 217 chromatogram of CH-03

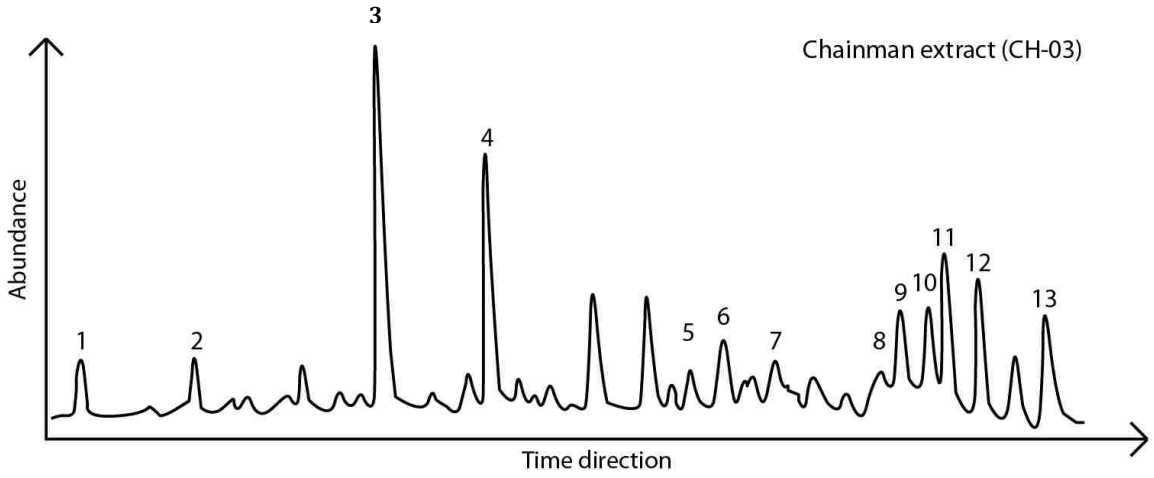

APPENDIX 4

GC CHROMATOGRAM OF OIL SAMPLES

(All numbered peaks correlate to different biomarker compounds as listed in Appendix 7)

A. GC trace of group 1 oil (Trap Spring and Grant Canyon)

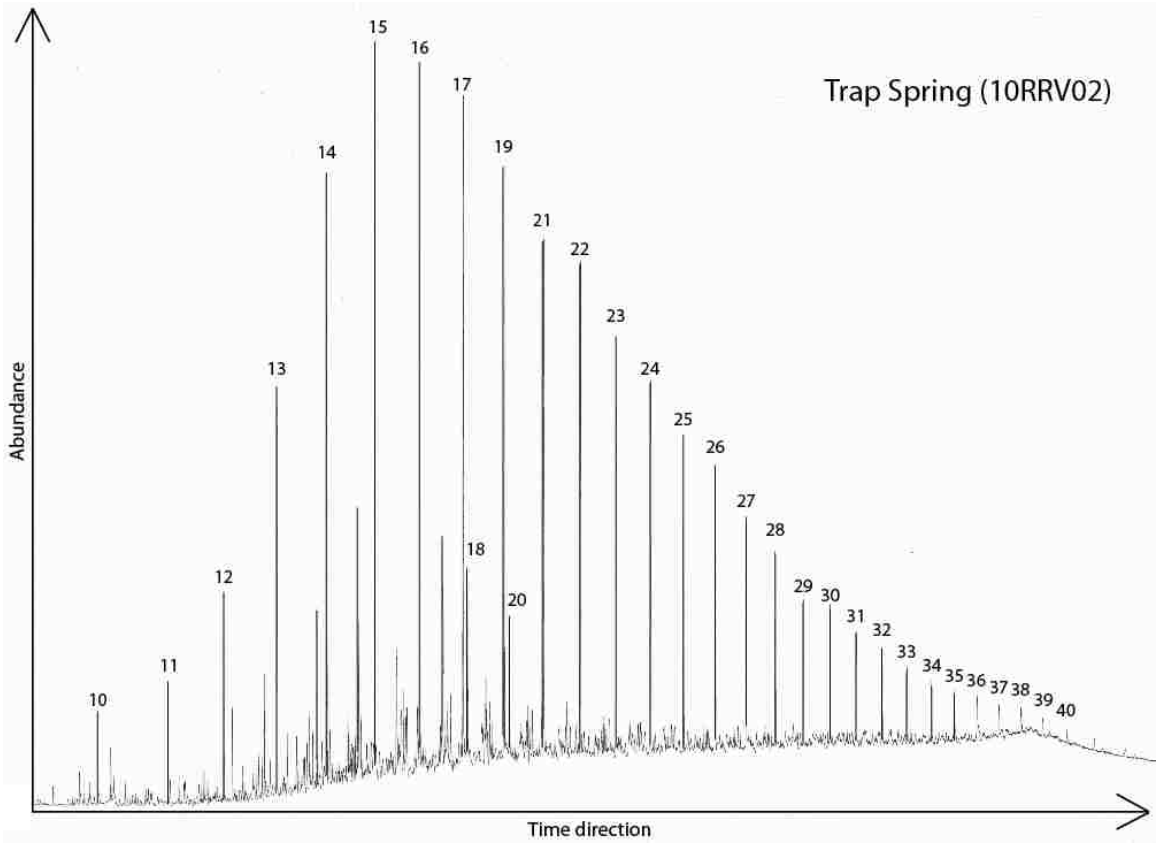

B. GC trace of group 2 oil (Eagle Spring, Kate Spring, and Ghost Ranch)

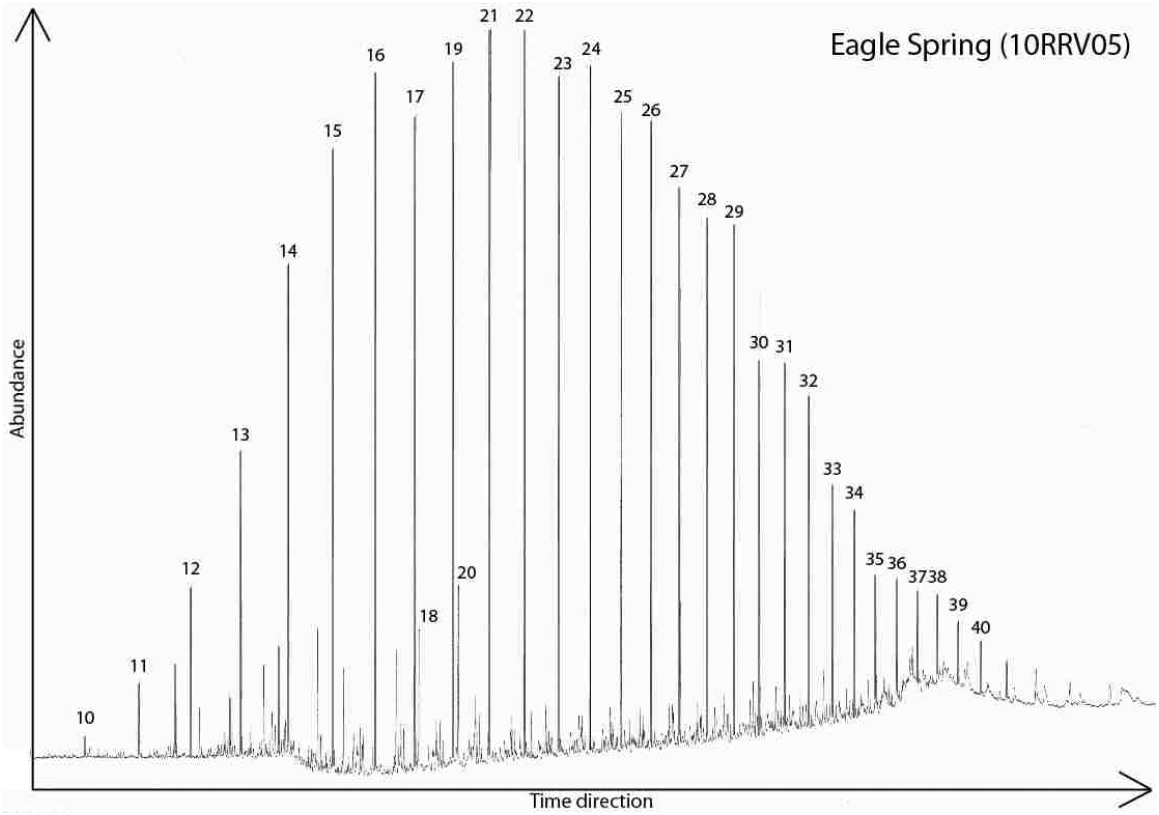

APPENDIX 5

GC-MSD CHROMATOGRAMS OF OIL SAMPLES

(All numbered peaks correlate to different biomarker compounds as listed in Appendix 7)

A.1. m/z 191 chromatogram of group 1 oil (Trap Spring and Grant Canyon)

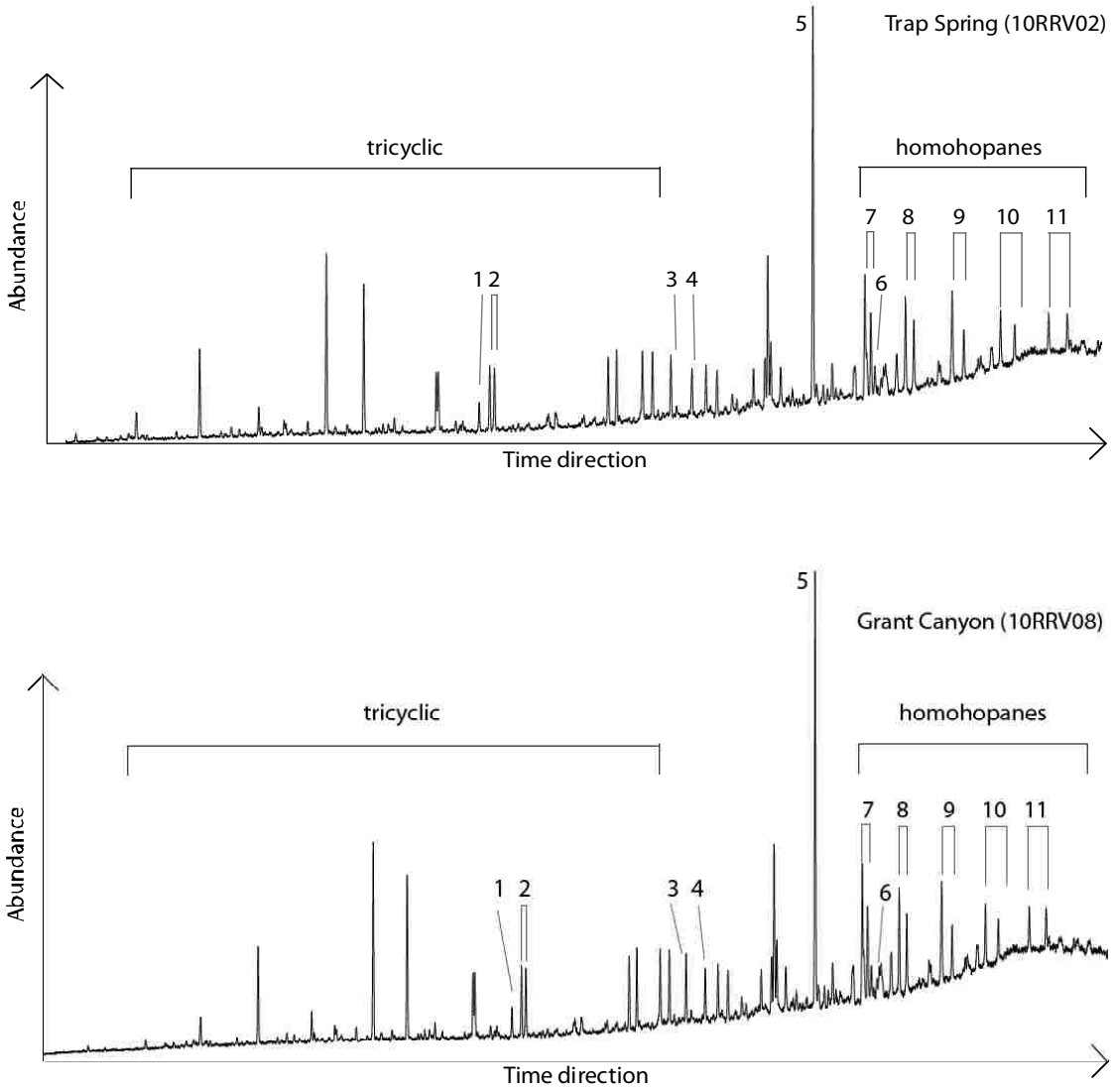

A.2. m/z 191 chromatogram of group 2 oil (Eagle Spring, Kate Spring, and Ghost Ranch)

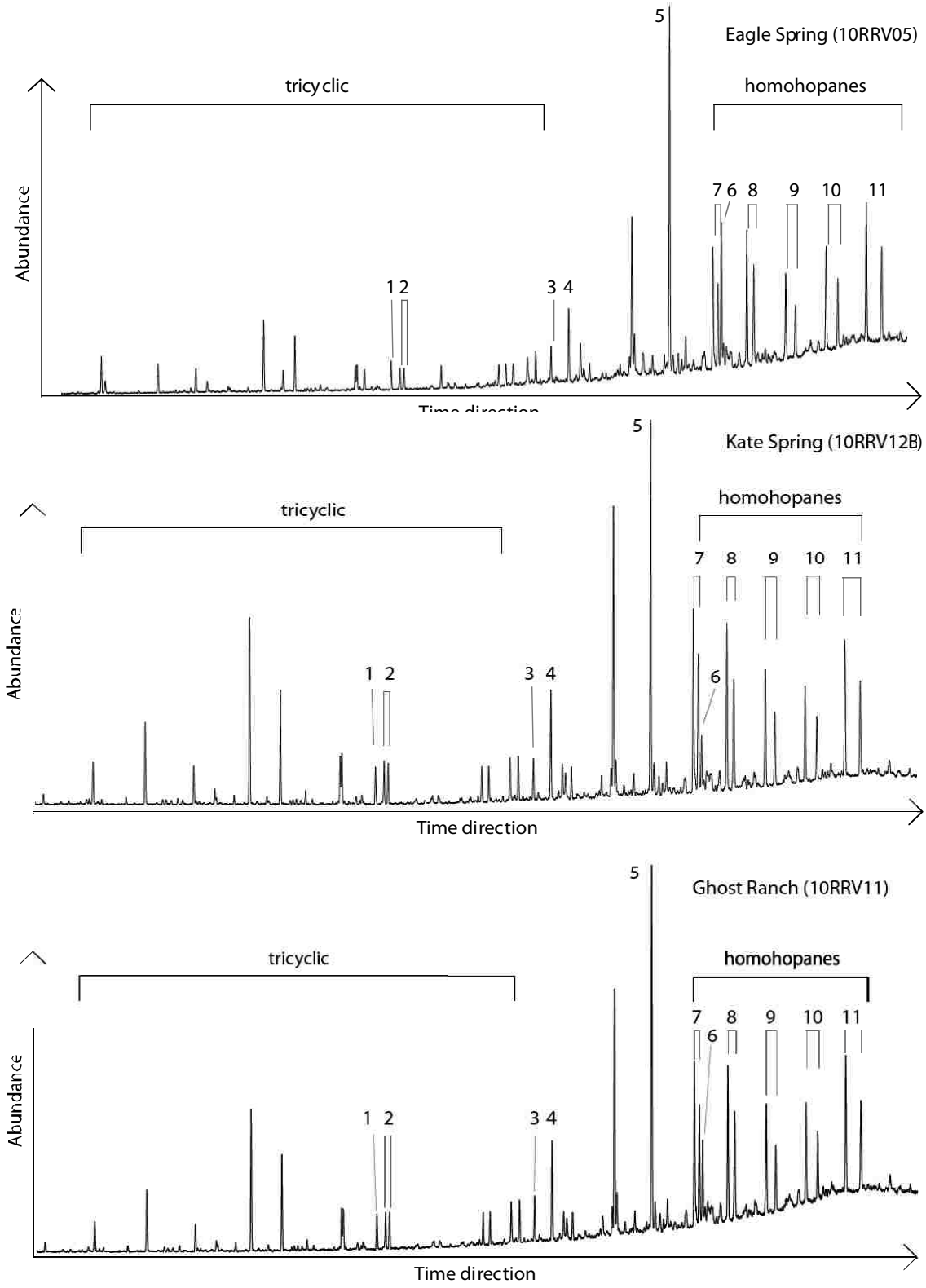

B.1. m/z 217 chromatogram of group 1 oil (Trap Spring and Grant Canyon)

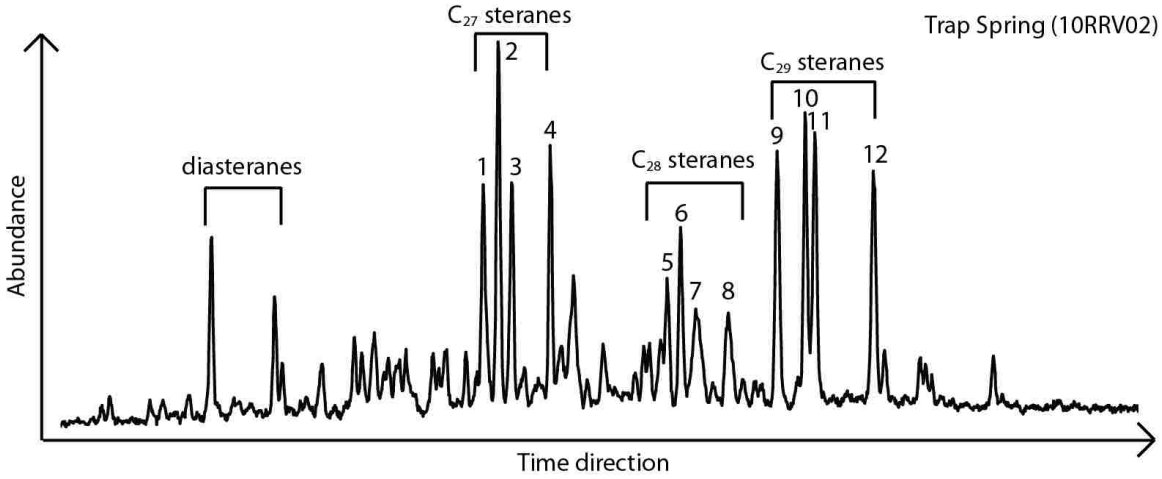

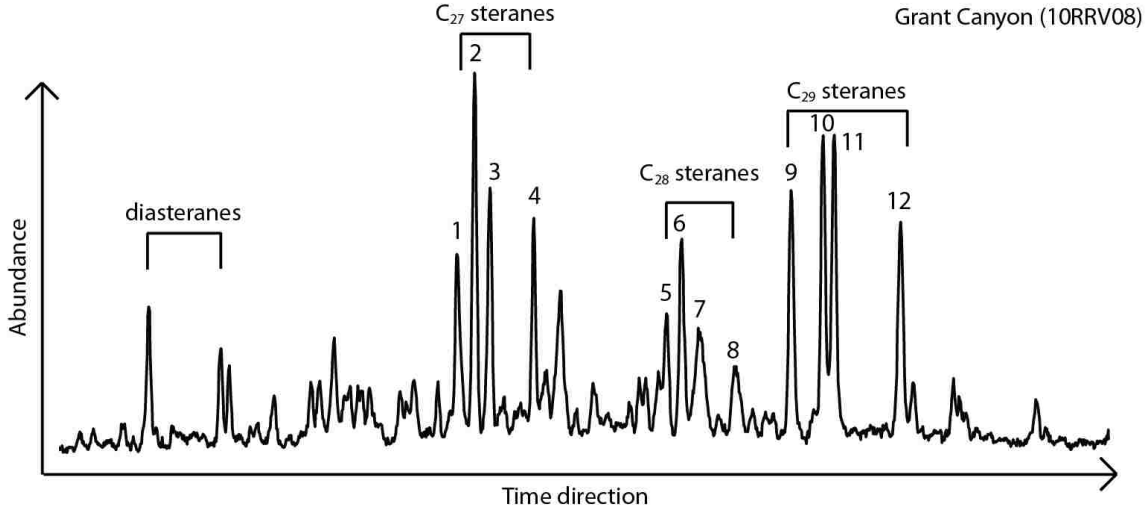

B.2. m/z 217 chromatogram of group 2 oil (Eagle Spring, Kate Spring, and Ghost Ranch)

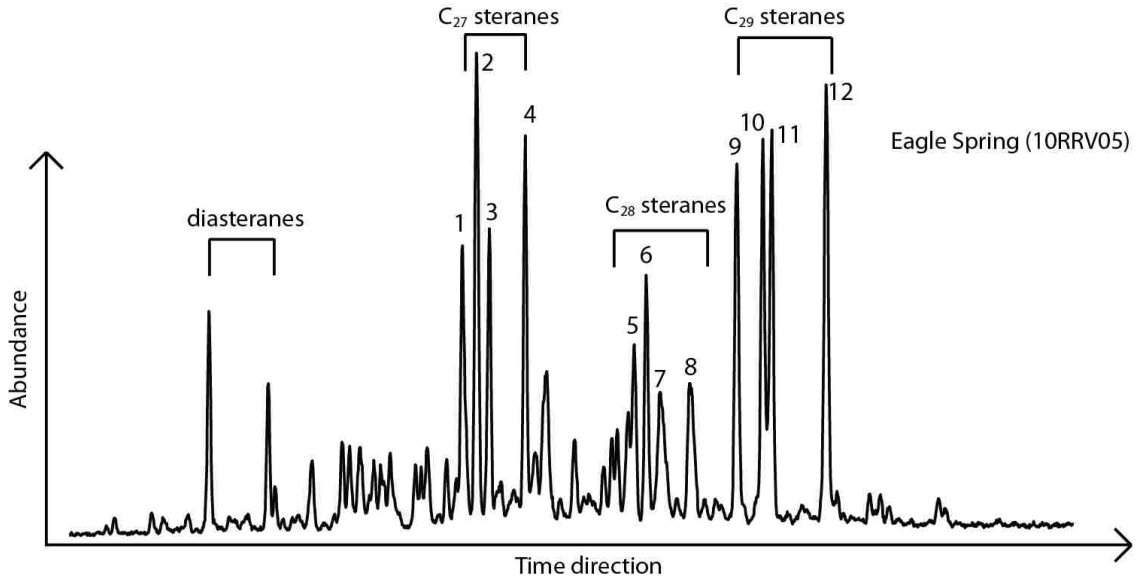

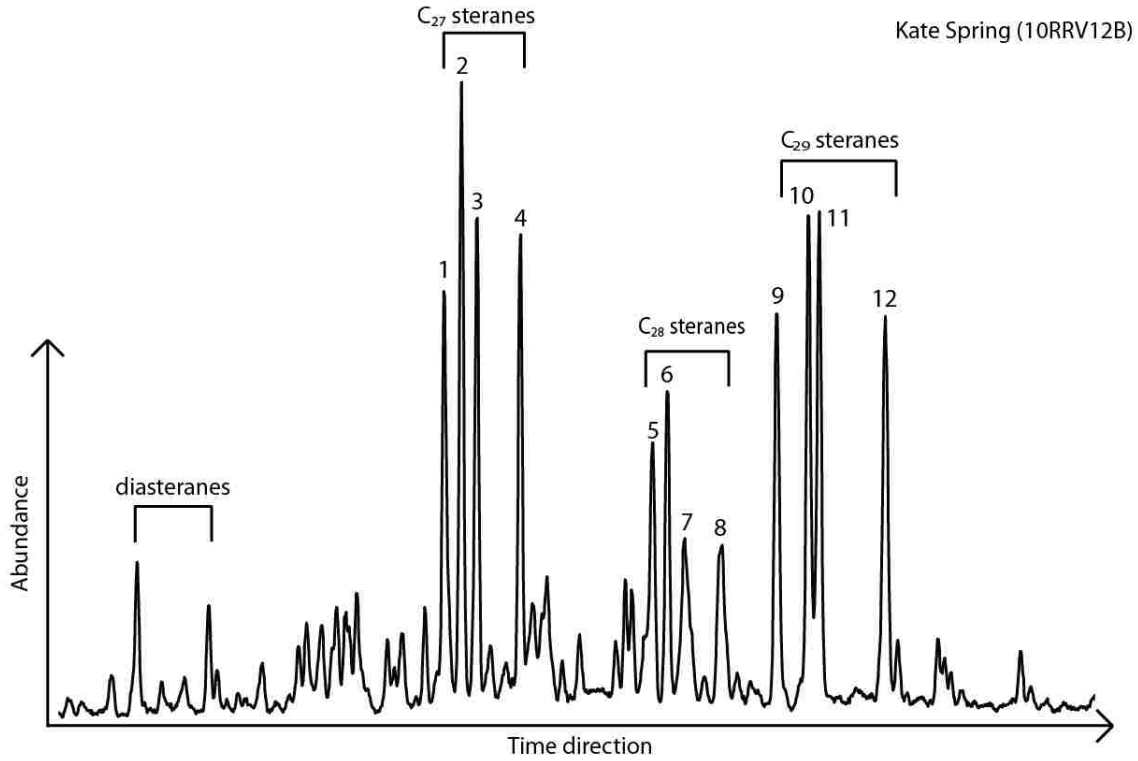

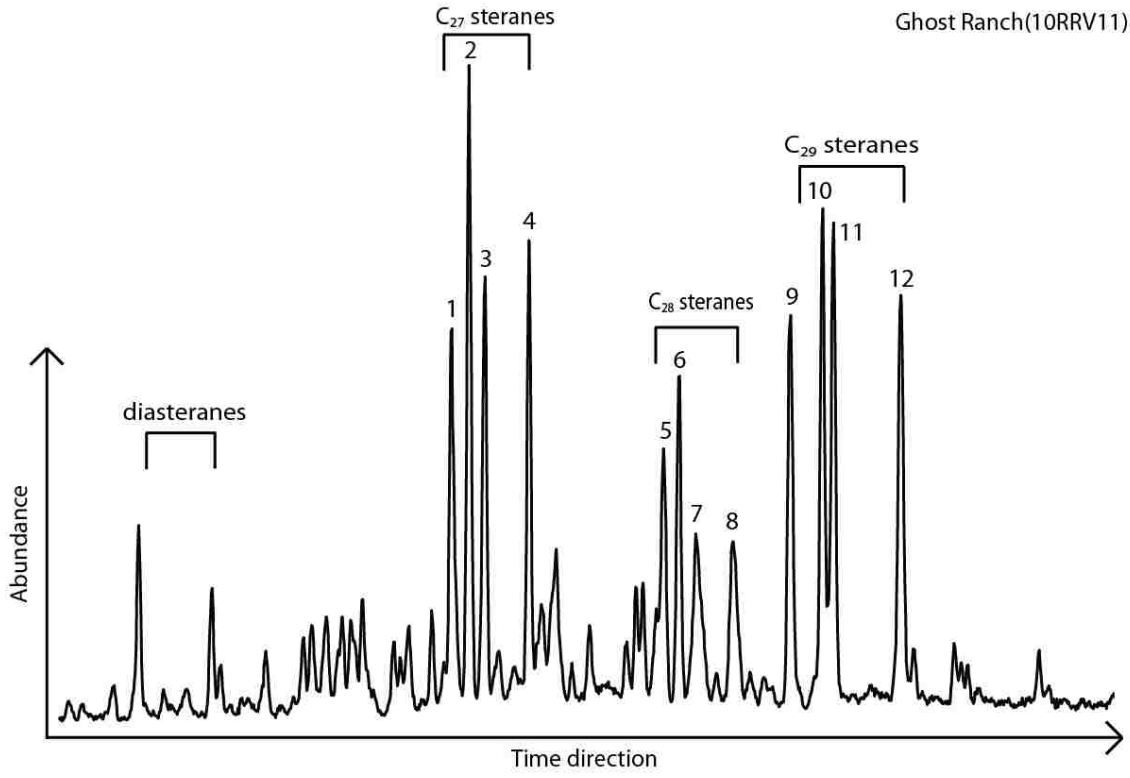
Ghost Ranch(10RRV11)
C27 steranes
2
C29 steranes
10
11
4
3
12
1
C28 steranes
9
6
diasteranes
5
7
8
Abundance
Time direction

C.1. m/z 231 chromatogram of group 1 oil (Trap Spring and Grant Canyon)

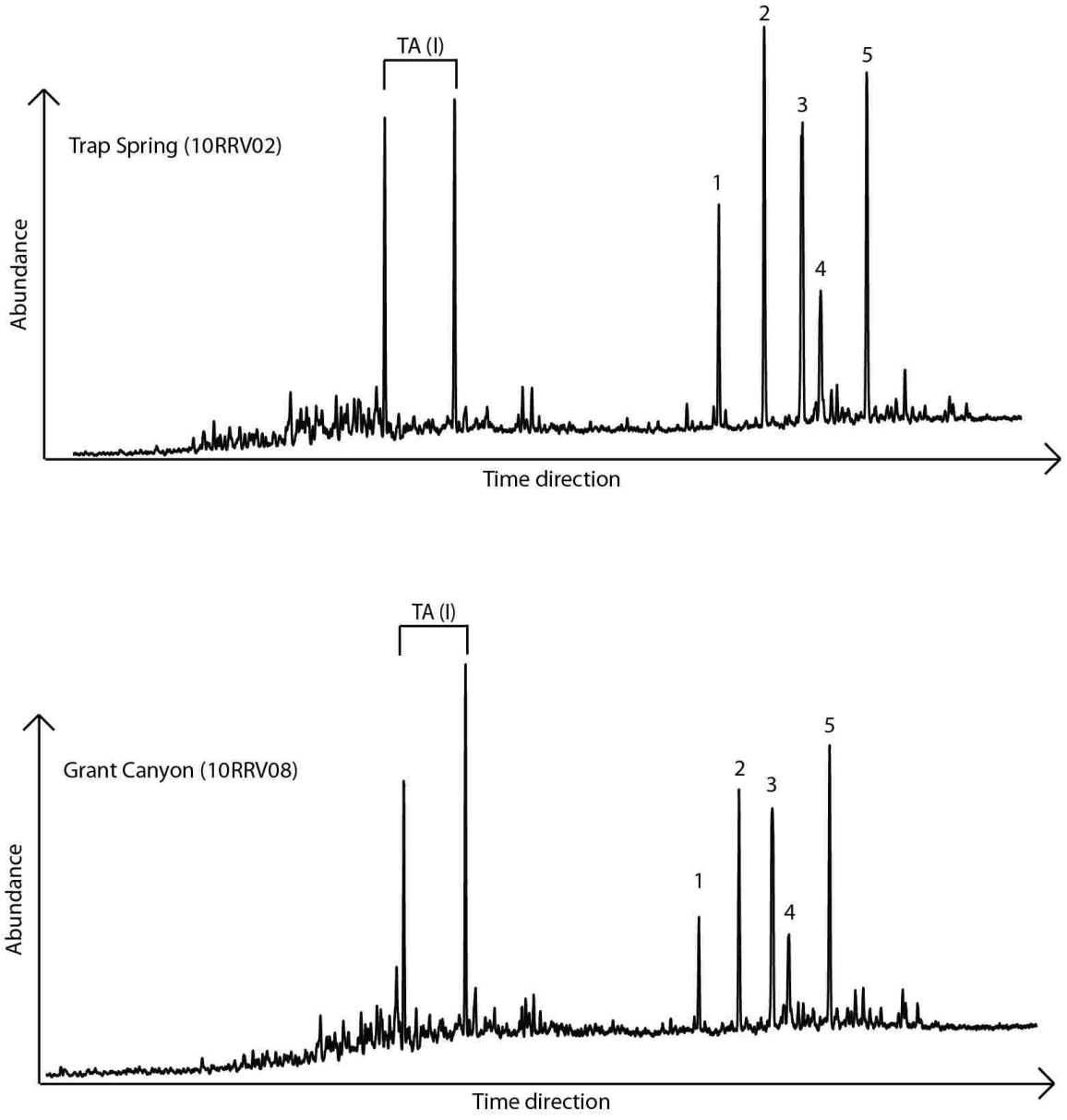

C.2. m/z 231 chromatogram of group 2 oil (Eagle Spring, Kate Spring, and Ghost Ranch)

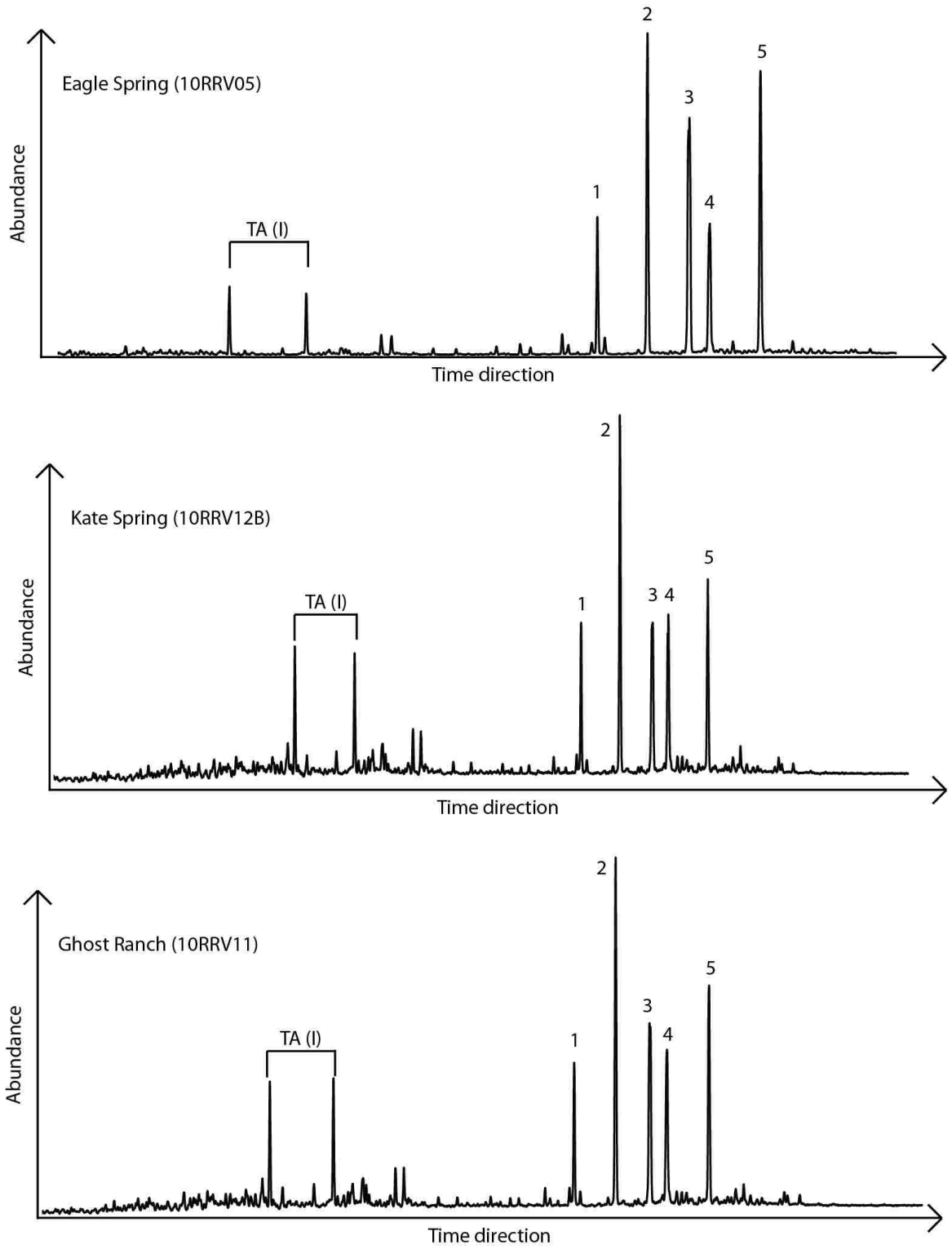

D.1. m/z 253 chromatogram of group 1 oil (Trap Spring and Grant Canyon)

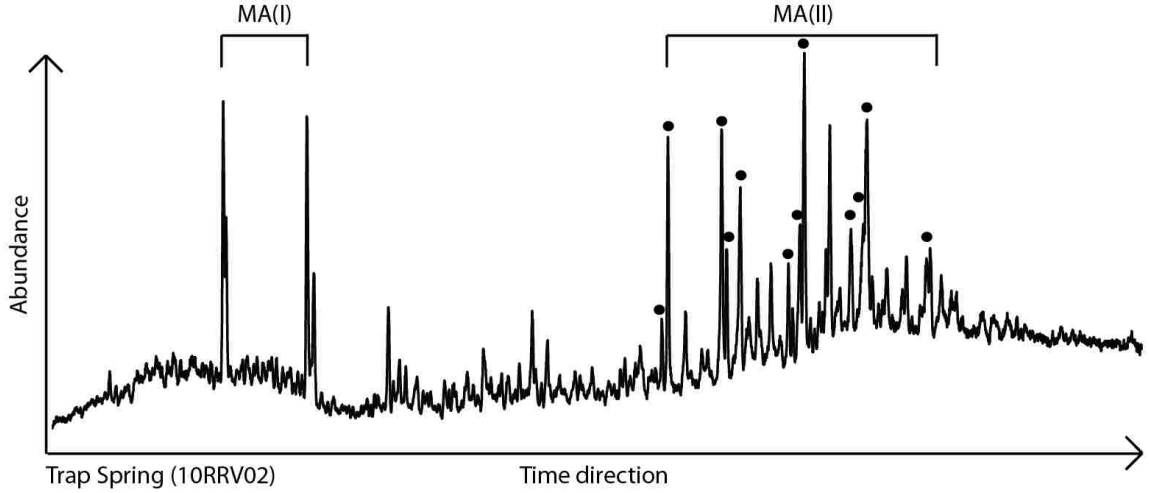

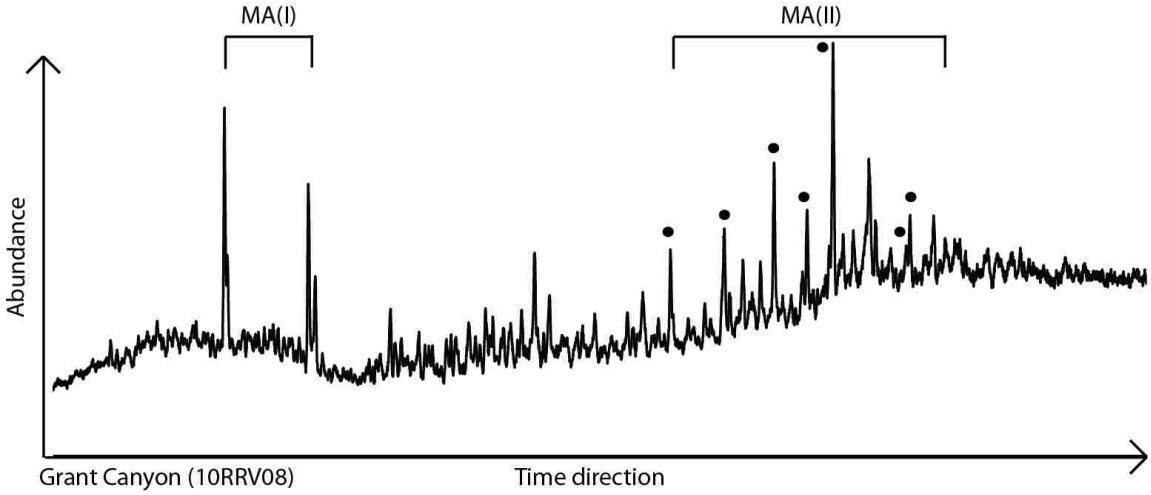

D.2. m/z 253 chromatogram of group 2 oil (Eagle Spring, Kate Spring, and Ghost Ranch)

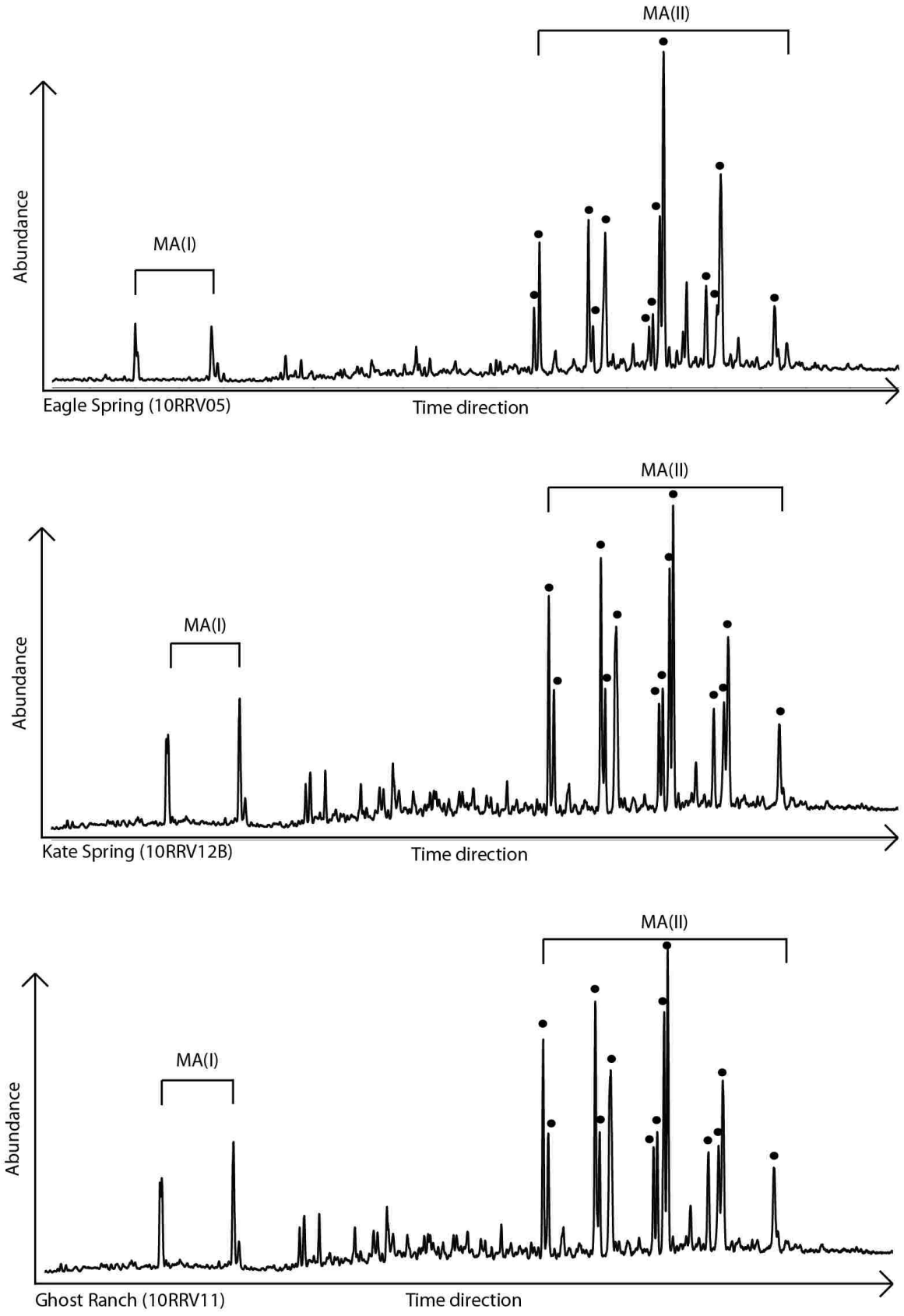

E.1. m/z 245 chromatogram of group 1 oil (Trap Spring and Grant Canyon)

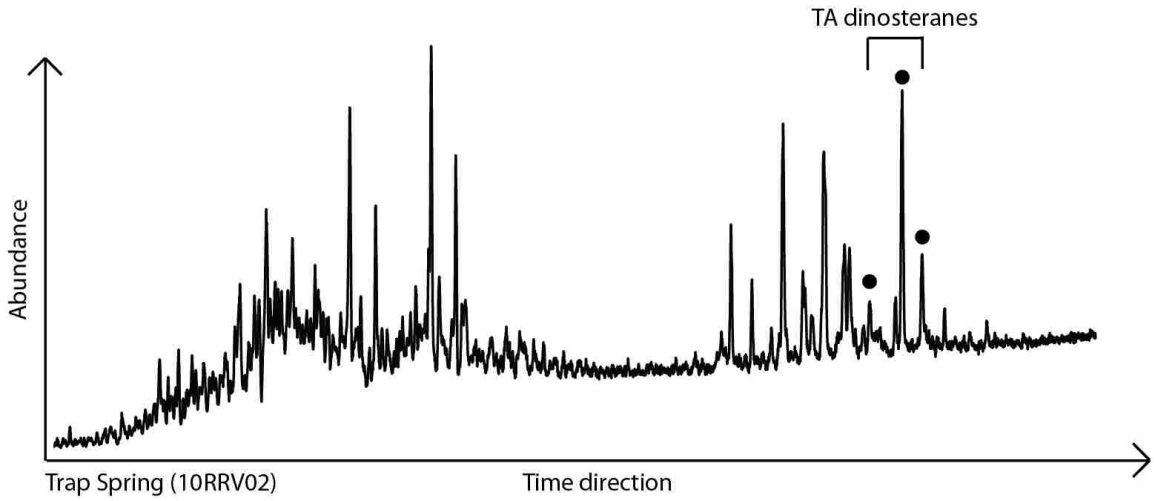

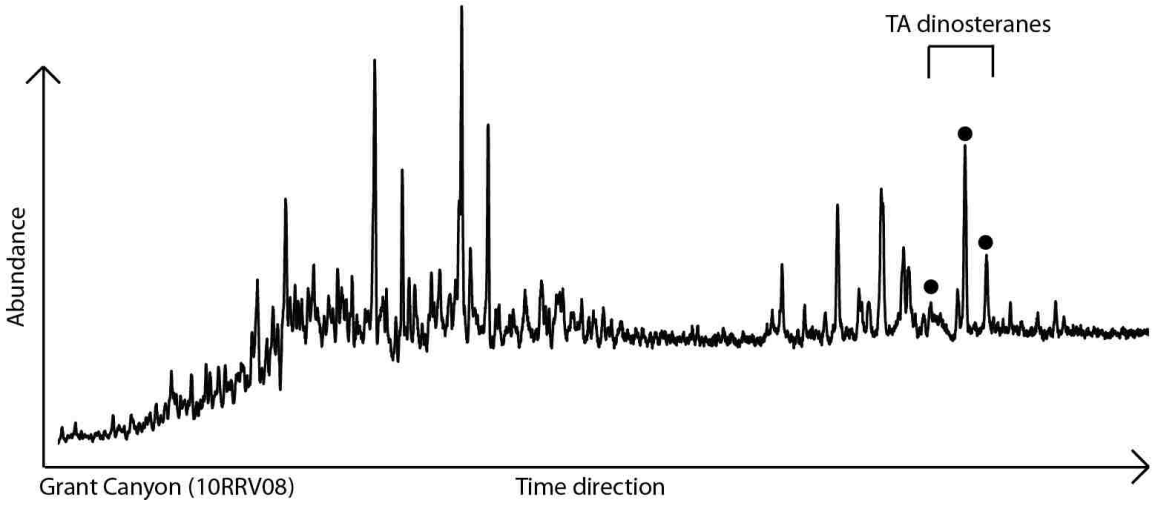

E.2. m/z 245 chromatogram of group 2 oil (Eagle Spring, Kate Spring, and Ghost Ranch)

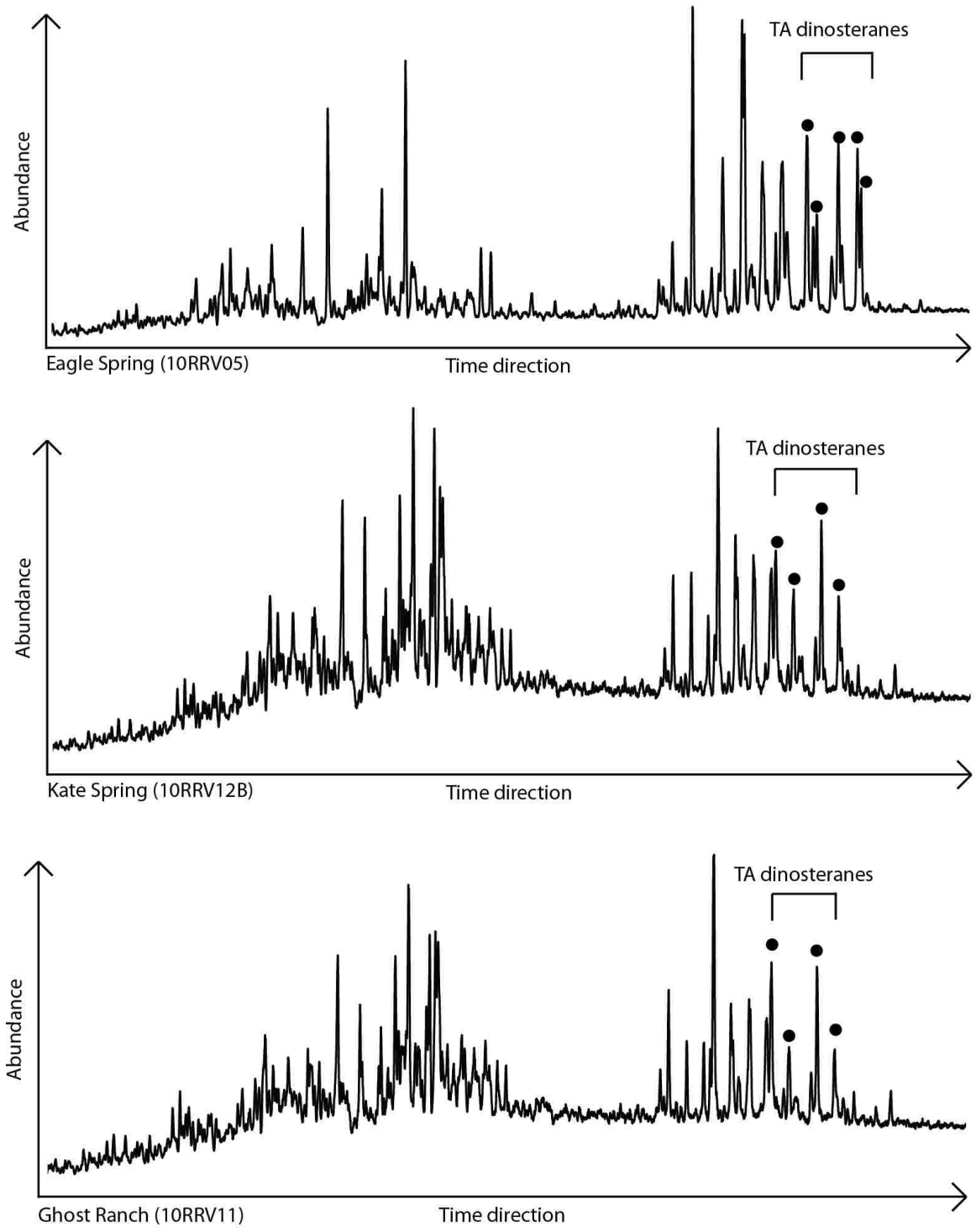

APPENDIX 6

GCMS-MRM CHROMATOGRAMS OF REPRESENTATIVE OIL SAMPLES

(All numbered peaks correlate to different biomarker compounds as listed in Appendix 7)

A. m/z 358 → 217 chromatogram of group 1 oil (Trap Spring)

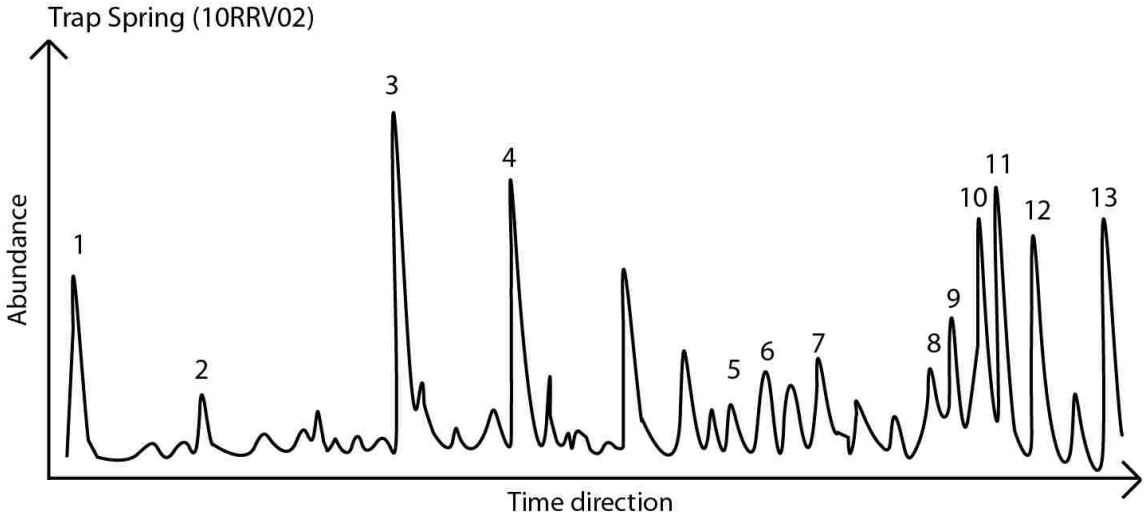

B. m/z 358 → 217 chromatogram of group 2 oil (Eagle Spring)

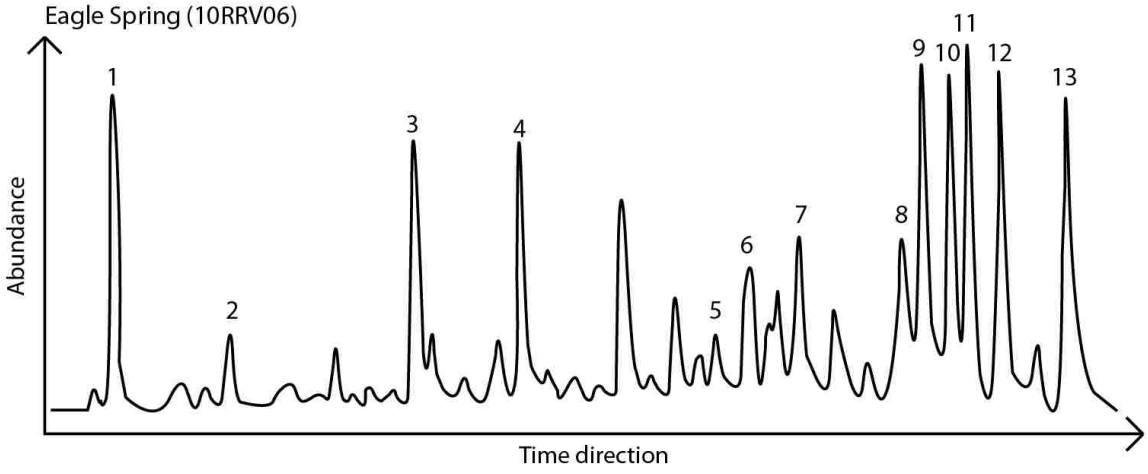

APPENDIX 7

KEY FOR PEAK NUMBERS USED TO IDENTIFY PEAKS

ON THE CHROMATOGRAMS

A. Peaks in the GC trace

10 : $n-C_{10}$	21 : $n-C_{19}$	32 : $n-C_{30}$
11 : $n-C_{11}$	22 : $n-C_{20}$	33 : $n-C_{31}$
12 : $n-C_{12}$	23 : $n-C_{21}$	34 : $n-C_{32}$
13 : $n-C_{13}$	24 : $n-C_{22}$	35 : $n-C_{33}$
14 : $n-C_{14}$	25 : $n-C_{23}$	36 : $n-C_{34}$
15 : $n-C_{15}$	26 : $n-C_{24}$	37 : $n-C_{35}$
16 : $n-C_{16}$	27 : $n-C_{25}$	38 : $n-C_{36}$
17 : $n-C_{17}$	28 : $n-C_{26}$	39 : $n-C_{37}$
18 : Pristane (Pr)	29 : $n-C_{27}$	40 : $n-C_{38}$
19 : $n-C_{18}$	30 : $n-C_{28}$	
20 : Phytane (Ph)	31 : $n-C_{29}$	

B. Peaks in the m/z 191 chromatogram

1 : C_{24} tetracyclic terpane

2 : C_{26} tricyclic terpane (S+R)

3 : Ts 18α (H)-trisnorhopane

4 : Tm 17α (H)-trisnorhopane

5 : C_{30} 17α (H)-hopane

6 : Gammacerane

7 : C_{31} homohopane

8 : C_{32} homohopane

9 : C_{33} homohopane

10 : C_{34} homohopane

11 : C_{35} homohopane

C. Peaks in the m/z 217 chromatogram

1 : C_{27} ααα 20S

2 : C_{27} αββ 20R

3 : C_{27} αββ 20S

4 : C_{27} ααα 20R

5 : C_{28} ααα 20S

6 : C_{28} αββ 20R

7 : C_{28} αββ 20S

8 : C_{28} ααα 20R

9 : C_{29} ααα 20S

10 : C_{29} αββ 20R

11 : C_{29} αββ 20S

12 : C_{29} ααα 20R

D. Peaks in the m/z 217 chromatogram

TA (I) : Triaromatic steroid (C_{20} pregnane + C_{21} 20-methylpregnane)

TA (II) :

1 : C_{26} cholestane 20S

2 : C_{26} + C_{27} cholestane 20R + ergostane 20S

3 : C_{28} stigmastane 20S

4 : C_{27} ergostane 20R

5 : C_{28} stigmastane 20R

E. Peaks in the m/z 358 → 217 chromatogram

1 : C_{26} 24-nordiacholestanes 20S

2 : C_{26} 24-nordiacholestanes 20R

3 : C_{26} 27-nordiacholestanes 20S

4 : C_{26} 27-nordiacholestanes 20R

5 : C_{26} ααα 24-norcholestanes 20S

6 : C_{26} αββ 24-norcholestanes 20R

7 : C_{26} αββ 24-norcholestanes 20S

8 : C_{26} ααα 24-norcholestanes 20R

9 : C_{26} 21-norcholestanes ααα + αββ

10 : C_{26} ααα 27-norcholestanes 20S

11 : C_{26} αββ 27-norcholestanes 20R

12 : C_{26} αββ 27-norcholestanes 20S

13 : C_{26} ααα 27-norcholestanes 20R

APPENDIX 8

INPUT PARAMETERS FOR THE CLUSTER ANALYSIS

1. Pr/Ph
2. OEP 5
3. Tricyclic / hopane
4. C_{24} tetracyclic / C_{26} tricyclic
5. Ts / (Ts+Tm)
6. Oleanane
7. Diahopane / (diahopane + C_{29})
8. Diahopane / (diahopane + C_{30})
9. C_{29} Ts / (C_{29}Ts + C_{29})
10. Moretane / hopane
11. Gammacerane
12. Homohopane
13. Diasteranes / steranes
14. C_{26} 21, 24, 27-norcholestance
15. C_{27} steranes
16. C_{30} diasteranes
17. TPP ratio
18. TA dinosteranes
19. C_{28} Triaromatic
20. C_{27} / C_{28}S Triaromatic
21. MA (I) / (MA (I) + MA (II)) and TA (I) / (TA (I) + TA (II))

Table 1. List of oil samples

No	Sample Number	Well name	Coordinates	Production interval (Formation and depth); Cumulative Production (Barrels) (2006)	Field; Operator; Status (2006);
1	LA - 02	Munson Ranch #13-14	N 38^0 38' 10.0"	(1) Oligocene Pritchard Station	**Trap Spring (MR);**
			W 115^0 37' 44.3"	3,210 - 4,950 feet; Average: 4,005 ft	Makoil
2	LA - 03	Munson Ranch #14-44	N 38^0 38' 07.7"	API: 24.8	33 producers,
			W 115^0 38' 14.9"	13,752,356 barrels	10 shut-in,1 P&A
3	LA - 04	Munson Ranch #13-45	N 38^0 38' 23.4"		
			W 115^0 37' 43.7"		
4	LA - 13	Zuspam 24-3	N 38^0 37' 41.4"		
			W 115^0 37' 40.4"		
5	LA - 14	Munson Ranch 13-24	N 38^0 38' 06.4"		
			W 115^0 37' 52.0"		
6	LA - 15	Trap Spring #19	N 38^0 37' 38.8"		
			W 115^0 38' 46.8"		
7	LA - 05	Eagle Spring 73-35	N 38^0 34' 59.7"	(2) Oligocene Garret Ranch Group	**Eagle Spring**
			W 115^0 31' 41.4"	(3) Eocene Sheep Pass Fm	Meritage Energy

8	LA - 06	Eagle Spring 74-35	N 38^0 35' 41.3"	(4) Pennsylvanian Ely limestone	15 producers,
			W 115^0 31' 39.3"		6 shut-in, 1injection
9	LA - 07	Eagle Spring 23-36	N 38^0 37' 47.3"	5,780 - 7,360 feet; Average: 6,508 ft	
			W 115^0 31' 10.4"	API: 30.8 - 27.8	
10	LA - 10	Eagle Spring	-	5,218,259 barrels	
11	ES - 1	Eagle Spring #1	-		
12	LA - 11	Ghost Ranch	-	(5) Neogene Horse Camp Fm Breccia	**Ghost Ranch**; Meritage
				API: 22.5; 502,023 barrels	4 producers, 1 shut-in
13	LA - 12A	Kate Spring #1	N 38^0 34' 42.5"	(5) Neogene Horse Camp Fm Breccia	**Kate Spring**
14	LA - 12B		W 115^0 32' 26.7"	API: 22.5; 502,023 barrels	Western General
15	LA - 12C				4 producers, 2 shut-in
16	LA - 08	Grant Canyon #7	N 38^0 27' 27.5"	(6) Devonian Simonson Fm	**Grant Canyon**
			W 115^0 34' 39.1"	and Guilmette Fm	Grant Canyon O&G
17	LA - 09	Grant Canyon #9	N 38^0 27' 23.6"	4,374 - 4,426 feet; Average: 3,979 ft	2 producers, 4 shut-in
			W 115^0 34' 44.5"	20,938,790 barrels	
18	GC - 3	Grant Canyon #3	-		
19	TR	Foreland-Southern Pacific Land Co. No. 1-5	-	(7) Oligocene Indian Well Fm	**Tomera Ranch**; Dixie Co,
				1,150 - 1,950 feet; Average: 1,670 ft; 36,4	2 shut-in, 1 P&A, 1 injection

Table 2. Total organic carbon, Rock Eval Pyrolysis, vitrinite reflectance, and thermal alteration index results for source rock samples

Region	Age	Formation	Lithology	Sample Name	Location		Elevation (m)	Leco TOC	RE			Tmax (°C)	**	Ro %	TAI	HI	OI	S2/S3	S1/TOC *100	PI
					Latitude	Longitude			S1	S2	S3									
Egan Range	Paleo-gene	Sheep Pass Fm member B	Mud-supported carbonate	10SP06	N38^{0}44'18.1"	N114^{0}57'36.5"	2102	-	-	-	-	-	-	0.46	2 to 2+	-	-	-	-	-
				10SP05	N38^{0}44'18.7"	N114^{0}57'37.5"	2091	0.19	0.04	0.27	0.29	438	**			146	157	0.9	22	0.13
				10SP07	N38^{0}44'18.1"	N114^{0}57'36.5"	2102	0.07	0.02	0.12	0.23	441	**			171	329	0.5	29	0.14
				10SP08	N38^{0}44'17.5"	N114^{0}57'35.8"	2121	0.06	0.02	0.11	0.35	487	**			180	574	0.3	33	0.15
				10SP09	N38^{0}44'17.3"	N114^{0}57'34.8"	2114	0.24	0.06	1.09	1.08	436				447	443	1.0	25	0.05
				10SP10	N38^{0}44'17.0"	N114^{0}57'34.5"	2125	0.06	0.02	0.10	0.21	445	**			169	356	0.5	34	0.17
				10SP11	N38^{0}44'16.7"	N114^{0}57'33.8"	2119	0.05	0.02	0.13	0.22	442	**			289	489	0.6	44	0.13
				10SP12	N38^{0}44'16.4"	N114^{0}57'33.5"	2122	0.17	0.02	0.27	0.45	438	**			163	271	0.6	12	0.07
				10SP13	N38^{0}44'16.1"	N114^{0}57'32.0"	2118	0.20	0.03	0.37	0.44	436	**			189	224	0.8	15	0.07
				10SP14	N38^{0}44'16.1"	N114^{0}58'30.0"	2114	0.12	0.02	0.21	0.25	447	**			174	207	0.8	17	0.09
				10SP15	N38^{0}44'17.7"	N114^{0}57'22.3"	2098	0.05	0.01	0.13	0.31	443	**			283	674	0.4	22	0.07
	Missis-sippian	Chainman Shale	Shale	10CH01	N38^{0}44'04.3"	N114^{0}58'37.7"	1960	1.10	0.02	0.14	0.28	455	**	0.90	2+/2+ to 3	13	25	0.5	2	0.13
				10CH02	N38^{0}44'10.3"	N114^{0}58'31.0"	2008	0.79	0.03	0.07	0.62	453	**	1.01	2+/2+ to 3	9	78	0.1	4	0.30
				10CH03	N38^{0}44'39.7"	N114^{0}58'09.4"	2108	2.60	0.05	2.31	1.13	442		0.68	4.00	89	43	2.0	2	0.02
				10CH04	N38^{0}44'39.2"	N114^{0}58'09.6"	2108	4.31	0.18	5.00	1.37	444		0.72	4.00	116	32	3.6	4	0.03

Notes:

TOC : Total Organic Carbon, wt%

S1 : Volatile hydrocarbon (HC) content, mg HC/g rock

S2 : Remaining HC generative potential, mg HC/g rock

S3 : Carbon dioxide content, mg CO_2/g rock

** : Low S2, Tmax is unreliable

%Ro : Measured vitrinite reflectance

HI : Hydrogen Index = S2 x 100 / TOC, mg HC/ g TOC

OI : Oxygen Index = S3 x 100 / TOC, mg CO2/ g TOC

TAI : Thermal Alteration Index

PI : Production index = S1/ (S1+S2)

Table 3. Stable carbon isotope values of source rock samples

ID#1	ID#2	ID#3	Wt (mg)	Amp(V) C	Wt. % C	$d^{13}C$ VPDB	Run
CH3	Saturate	SRE	0.220	1.309	76.46	-29.11	25
CH4	Saturate	SRE	0.211	1.257	76.68	-30.04	28
CH3	Aromatic	SRE	0.233	1.580	87.67	-29.06	46
CH4	Aromatic	SRE	0.310	2.122	88.49	-29.93	47

Notes:

ID#1 : Sample number

ID#2 : Fraction

ID#3 : Sample type

SRE : Source rock extracts

Wt : Weight (mg)

Amp :

Wt %C : Weight (%)

$d^{13}C$ VPDB : $((R_{sam}/R_{std}) - 1))*1000$, where R equals $^{13}C/^{12}C$ and the subscripts "sam" and "std" refer to the unknown sample and a standard (Pee Dee Belemnite, PDB), respectively

Run : Run number

Table 4. Measured peak heights for different biomarker compounds

Peak height	Sample Number																				
	TS			ES			GC		ES	GR	KS			TS			ES	GC	TR	Chainman	
	LA-02	LA-03	LA-04	LA-05	LA-06	LA-07	LA-08	LA-09	LA-10	LA-11	LA-12	LA-12	LA-12	LA-13	LA-14	LA-15	ES-1	GC-3	TR	CH-3	CH-4
GC trace																					
n-C_9	0	0	0	0	0	2	0	0	7.8	8.6	-	0	16.8	10.1	9.8	12.9	11.4	5.5	0	0	0
n-C_{10}	1.9	0	0	0	0	3.9	0	0	13.3	9.9	-	6.5	13.2	14.9	14.6	15.9	13.5	10.8	0	0	0
n-C_{11}	2.5	0	1.6	1.6	0.9	6.1	0	0	16.5	10.3	-	5.6	11	16.6	16.7	16.6	14.7	14.3	1.8	0	0
n-C_{12}	4.2	2.8	2.4	3.5	2.6	7.9	0.5	0	16.7	10.1	-	5.2	7.5	14.7	15	13.2	14.1	14.5	7.3	0	0
n-C_{13}	8	6.4	4.35	6.4	5.7	9.8	1	0	16.4	10.9	-	5.3	7.7	15	15.2	14.1	13.8	13.8	12	0	0
n-C_{14}	12.1	10.7	7	9.9	9.2	11.8	3.5	0	15.7	11.9	-	4.9	7.1	14.3	14.7	14.1	13.5	12.7	14.1	8.8	0
n-C_{15}	14.4	14.2	10.1	12.5	12.1	13.6	9	1.8	15.5	13.8	-	4.8	7	13.5	13.8	14.4	13.1	11.6	14.3	12	12.6
n-C_{16}	14.3	15.6	12.8	13.9	13.7	15.3	14.1	6.9	14.7	14.7	-	4.8	7	12.2	13	13.6	12.9	10	13.1	7	9.5
Pr	3.9	5.1	4.8	2.9	2.5	3.8	3.5	2.8	2.7	3.9	-	1.6	2.9	3.7	3.7	3.8	2.5	1.9	2.3	2.4	7.1
Ph	2.7	3.7	3.2	3.8	3.7	5.3	2.5	2.6	3.7	5	-	2.1	3.7	2.4	2.5	2.5	2.9	1.3	1.6	1.9	5.1
n-C_{17}	13.1	16	14.2	13.9	14.1	15.5	16.2	12.2	14.5	14	-	4.2	6.2	10.6	11.4	12.5	13.2	9	12	5.8	7.5
n-C_{18}	11.8	15.2	13.8	14.6	14.1	16	15.8	15.3	14.3	13.8	-	3.7	5.6	9.5	10	11.2	12.5	8	10.1	5.9	7.7
n-C_{19}	10.2	13.9	12.6	14.6	13.8	15.8	14.5	15.7	13.8	12.9	-	3.3	4.8	8.7	8.85	10	12.3	7.1	9.1	5	7.3
n-C_{20}	9.7	12.8	12	14.7	14	16	13.6	15.1	14	13.5	-	3	4.55	8.65	8.5	9.15	12.8	6.55	8.3	4.9	7.5

n-C_{21}	8.3	11.4	10.6	13.9	13.2	15.9	12	13.1	13.5	12	-	2.15	3.3	7.35	7.25	8.1	12	5.6	7.4	4.15	6.5
n-C_{22}	7.85	10.3	9.6	14.1	13	16.4	10.5	11.8	13.5	11.3	-	1.6	2.6	6.45	6.3	7.15	11.4	4.95	6.6	3.9	6.7
n-C_{23}	6.3	8.9	8.4	12.7	12.2	15.3	8.9	10	12	10	-	1	1.7	5.35	5.3	6.15	11	4.3	5.8	3.4	5.4
n-C_{24}	5.7	8.1	7.7	12.4	11.4	15.3	7.7	8.8	12	9.3	-	0.7	1.1	4.7	4.55	5.2	10.4	3.7	5.2	3.2	4.6
n-C_{25}	4.6	6.65	6.7	11	9.5	13.2	6.8	7.6	10.5	7.5	-	0.3	0.7	4	4.1	4.6	9	3.2	4.5	2.8	4.25
n-C_{26}	3.95	5.8	6.05	11.5	9.8	13.5	6	7.1	10.5	7.4	-	0	0	3.5	3.5	4.1	9.2	2.8	3.95	2.65	3.9
n-C_{27}	3.3	4.8	5.4	10.2	8.5	11.5	5.3	5.9	9	6	-	0	0	3	2.9	3.45	8	2.3	3.25	2.4	3.1
n-C_{28}	2.8	4.1	4.85	9.3	8.5	10.9	4.7	5.4	9	6	-	0	0	2.8	2.5	2.95	7.65	2	2.8	2.25	3.2
n-C_{29}	2.3	3.3	4	7.4	6.3	8.65	3.8	4.5	7.3	4.5	-	0	0	2.15	2.1	2.45	6.1	1.95	2.3	1.9	2.2
n-C_{30}	1.95	2.8	3.5	6.7	5.8	7.6	3.5	3.9	6.5	4.2	-	0	0	1.8	1.7	1.95	5.2	1.15	1.85	1.7	1.8
n-C_{31}	1.6	2.3	2.7	4.8	4.2	5.5	2.7	3.2	5	2	-	0	0	1.5	1.5	2.65	4	0.85	1.65	1.35	1.7
n-C_{32}	1.3	2	2.25	4.2	3.5	4.6	2.4	2.4	4.2	2.5	-	0	0	1.2	1.1	1.3	3.3	0.65	1.3	1.2	1.2
n-C_{33}	1.15	1.7	2.15	3.2	2.7	3.3	2.1	2.5	3.3	2	-	0	0	1.15	1	1.2	2.5	0.6	1.1	1.2	1.3
n-C_{34}	0.95	1.5	1.7	2.7	2.6	2.9	1.9	2.3	2.8	1.9	-	0	0	0.9	0.85	1	2.1	0.4	1	1	0.9
Carotanes	No																				
Botryococcus	No																				
Biodegraded		Yes						Yes			Yes										
m/z 238																					
HBI	No			Abundant			No		Abundant					No			Abndn	No			

m/z 191																					
C_{19} Tricyclic	0.3	0	0.3	0.1	0.1	0	0.65	0.4	0.25	0.3	0.2	0.4	0.1	0.7	0.65	0.6	0.3	0.65	0.4	1.7	1
C_{20} Tricyclic	0.75	0.25	1	0.4	0.4	0.25	2	1.2	0.75	0.95	1.05	1.35	0.55	1.8	1.65	1.6	0.75	1.95	0.85	3.55	2.65
C_{21} Tricyclic	2.55	1.2	2.75	0.95	0.9	0.55	4.5	2.2	1.25	1.95	2.1	2.6	1.35	4.55	4.05	3.8	1.25	3.4	2.2	9.25	7.75
C_{22} Tricyclic	0.85	0.5	0.9	0.4	0.5	0.3	1.5	0.65	0.5	0.85	1.05	1.25	0.75	1.2	1.15	1	0.45	1.05	0.6	2.2	1.85
C_{23} Tricyclic	5.05	3.75	5.75	2.3	2.6	1.65	8.05	3.6	2.6	4.45	5.05	5.9	3.8	6.75	6.5	6.15	2.4	5.7	3.45	11.3	11.4
C_{24} Tricyclic	4.2	3.25	4.9	1.8	1.9	1.3	6.8	2.95	1.9	3	3.45	3.65	2.4	5.5	5	4.95	2.05	5.1	2.85	9.7	11.4
C_{25} Tricyclic	3.5	2.6	3.8	1.85	1.8	1.4	4.8	2.3	1.8	2.7	3.1	3.2	2.3	4	3.8	3.65	1.8	3.85	2.5	5.8	6.7
C_{24}* Tetracyclic	0.8	0.9	0.85	0.95	1.2	0.8	1.5	1	1.1	1.15	1.2	1.2	0.95	1	0.95	0.9	0.9	1.1	0.75	1.1	0.75
C_{26} Tricyclic	3.7	2.25	4	1.4	1.5	1.2	5.4	2.5	1.45	2.4	2.7	2.7	2	4.45	4.25	3.85	1.4	4	2.4	7.8	9.7
C_{27} Tricyclic	1	0.9	1	0.5	0.4	0.45	1.2	0.8	0.5	0.5	0.5	0.6	0.6	1	1	0.95	0.45	1.1	0.75	1.8	2.25
C_{28} Tricyclic	4.1	5.3	4.6	1.4	1.4	1.1	5.1	2.7	1.4	2.2	2.4	2.3	2	4.3	4.3	4.15	1.5	4	3.05	7.15	9.1
C_{29} Tricyclic	4.1	3.4	4.6	2	1.9	1.6	5.3	2.7	0.85	2.7	2.9	2.8	2.55	4.3	4.3	4	1.9	4.4	3.3	6.5	9.3
Ts	1.9	1.8	1.95	1.2	1.3	1.05	2.45	2.2	1.3	1.45	1.45	1.4	1.35	1.95	1.9	1.95	1.25	2.1	1.3	6.9	5.7
Tm	1.45	1.75	1.5	2.35	2.5	2.2	1.9	1.5	2.4	3.15	3.7	3.55	3.1	1.7	1.6	1.5	2.25	1.45	1.85	1.35	1.1
C_{29} Ts	1.9	2.05	2.15	1.4	1.3	1.15	2	1.7	1.4	1.35	1.15	1.15	1.1	1.85	1.85	2	1.4	1.75	2.55	2.7	2.2
C_{29} hopane	4.25	4.75	4.35	5.1	6.05	4.4	5.1	6.1	6	7.75	8.6	9.15	7.75	4.9	4.15	4.85	5.5	4.6	5.8	1.5	1.35
Diahopane	1.2	1.05	1.4	0.8	0.45	0.45	1.2	0.75	0.45	0.4	0.55	0.35	0.35	1.2	1.25	1.2	0.45	0.9	1	2.7	1
Oleanane	0	0	0	0	0	0	0	0	0	0	0	0	0	0	0	0	0	0	0	0	0

C_{30} hopane	11.1	9.7	11.4	11.7	11.7	11.8	10.7	9.55	11.5	11.5	11.4	11.9	10.4	11.2	11	11.5	11.7	11.1	11.3	4.35	4.2
Moretane	1.15	1.45	1.2	1.2	1.15	1.15	1.1	1	1.05	1	1	1.1	1	1.25	1.15	1.2	1.1	0.9	1.15	1	0.8
Gammacerane	0.95	0.75	0.9	4.7	3.85	4.9	0.95	1.4	4.4	2.7	1.8	1.85	1.35	0.95	0.9	0.9	4.35	1	1.2	0.5	0.5
C_{31} 22S	3.55	3	3.55	3.9	4	3.45	3.5	4.5	4	5.25	5.55	5.85	4.6	3.7	3.45	3.8	3.9	3.25	4.9	1.35	1.4
C_{31} 22R	2.45	2.5	2.65	2.75	2.9	2.45	2.4	3.45	3.1	3.8	3.9	4.45	3.1	2.65	2.6	2.6	3	2.25	3.7	1.15	1.1
C_{31} 22S+22R homohopane	6	5.5	6.2	6.65	6.9	5.9	5.9	7.95	7.1	9.05	9.45	10.3	7.7	6.35	6.05	6.4	6.9	5.5	8.6	2.5	2.5
C_{32} 22S	2.8	2.1	2.85	4.35	4.45	4	2.85	3.6	4.55	4.95	4.75	5.35	3.55	2.8	2.85	2.9	4.65	2.75	4.2	1.4	1.4
C_{32} 22R	2.1	1.75	2.25	3.2	3.2	3.1	1.9	2.7	3.3	3.4	3.25	3.55	2.45	2	1.95	2.05	3.25	1.7	2.65	1	1.05
C_{32} 22S+22R homohopane	4.9	3.85	5.1	7.55	7.65	7.1	4.75	6.3	7.85	8.35	8	8.9	6	4.8	4.8	4.95	7.9	4.45	6.85	2.4	2.45
C_{33} 22S	2.6	1.8	2.8	2.8	2.8	2.35	2.6	4.4	2.8	3.45	3.35	3.75	2.4	2.65	2.4	2.7	2.8	3.4	3.95	1.45	1.8
C_{33} 22R	1.45	1.2	1.5	1.7	1.7	1.5	1.4	2.15	2	2.15	2.05	2.4	1.4	1.45	1.95	1.35	1.95	1.2	1.95	0.55	0.6
C_{33} 22S+22R homohopane	4.05	3	4.3	4.5	4.5	3.85	4	6.55	4.8	5.6	5.4	6.15	3.8	4.1	4.35	4.05	4.75	4.6	5.9	2	2.4
C_{34} 22S	1.7	1.15	1.6	3.3	3	3	1.35	3	3.7	3.15	2.6	3.1	1.7	1.55	1.5	1.5	3.5	1.85	2.15	0.55	0.55
C_{34} 22R	1.1	0.85	1.2	2.25	2.1	2.25	1.05	1.9	2.6	2.2	1.95	2.05	1.3	1.1	1	1.05	2.5	1.05	1.6	0.45	0.45
C_{34} 22S+22R homohopane	2.8	2	2.8	5.55	5.1	5.25	2.4	4.9	6.3	5.35	4.55	5.15	3	2.65	2.5	2.55	6	2.9	3.75	1	1
C_{35} 22S	1.2	0.8	1.2	4.5	4.35	4.2	0.9	2.6	4.7	4.35	3.85	4.35	2.4	1.15	1.05	1	4.5	0.8	1.75	0.3	0.25
C_{35} 22R	1.15	0.9	1.1	3	3.05	3	1	2.25	3.4	2.9	2.7	3.05	1.75	1	1.1	1.05	3.2	1	1.6	0.55	0.55
C_{35} 22S+22R homohopane	2.35	1.7	2.3	7.5	7.4	7.2	1.9	4.85	8.1	7.25	6.55	7.4	4.15	2.15	2.15	2.05	7.7	1.8	3.35	0.85	0.8
Total homohopane (C_{31} - C_{35})	20.1	16.1	20.7	31.8	31.6	29.3	19	30.6	34.2	35.6	34	37.9	24.7	20.1	19.9	20	33.3	19.3	28.5	8.75	9.15

m/z 217 and GCMS - MRM traces																					
C_{27} diasterane ααα 20S	15.2	15	15	13.6	9.5	13.8	12.3	13.8	11.7	9.35	7.55	7.1	7.9	14.9	15	15.1	14.9	11.7	14.8	15.1	15
C_{27} diasterane αββ 20S	3.7	3.5	3.4	3.1	2.35	3.1	2.9	3.2	2.75	2.15	1.7	1.65	1.9	3.5	3.4	3.6	3.4	2.6	3.45	3.15	3.6
C_{27} diasterane ααα 20R	4.9	4	4.6	3.9	2.9	4.1	3.8	4.65	3.55	2.75	2.2	2.05	2.45	4.5	4.85	4.95	4.25	3.5	4.5	4.4	4.8
C_{27} diasterane αββ 20R	10.1	10.3	10	9.05	6.85	9.2	8.15	9.75	8.95	6.85	4.5	4.5	5.3	9.6	10.5	10.7	10.8	7.65	10.2	9.55	10
C_{27} diasteranes total	33.9	32.8	33	29.7	21.6	30.2	27.2	31.4	26.9	21.1	16	15.3	17.6	32.5	33.7	34.3	33.3	25.5	32.9	32.2	33.4
C_{28} diasterane ααα 20S	14.6	17.5	13.2	14.2	11.8	15	11.6	14.6	12.8	9.3	8	6.9	8.05	16.6	13.2	15.2	15.9	10.7	15.6	25.3	19.6
C_{28} diasterane αββ 20S	0	0	0	0	0	0	0	0	0	0	0	0	0	0	0	0	0	0	0	0	0
C_{28} diasterane ααα 20R	0	0	0	0	0	0	0	0	0	0	0	0	0	0	0	0	0	0	0	0	0
C_{28} diasterane αββ 20R	10.8	12.4	10.7	10.1	8.3	10.3	9.2	11.5	9.75	6.55	5.6	5	5.7	11.5	10.3	10.9	11	8.45	11.6	17.7	14.5
C_{28} diasteranes total	25.4	29.9	23.9	24.3	20.1	25.3	20.8	26.1	22.6	15.9	13.6	11.9	13.8	28.1	23.5	26.1	26.8	19.2	27.2	43	34
C_{29} diasterane ααα 20S	8.55	9.3	10.1	8.9	7.1	9.5	6.6	7.9	8.3	6.45	4.95	4.5	5.05	9.05	8.35	8.1	11.1	6.6	10.7	14.7	11.2
C_{29} diasterane αββ 20S	0	0	0	0	0	0	0	0	0	0	0	0	0	0	0	0	0	0	0	0	0
C_{29} diasterane ααα 20R	0	0	0	0	0	0	0	0	0	0	0	0	0	0	0	0	0	0	0	0	0
C_{29} diasterane αββ 20R	7.15	7.3	7.9	6.6	5	6.9	6.7	6.8	5.95	4.7	3.65	3.4	3.9	7.45	6.75	6.2	8.1	6.65	8.2	10.6	9.1
C_{29} diasteranes total	15.7	16.6	18	15.5	12.1	16.4	13.3	14.7	14.3	11.2	8.6	7.9	8.95	16.5	15.1	14.3	19.2	13.3	18.9	25.3	20.3
C_{30} diasterane ααα 20S	8.5	10.3	10.3	6.6	5	7.4	9.4	8.9	6.6	5.1	4.7	4.7	4.9	10.1	8.5	8.7	6.9	8.85	9	17.7	13.4
C_{30} diasterane αββ 20R	7.1	8	7.25	5.8	4.5	5.8	7.7	8.1	5.25	4.7	4.35	3.85	5.2	4.8	6.4	6.65	4.8	6	6.2	12.1	9.7
C_{30} diasteranes total	15.6	18.3	17.6	12.4	9.5	13.2	17.1	17	11.9	9.8	9.05	8.55	10.1	14.9	14.9	15.4	11.7	14.9	15.2	29.8	23.1

C_{27} ααα 20S	11.8	11.5	11.9	11.1	11	11.7	9.9	10.4	11.1	11.6	11.5	11.4	11.8	12.1	12.9	12.8	12.1	10.6	10.5	4.65	6.1
C_{27} αββ 20S	12	11.4	11.7	10.9	10.6	11.8	12.6	11.4	15.3	12.4	12.6	12.9	14	11.5	12.2	11.8	15.2	12.6	11.1	6	7.9
C_{27} ααα 20R	12.9	12.3	12.9	15.4	15.4	15.4	11.5	12.1	15.5	13.2	12.9	12.3	13.2	11.9	14.7	13.7	15.4	11	10.5	4.9	6.5
C_{27} αββ 20R	13.5	12.1	12.7	12.6	12.7	13.5	14.9	14.4	13	15.3	15.5	15.4	15.4	11.9	13.4	14.2	13.6	14.8	11.6	7.1	8.5
C_{27} Steranes total	50.1	47.3	49.1	49.9	49.6	52.3	48.9	48.3	54.7	52.4	52.5	51.9	54.3	47.4	53.2	52.5	56.2	48.9	43.7	22.7	29
C_{28} ααα 20S	14	13.8	13.2	13.8	14.2	14.1	11.3	11.5	13.6	11.9	12.6	11.2	12	14.8	14	14	14.3	11.2	12.5	10.9	11.6
C_{28} αββ 20S	14.7	14.7	14.1	14.5	15.1	15.1	14.5	13.1	15	15.2	15.3	15.1	15.3	14.5	14.6	14.7	14.1	14.3	13.7	13.7	14.2
C_{28} ααα 20R	9.3	9.5	9.5	11	11.8	10.9	6.8	7.6	11.1	8.4	8.5	7.95	8.25	9.55	9.6	9.75	10.4	7.35	9.6	6.3	7.35
C_{28} αββ 20R	14.7	14.7	14.1	14.5	15.1	15.1	14.5	13.1	15	15.2	15.3	15.1	15.3	14.5	14.6	14.7	14.1	14.3	13.7	13.7	14.2
C_{28} Steranes total	52.7	52.7	50.9	53.8	56.2	55.2	47	45.2	54.7	50.6	51.7	49.4	50.9	53.4	52.8	53.2	52.8	47.2	49.5	44.5	47.4
C_{29} ααα 20S	14.1	13	14.1	12.7	13.6	14	11.6	11.9	14.4	11.9	13.1	12.2	12.1	13	13.9	12.9	15.2	11.8	14.8	9.2	9.65
C_{29} αββ 20S	14.9	15	14.6	12.9	13.5	15.2	14.9	14.1	13.6	15.2	15.2	15.3	14.9	14.8	14.8	15	13.2	14.8	14.8	14.9	14.6
C_{29} ααα 20R	12	12.1	13	15.3	15.3	14.9	9.6	11.8	15.3	11.5	11.4	11.8	11.6	11.5	13.3	12	14.2	10.7	13.6	7.7	8.3
C_{29} αββ 20R	13.5	14.7	14.1	13	13.6	15.3	13.9	13	13.7	14.4	14.9	15.1	15.3	13.7	13	13.3	14.5	14.4	13.4	12.1	12.9
C_{29} Steranes total	54.5	54.8	55.8	53.9	56	59.4	50	50.8	57	52.9	54.5	54.4	53.8	53	55	53.2	57.1	51.7	56.6	43.9	45.5
C_{30} ααα 20S	10.9	10.7	10.8	9.5	10	9.1	9.6	7.45	11.4	11	11.3	10.4	10	10.4	10.3	9.85	8.45	9.4	5.9	9.1	9
C_{30} αββ 20S	10.3	10.8	10.9	10.7	11.7	10.8	12.5	8.45	13	13.9	14	14.1	13.6	9.6	9.9	10.7	9.65	11.4	7.75	12.2	12.2
C_{30} ααα 20R	13.9	13.6	13	13.1	13.4	13.6	12.3	10.1	13.5	14.2	13.9	14.1	13.4	13.5	13.5	13.6	10.1	11	7.5	9.75	10.3
C_{30} αββ 20R	11.1	10.7	11.6	11.8	12.3	9.6	12.7	9.1	12.8	13.3	14.5	14.1	14.4	10.5	10.5	10.5	9.85	12.3	8	11.5	12.6

C_{30} Steranes total	46.2	45.8	46.2	45.1	47.4	43.1	47.1	35.1	50.7	52.3	53.7	52.7	51.4	44	44.2	44.6	38.1	44	29.2	42.6	44.1
% C_{30} Steranes total	22.7	22.8	22.9	22.3	22.7	20.5	24.4	19.5	23.4	25.1	25.3	25.3	24.4	22.2	21.6	21.9	18.6	23	16.3	27.7	26.6
MRM trace																					
C_{26} 24-nordiacholestane 20S	7.85	14.3	5.75	12.7	13.9	15	12.1	12.7	7.25	11.7	7.15	5.35	14.3	10.1	9.1	5.4	4.5	5.2	3.8	2.45	2.45
C_{26} 24-nordiacholestane 20R	2.7	1.7	2.25	4.15	3.25	2.65	2.45	2.1	3.45	2.45	2.1	1.9	2.1	2.5	2.35	2.05	3.4	4.1	2.4	2.3	2.25
Total	10.6	16	8	16.8	17.1	17.7	14.6	14.8	10.7	14.2	9.25	7.25	16.4	12.6	11.5	7.45	7.9	9.3	6.2	4.75	4.7
C_{26} 27-nordiacholestane 20S	13.3	8.8	12.8	13.8	10.7	9.65	12.3	9.1	12.3	9.45	8.05	8.45	7.5	13	12.7	13.2	11.1	11.5	11.8	13.5	13.4
C_{26} 27-nordiacholestane 20R	10.7	6.7	10.3	14	10.5	8.55	9.75	7.65	14.5	7.9	7	7.4	7.3	9.3	10.1	9.75	12.8	8.75	9.6	9.6	9.95
C_{26} ααα 24-norcholestane 20S	2.3	1.5	2.3	3.05	2.85	2.85	3.15	2.65	2.75	2.6	2.75	2.6	2.55	2	2.1	1.9	2.35	3.5	1.85	1.75	2.05
C_{26} αββ 24-norcholestane 20R	3.55	2.5	3.75	6.4	5.6	4.85	3.35	3.55	5.4	4.25	4.2	4.05	4.15	3.5	4.45	3.9	4.75	3.2	3.3	2.75	2.95
C_{26} αββ 24-norcholestane 20S	4.3	2.75	4.05	6.4	6.8	5.1	4.3	4.1	6.55	5.7	5.7	5.65	5.55	4.95	4.5	4.15	4.8	4	3.45	2.2	2.45
C_{26} ααα 24-norcholestane 20R	3.95	2.7	3.9	6.65	6.8	4.65	3.75	4.3	6.45	5.3	5.05	4.6	4.8	3.6	4.4	3.9	4.4	3.75	2.9	2	2.2
Total	14.1	9.45	14	22.5	22.1	17.5	14.6	14.6	21.2	17.9	17.7	16.9	17.1	14.1	15.5	13.9	16.3	14.5	11.5	8.7	9.65
C_{26} 21-norcholestane ααα + αββ	5.9	3.5	5.65	10.5	13.4	5.95	8.05	7.2	11.3	10.9	10.5	10.8	11.1	5	5.85	5.2	6.9	7.1	3.45	4.05	4.65
C_{26} ααα 27-norcholestane 20S	9.5	5.3	9.3	11.9	13.3	7.9	9.75	7.35	12.3	12.5	13	12.7	12.2	8.7	10.1	9.2	10.2	9.4	8.25	4.35	5
C_{26} αββ 27-norcholestane 20R	10.8	6.7	9.7	13.4	14.3	8.65	11.3	9.9	13.6	14.3	15	14.8	14.6	9.55	12.2	10.7	10.5	10.8	9.15	6.4	7.5
C_{26} αββ 27-norcholestane 20S	9.35	5.75	8.45	12.3	13.4	7.75	10.2	8.35	12.7	13.3	14.4	14.3	13.6	8.65	9.2	9.55	9.35	9.4	8.55	5.55	6.5
C_{26} ααα 27-norcholestane 20R	9.85	5.95	8.95	11.9	12.5	8.05	8.75	8.05	11.5	10.9	11	11	10.4	8.05	10	9.3	9.15	8.1	8.15	4.35	5.1
Total	39.5	23.7	36.4	49.4	53.4	32.4	39.9	33.7	50.1	50.9	53.3	52.8	50.8	35	41.5	38.8	39.2	37.7	34.1	20.7	24.1

Oleanane	0	0	0	1.5	1.05	1.45	0	0	1.2	0.75	0.5	0.5	0.75	0	0	0	1.55	0	0	2.4	2.2
Hopane	15.5	15.5	15.5	15.5	15.5	15.5	15.5	15.5	15.5	15.5	15.5	15.5	15.5	15.5	15.5	15.5	15.6	15.5	15.5	15.2	12.2
Gammacerane	1	0.65	0.9	4.75	3.9	4.75	0.95	1.4	4.2	2.45	1.75	1.85	1.8	1	0.9	0.9	4.65	0.95	1.4	1.65	1
m/z 253																					
C_{21} 20S	8.35	6.15	8.1	2.25	1.85	1.65	7.6	6.7	1.85	2.5	3.05	3.2	3	7.85	6	6.1	4.1	6	0	0.5	0.1
C_{21} 20R	0	0	0	0	0	0	0	0	0	0	0	0	0	0	0	0	0	0	0	0	0
C_{21} (20S + 20R) Monoaromatic	8.35	6.15	8.1	2.25	1.85	1.65	7.6	6.7	1.85	2.5	3.05	3.2	3	7.85	6	6.1	4.1	6	0	0.5	0.1
C_{22} 20S	8.4	6.25	8.5	2.1	1.9	1.65	5.95	5.5	1.85	3.6	4.8	4.8	4.8	7.9	6.4	6.3	3.4	3.4	0	0.4	0.2
C_{22} 20R	0	0	0	0	0	0	0	0	0	0	0	0	0	0	0	0	0	0	0	0	0
C_{22} (20S + 20R) Monoaromatic	8.4	6.25	8.5	2.1	1.9	1.65	5.95	5.5	1.85	3.6	4.8	4.8	4.8	7.9	6.4	6.3	3.4	3.4	0	0.4	0.2
C_{27} 5β 20S	2.35	2.2	2.3	2.6	3.35	2.65	3.2	1.4	3.05	6.05	8.2	8.15	8.15	2.15	2.35	2.25	1.55	0.75	0	0.6	1
C_{27} diacholestane 20S	7.55	6.65	7.8	5	4.4	4.2	1.25	4.4	4.3	4.5	4.7	4.7	4.75	7.3	7.15	6.95	3.5	1.35	0	1.75	2.6
C_{27} 5β 20S + diacholestane 20S	7.4	7.3	7.9	5.8	6.1	5.6	3.5	4.8	5.7	7.7	9.8	9.5	9.9	7.5	7.15	7.55	4.7	2	0	1.1	1.6
C_{27} 5α 20S	3.9	3.7	4.25	1.9	2.3	1.8	1.5	2.15	2.05	3.6	4.6	4.7	4.6	4	3.65	3.4	1.55	1.1	0	0.35	1
C_{27} 5α 20R	3	2.95	3	1.85	2.2	1.7	0.95	1.35	1.95	3.05	4.15	4.1	3.9	3.05	2.65	2.65	1.6	2.3	0	1.15	1
C_{27} (20S + 20R) Monoaromatic	24.2	22.8	25.3	17.2	18.4	16	10.4	14.1	17.1	24.9	31.5	31.2	31.3	24	23	22.8	12.9	7.5	0	4.95	7.2
C_{28} 5β 20S + diaergostane 20S	5.55	5.6	6.1	5.35	5.1	5.1	2.35	4.1	4.9	6.1	7	7	6.7	5.5	5.3	5.2	0.7	1.3	0	0.4	0.7
C_{28} 5a 20S	1.65	2.05	1.7	2.3	2.75	2.2	0.55	1.6	2.45	3.85	4.6	4.65	4.7	1.75	1.6	1.55	1.6	1.65	0	1	1.6
C_{28} 5β 20R + diaergostane 20R	3.95	4.2	4.1	5.9	6	5.4	1.55	3.45	5.5	7.85	8.9	9.1	9	4.65	4.25	4.5	4.8	5.2	0	4.9	4.8

C_{28} 5α 20R	3.2	3.3	3.2	2.6	2.65	2.4	2	2.25	2.6	3.45	4	4.1	4.05	3.3	2.8	2.95	0.85	1.5	0	0.6	0.85
C_{28} (20S + 20R) Monoaromatic	14.4	15.2	15.1	16.2	16.5	15.1	6.45	11.4	15.5	21.3	24.5	24.9	24.5	15.2	14	14.2	7.95	9.65	0	6.9	7.95
C_{29} 5β 20S+diastigmastane 20S	8.9	8.9	9	12	12	12.1	3.35	6.4	11.9	11.5	11.2	11.4	11.3	8.95	9.25	9.25	4.8	5.2	0	4.9	4.8
C_{29} 5α 20S	3.15	3.25	3.5	3.3	3.5	3.2	1.85	2.85	3.4	3.6	3.8	3.9	3.8	3.5	4.9	3.25	0.5	8.1	0	0.4	0.5
C_{29} 5β 20S+diastigmastane 20R	6.15	5.9	6.4	7.4	7.1	7.1	3.9	4.45	7.3	6.7	6.5	6.5	6.5	7.5	7	7.2	11.5	2.1	0	11.9	11.5
C_{29} 5α 20R	2.3	2.3	2.2	2.55	2.8	2.6	1.8	1.1	2.7	2.95	3.35	3.25	3.1	2.5	2.3	2.25	0.8	1.9	0	0.65	0.8
C_{29} (20S + 20R) Monoaromatic	20.5	20.4	21.1	25.2	25.4	25	10.9	14.8	25.3	24.8	24.9	25.1	24.7	22.5	23.5	22	17.6	17.3	0	17.9	17.6
m/z 231																					
C_{20} 20S	8.95	9.1	9.7	2.65	2.65	2.3	8	8.25	2.65	4.4	3.8	4.3	4.1	6.65	7.3	8.5	2.65	7.85	0	7.85	3
C_{20} 20R	0	0	0	0	0	0	0	0	0	0	0	0	0	0	0	0	0	0	0	0	0
C_{20} (20S + 20R) Triaromatic	8.95	9.1	9.7	2.65	2.65	2.3	8	8.25	2.65	4.4	3.8	4.3	4.1	6.65	7.3	8.5	2.65	7.85	0	7.85	3
C_{21} 20S	10	9.55	11.4	2.4	2.45	2.15	11.1	11.2	2.4	4.5	4.05	4.05	4.3	7.6	8.25	9.05	2.55	11.2	0	11.6	6.25
C_{21} 20R	0	0	0	0	0	0	0	0	0	0	0	0	0	0	0	0	0	0	0	0	0
C_{21} (20S + 20R) Triaromatic	10	9.55	11.4	2.4	2.45	2.15	11.1	11.2	2.4	4.5	4.05	4.05	4.3	7.6	8.25	9.05	2.55	11.2	0	11.6	6.25
C_{26} 20S	6.6	6.45	6.35	5.3	5.3	4.9	3.5	3.9	5.25	4.95	4.9	5.05	5	6.7	6.5	6.55	5.2	3.9	0	2.25	1.35
C_{26} 20R	11.6	11.4	11.5	12.3	12.2	12.3	7.2	8.3	12.3	12	11.9	11.9	11.9	11.7	11.6	11.6	12.3	7.95	0	3.3	2.1
C_{26} (20S + 20R) Triaromatic	18.2	17.9	17.9	17.6	17.5	17.2	10.7	12.2	17.5	16.9	16.8	17	16.9	18.4	18.1	18.1	17.5	11.9	0	5.55	3.45
C_{27} 20S	0	0	0	0	0	0	0	0	0	0	0	0	0	0	0	0	0	0	0	0	0
C_{27} 20R	4	3.9	4.1	4.95	5.3	5.6	2.85	3.25	5.5	5.4	5.05	5.35	4.8	4.35	4.05	4.2	5.25	3.15	0	1.2	0.8

C_{27} (20S + 20R) Triaromatic	4	3.9	4.1	4.95	5.3	5.6	2.85	3.25	5.5	5.4	5.05	5.35	4.8	4.35	4.05	4.2	5.25	3.15	0	1.2	0.8
C_{28} 20S	8.8	8.3	8.4	8.55	8.25	9.6	6.6	7.2	8.5	6.3	4.75	4.9	4.6	9.15	8.95	9.15	9.5	7.55	0	2.85	1.7
C_{28} 20R	10.4	10	9.9	10.8	10.5	12.1	8.35	8.85	10.5	7.55	6.15	6.5	6.15	11.4	11	10.9	10.7	9.65	0	3.2	1.95
C_{28} (20S + 20R) Triaromatic	19.2	18.3	18.3	19.3	18.8	21.7	15	16.1	19	13.9	10.9	11.4	10.8	20.5	19.9	20.1	20.2	17.2	0	6.05	3.65
C_{29} 20S	2	2.4	2	0.5	0.55	0.6	1.7	2	0.6	1	1.3	1.3	1.2	2.7	2.5	2.6	0.55	1.8	0	1.5	0.45
C_{29} 20R	1.6	1.5	1.55	0.5	0.55	12.7	1.2	1.4	0.7	0.75	0.95	0.5	0.95	1.95	1.9	1.9	0.6	1.5	0	0.8	0.55
C_{29} (20S + 20R) Triaromatic	3.6	3.9	3.55	1	1.1	13.3	2.9	3.4	1.3	1.75	2.25	1.8	2.15	4.65	4.4	4.5	1.15	3.3	0	2.3	1
m/z 245																					
Triaromatic dinosteranes	Low	Low	Low	High	High	High	Low	Low	High	High	High	High	High	Low	Low	Low	High	Low	Low	Low	Low

Note:

Mark (-) : no data
TS : Trap Spring
ES : Eagle Spring
GC : Grant Canyon
KS : Kate Spring
TR : Tomaro Ranch

Table 5. Calculated biomarker ratios for oil and rock samples

Calculated Ratio	Sample Number																				
	TS			ES			GC		ES	GR	KS			TS			ES	GC	TR	Chainman	
	LA-02	LA-03	LA-04	LA-05	LA-06	LA-07	LA-08	LA-09	LA-10	LA-11	LA-12 A	LA-12B	LA-12C	LA-13	LA-14	LA-15	ES-1	GC-3	TR	CH-3	CH-4
GC trace																					
Pr/Ph	1.44	1.38	1.50	0.76	0.68	0.72	1.40	1.08	0.73	0.78	-	0.76	0.78	1.54	1.48	1.52	0.86	1.46	1.44	1.26	1.39
Pr/(Pr+Ph)	0.59	0.58	0.60	0.43	0.40	0.42	0.58	0.52	0.42	0.44	-	0.43	0.44	0.61	0.60	0.60	0.46	0.59	0.59	0.56	0.58
Ph / *n*-C_{18}	0.23	0.24	0.23	0.26	0.26	0.33	0.16	0.17	0.26	0.36	-	0.57	0.66	0.25	0.25	0.22	0.23	0.16	0.16	0.32	0.66
Pr / *n*-C_{17}	0.30	0.32	0.34	0.21	0.18	0.25	0.22	0.23	0.19	0.28	-	0.38	0.47	0.35	0.32	0.30	0.19	0.21	0.19	0.41	0.95
OEP 1 (C_9 - C_{13})	0.94	0.57	1.45	1.14	1.07	1.03	0.50	0.00	1.03	1.02	-	0.83	1.09	1.05	1.06	1.09	1.03	1.04	0.78	0.00	0.00
OEP 2 (C_{13} - C_{17})	1.02	1.02	1.00	1.00	1.01	0.99	1.01	0.83	1.00	1.01	-	0.99	0.99	1.01	0.99	1.02	1.00	1.02	1.01	1.23	2.19
OEP 3 (C_{17} - C_{21})	0.96	0.99	0.97	0.98	0.98	0.98	0.98	0.98	0.98	0.95	-	0.98	0.94	0.97	0.97	0.99	0.98	0.98	1.01	0.92	0.95
OEP 4 (C_{21} - C_{25})	0.94	0.97	0.98	0.95	0.98	0.95	0.99	0.98	0.94	0.96	-	0.92	0.96	0.97	0.99	1.00	1.00	1.00	0.99	0.96	0.95
OEP 5 (C_{25} - C_{27})	0.38	0.37	0.37	0.34	0.33	0.34	0.37	0.36	0.34	0.34	-	0.00	0.00	0.36	0.38	0.37	0.34	0.39	0.37	0.36	0.34
m/z 191 trace																					
C_{22} tricyclic / C_{21} tricyclic	0.33	0.42	0.33	0.42	0.56	0.55	0.33	0.30	0.40	0.44	0.50	0.48	0.56	0.26	0.28	0.26	0.36	0.31	0.27	0.24	0.24
C_{24} tricyclic / C_{23} tricyclic	0.83	0.87	0.85	0.78	0.73	0.79	0.84	0.82	0.73	0.67	0.68	0.62	0.63	0.81	0.77	0.80	0.85	0.89	0.83	0.86	1.00
C_{26} tricyclic / C_{25} tricyclic	1.06	0.87	1.05	0.76	0.83	0.86	1.13	1.09	0.81	0.89	0.87	0.84	0.87	1.11	1.12	1.05	0.78	1.04	0.96	1.34	1.45
C_{29} tricyclic / C_{30} tricyclic	0.37	0.35	0.40	0.17	0.16	0.14	0.50	0.28	0.07	0.23	0.25	0.24	0.25	0.38	0.39	0.35	0.16	0.40	0.29	1.49	2.21

C_{23} tricyclic / (C_{23} + C_{29}) tricyclic	0.55	0.52	0.56	0.53	0.58	0.51	0.60	0.57	0.75	0.62	0.64	0.68	0.60	0.61	0.60	0.61	0.56	0.56	0.51	0.63	0.55
C_{23} tricyclic / (C_{23} tricyclic + C_{30} hopane)	0.31	0.28	0.34	0.16	0.18	0.12	0.43	0.27	0.19	0.28	0.31	0.33	0.27	0.38	0.37	0.35	0.17	0.34	0.23	0.72	0.73
C_{24} tetracyclic / (C_{24} tetracyclic + C_{26} tricyclic)	0.18	0.29	0.18	0.40	0.44	0.40	0.22	0.29	0.43	0.32	0.31	0.31	0.32	0.18	0.18	0.19	0.39	0.22	0.24	0.12	0.07
C_{26} tricyclic / C_{24} tetracyclic	4.63	2.50	4.71	1.47	1.25	1.50	3.60	2.50	1.32	2.09	2.25	2.25	2.11	4.45	4.47	4.28	1.56	3.64	3.20	7.09	12.93
C_{24} tetracyclic / (C_{24} tetracyclic + C_{30} hopane)	0.07	0.08	0.07	0.08	0.09	0.06	0.12	0.09	0.09	0.09	0.10	0.09	0.08	0.08	0.08	0.07	0.07	0.09	0.06	0.20	0.15
C_{25} / C_{24} tricyclic	4.38	2.89	4.47	1.95	1.50	1.75	3.20	2.30	1.64	2.35	2.58	2.67	2.42	4.00	4.00	4.06	2.00	3.50	3.33	5.27	8.93
C_{25} / C_{26} tricyclic	0.95	1.16	0.95	1.32	1.20	1.17	0.89	0.92	1.24	1.13	1.15	1.19	1.15	0.90	0.89	0.95	1.29	0.96	1.04	0.74	0.69
(C_{28}+C_{29}) tricyclic/(C_{28}+C_{29})+hopanes	0.42	0.47	0.45	0.23	0.22	0.19	0.49	0.36	0.16	0.30	0.32	0.30	0.30	0.43	0.44	0.41	0.23	0.43	0.36	0.76	0.81
C_{29} Hopane / (C_{29} Hopane + C_{30} Hopane)	0.28	0.33	0.28	0.30	0.34	0.27	0.32	0.39	0.34	0.40	0.43	0.43	0.43	0.30	0.27	0.30	0.32	0.29	0.34	0.26	0.24
C_{29} Ts / (C_{29}Ts + C_{29} Hopane)	0.31	0.30	0.33	0.22	0.18	0.21	0.28	0.22	0.19	0.15	0.12	0.11	0.12	0.27	0.31	0.29	0.20	0.28	0.31	0.64	0.62
Ts/(Ts+Tm)	0.57	0.51	0.57	0.34	0.34	0.32	0.56	0.59	0.35	0.32	0.28	0.28	0.30	0.53	0.54	0.57	0.36	0.59	0.41	0.84	0.84
Oleanane / (Oleanane + Hopane)	0.00	0.00	0.00	0.09	0.06	0.09	0.00	0.00	0.07	0.05	0.03	0.03	0.05	0.00	0.00	0.00	0.09	0.00	0.00	0.14	0.15
Gammacerane / C_{31} 22S	0.27	0.25	0.25	1.21	0.96	1.42	0.27	0.31	1.10	0.51	0.32	0.32	0.29	0.26	0.26	0.24	1.12	0.31	0.24	0.37	0.36
C_{31} 22R homohopane / C_{30} hopane	0.22	0.26	0.23	0.24	0.25	0.21	0.22	0.36	0.27	0.33	0.34	0.37	0.30	0.24	0.24	0.23	0.26	0.20	0.33	0.26	0.26
C_{31} 22S homohopane / (C_{31} 22S + 22R) homohopane	0.59	0.55	0.57	0.59	0.58	0.58	0.59	0.57	0.56	0.58	0.59	0.57	0.60	0.58	0.57	0.59	0.57	0.59	0.57	0.54	0.56
C_{32} 22S homohopane / (C_{32} 22S+22R) homohopane	0.57	0.55	0.56	0.58	0.58	0.56	0.60	0.57	0.58	0.59	0.59	0.60	0.59	0.58	0.59	0.59	0.59	0.62	0.61	0.58	0.57

C_{33} 22S homohopane / (C_{33} 22S + 22R) homohopane	0.64	0.60	0.65	0.62	0.62	0.61	0.65	0.67	0.58	0.62	0.62	0.61	0.63	0.65	0.55	0.67	0.59	0.74	0.67	0.73	0.75
C_{34} 22S homohopane / (C_{34} 22S + 22R) homohopane	0.61	0.58	0.57	0.59	0.59	0.57	0.56	0.61	0.59	0.59	0.57	0.60	0.57	0.58	0.60	0.59	0.58	0.64	0.57	0.55	0.55
C_{35} 22S homohopane / (C_{34} 22S homohopane)	0.71	0.70	0.75	1.36	1.45	1.40	0.67	0.87	1.27	1.38	1.48	1.40	1.41	0.74	0.70	0.67	1.29	0.43	0.81	0.55	0.45
C_{35} 22S homohopane / (C_{34} 22S + C_{35} 22S)	0.41	0.41	0.43	0.58	0.59	0.58	0.40	0.46	0.56	0.58	0.60	0.58	0.59	0.43	0.41	0.40	0.56	0.30	0.45	0.35	0.31
% C_{31} Homohopane	29.85	34.27	29.95	20.94	21.87	20.14	31.13	26.02	20.79	25.42	27.84	27.18	31.24	31.67	30.48	32.00	20.75	28.57	30.23	28.57	27.32
% C_{32} Homohopane	24.38	23.99	24.64	23.78	24.25	24.23	25.07	20.62	22.99	23.46	23.56	23.48	24.34	23.94	24.18	24.75	23.76	23.12	24.08	27.43	26.78
% C_{33} Homohopane	20.15	18.69	20.77	14.17	14.26	13.14	21.11	21.44	14.06	15.73	15.91	16.23	15.42	20.45	21.91	20.25	14.29	23.90	20.74	22.86	26.23
% C_{34} Homohopane	13.93	12.46	13.53	17.48	16.16	17.92	12.66	16.04	18.45	15.03	13.40	13.59	12.17	13.22	12.59	12.75	18.05	15.06	13.18	11.43	10.93
% C_{35} Homohopane	11.69	10.59	11.11	23.62	23.45	24.57	10.03	15.88	23.72	20.37	19.29	19.53	16.84	10.72	10.83	10.25	23.16	9.35	11.78	9.71	8.74
Tricyclic/hopane	0.61	0.60	0.65	0.26	0.29	0.22	0.88	0.41	0.28	0.38	0.43	0.43	0.43	0.74	0.71	0.68	0.28	0.71	0.40	1.66	2.12
Moretane / Hopane	0.10	0.15	0.11	0.10	0.10	0.10	0.10	0.10	0.09	0.09	0.09	0.09	0.10	0.11	0.11	0.10	0.09	0.08	0.10	0.23	0.19
Homohopane index	0.12	0.11	0.11	0.24	0.23	0.25	0.10	0.16	0.24	0.20	0.19	0.20	0.17	0.11	0.11	0.10	0.23	0.09	0.12	0.10	0.09
Gammacerane Index	0.08	0.07	0.07	0.29	0.25	0.29	0.08	0.13	0.28	0.19	0.14	0.13	0.11	0.08	0.08	0.07	0.27	0.08	0.10	0.10	0.11
10XGammacerane/(Gammacerane+C_{30}hopane)	0.79	0.72	0.73	2.87	2.48	2.93	0.82	1.28	2.78	1.90	1.36	1.35	1.15	0.78	0.76	0.73	2.72	0.83	0.96	1.03	1.06
Diahopane / (Diahopane + C_{30} Hopane)	0.10	0.10	0.11	0.06	0.04	0.04	0.10	0.07	0.04	0.03	0.05	0.03	0.03	0.10	0.10	0.09	0.04	0.08	0.08	0.38	0.19
Diahopane / (Diahopane + C_{29} Hopane)	0.22	0.18	0.24	0.14	0.07	0.09	0.19	0.11	0.07	0.05	0.06	0.04	0.04	0.20	0.23	0.20	0.08	0.16	0.15	0.64	0.43
Diahopane / (Diahopane + C_{29}Ts)	0.39	0.34	0.39	0.36	0.26	0.28	0.38	0.31	0.24	0.23	0.32	0.23	0.24	0.39	0.40	0.38	0.24	0.34	0.28	0.50	0.31

Tricyclic / (Tricyclic + Hopane)	0.35	0.33	0.37	0.16	0.16	0.13	0.44	0.23	0.15	0.21	0.23	0.23	0.22	0.39	0.39	0.37	0.16	0.39	0.24	0.64	0.70
m/z 217 and MRM traces*																					
C_{27} 20S (C_{27} ααα 20S + C_{27} αββ 20S)	23.75	22.90	23.55	21.95	21.50	23.40	22.45	21.75	26.30	23.95	24.10	24.25	25.75	23.55	25.10	24.60	27.25	23.10	21.55	10.65	14.00
C_{27} 20R (C_{27} ααα 20R + C_{27} αββ 20R)	26.35	24.40	25.50	27.95	28.10	28.90	26.40	26.54	28.40	28.45	28.35	27.65	28.55	23.80	28.05	27.85	28.95	25.80	22.10	12.00	15.00
C_{27} (20S + 20R)	50.10	47.30	49.05	49.90	49.60	52.30	48.85	48.29	54.70	52.40	52.45	51.90	54.30	47.35	53.15	52.45	56.20	48.90	43.65	22.65	29.00
C_{28} 20S (C_{28} ααα 20S + C_{28} αββ 20S)	28.70	28.50	27.30	28.30	29.30	29.20	25.70	24.50	28.60	27.05	27.90	26.30	27.30	29.30	28.55	28.70	28.35	25.50	26.20	24.55	25.80
C_{28} 20R (C_{28} ααα 20R + C_{28} αββ 20R)	24.00	24.20	23.60	25.50	26.85	26.00	21.25	20.65	26.10	23.55	23.80	23.05	23.55	24.05	24.20	24.45	24.45	21.65	23.30	19.95	21.55
C_{28} (20S + 20R)	52.70	52.70	50.90	53.80	56.15	55.20	46.95	45.15	54.70	50.60	51.70	49.35	50.85	53.35	52.75	53.15	52.80	47.15	49.50	44.50	47.35
C_{29} 20S (C_{29} ααα 20S + C_{29} αββ 20S)	29.00	27.95	28.70	25.60	27.10	29.15	26.50	26.00	28.00	27.00	28.25	27.45	26.95	27.80	28.65	27.85	28.35	26.55	29.60	24.10	24.25
C_{29} 20R (C_{29} ααα 20R + C_{29} αββ 20R)	25.45	26.80	27.10	28.25	28.85	30.20	23.50	24.80	28.95	25.90	26.25	26.90	26.85	25.20	26.30	25.30	28.70	25.10	27.00	19.80	21.20
C_{29} (20S + 20R)	54.45	54.75	55.80	53.85	55.95	59.35	50.00	50.80	56.95	52.90	54.50	54.35	53.80	53.00	54.95	53.15	57.05	51.65	56.60	43.90	45.45
C_{27} + C_{28} + C_{29} Steranes	157.3	154.8	155.8	157.6	161.7	166.9	145.8	144.2	166.4	155.9	158.7	155.6	159.0	153.7	160.9	158.8	166.1	147.7	149.8	111.1	121.8
C_{27} + C_{28} + C_{29} Diasteranes	75.00	79.30	74.85	69.45	53.75	71.80	61.25	72.15	63.70	48.10	38.15	35.10	40.25	77.05	72.25	74.70	79.25	57.85	78.90	100.5	87.70
Diasterane/sterane	0.68	0.69	0.67	0.59	0.44	0.58	0.56	0.65	0.49	0.40	0.30	0.29	0.32	0.69	0.63	0.65	0.59	0.52	0.75	1.42	1.15
C_{27} diasterane/(Dia+Reg) sterane	0.40	0.41	0.40	0.37	0.30	0.37	0.36	0.39	0.33	0.29	0.23	0.23	0.24	0.41	0.39	0.40	0.37	0.34	0.43	0.59	0.54
% C_{27} Sterane	31.86	30.57	31.49	31.67	30.67	31.35	33.50	33.48	32.88	33.61	33.06	33.35	34.16	30.81	33.04	33.04	33.85	33.11	29.15	20.40	23.81

% C_{28} Sterane	33.51	34.05	32.68	34.15	34.72	33.08	32.20	31.30	32.88	32.46	32.59	31.72	31.99	34.71	32.79	33.48	31.80	31.92	33.06	40.07	38.88
% C_{29} Sterane	34.63	35.38	35.83	34.18	34.60	35.57	34.29	35.22	34.24	33.93	34.35	34.93	33.85	34.48	34.16	33.48	34.36	34.97	37.80	39.53	37.32
% C_{27} Diasterane	45.20	41.36	44.02	42.69	40.19	41.99	44.33	43.52	42.23	43.87	41.81	43.59	43.60	42.18	46.64	45.92	42.02	43.99	41.63	32.06	38.08
% C_{28} Diasterane	33.87	37.70	31.93	34.99	37.30	35.17	33.96	36.11	35.40	32.95	35.65	33.90	34.16	36.40	32.46	34.94	33.82	33.10	34.41	42.76	38.77
% C_{29} Diasterane	20.93	20.93	24.05	22.32	22.51	22.84	21.71	20.37	22.37	23.18	22.54	22.51	22.24	21.41	20.90	19.14	24.16	22.90	23.95	25.19	23.15
C_{29} 20S / (20S+20R)	0.53	0.51	0.51	0.48	0.48	0.49	0.53	0.51	0.49	0.51	0.52	0.51	0.50	0.52	0.52	0.52	0.50	0.51	0.52	0.55	0.53
C_{29} αββ/(αββ+ααα)	0.52	0.54	0.51	0.48	0.48	0.51	0.58	0.53	0.48	0.56	0.55	0.56	0.56	0.54	0.51	0.53	0.48	0.57	0.50	0.62	0.61
C_{28}/C_{29} Steranes	0.97	0.96	0.91	1.00	1.00	0.93	0.94	0.89	0.96	0.96	0.95	0.91	0.95	1.01	0.96	1.00	0.93	0.91	0.87	1.01	1.04
C_{30} / (C_{27} - C_{30}) Steranes*	0.23	0.23	0.23	0.22	0.23	0.21	0.24	0.20	0.23	0.25	0.25	0.25	0.24	0.22	0.22	0.22	0.19	0.23	0.16	0.28	0.27
C_{26} 21/(21+27) Norcholestanes*	0.13	0.13	0.13	0.17	0.20	0.16	0.17	0.18	0.18	0.18	0.16	0.17	0.18	0.13	0.12	0.12	0.15	0.16	0.09	0.16	0.16
C_{26} 24/(24+27) Norcholestanes*	0.26	0.29	0.28	0.31	0.29	0.35	0.27	0.30	0.30	0.26	0.25	0.24	0.25	0.29	0.27	0.26	0.29	0.28	0.25	0.30	0.29
C_{26} 24/(24+27) Nordiacholestanes*	0.31	0.51	0.26	0.38	0.45	0.49	0.40	0.47	0.29	0.45	0.38	0.31	0.53	0.36	0.33	0.25	0.25	0.31	0.22	0.17	0.17
TPP ratio*	40.50	24.70	37.40	50.35	54.35	33.35	40.90	34.65	51.10	51.90	0.00	53.80	51.75	35.95	42.45	39.75	40.15	38.70	35.10	0.00	0.00
m/z 253																					
% 27s	40.98	39.11	41.09	29.32	30.46	28.48	37.48	34.99	29.50	35.12	38.92	38.43	38.93	38.93	38.03	38.68	33.55	21.77	0.00	16.67	21.98
% 28s	24.30	25.99	24.57	27.61	27.39	26.96	23.24	28.29	26.73	29.97	30.32	30.66	30.41	24.66	23.12	24.09	20.68	28.01	0.00	23.23	24.27
% 29s	34.72	34.91	34.34	43.08	42.16	44.55	39.28	36.72	43.77	34.91	30.75	30.91	30.66	36.42	38.86	37.23	45.77	50.22	0.00	60.10	53.74
MA (I) (Sum of C_{21} to C_{22})	16.75	12.40	16.60	4.35	3.75	3.30	13.55	12.20	3.70	6.10	7.85	8.00	7.80	15.75	12.40	12.40	7.50	9.40	0.00	0.90	0.30

MA (II) (Sum of C_{27} to C_{29})	59.05	58.30	61.45	58.50	60.25	56.00	27.75	40.30	57.80	70.90	80.80	81.05	80.40	61.65	60.35	58.95	38.45	34.45	0.00	29.70	32.75
MA (I) / ((MA (I) + MA (II))	0.22	0.18	0.21	0.07	0.06	0.06	0.33	0.23	0.06	0.08	0.09	0.09	0.09	0.20	0.17	0.17	0.16	0.21	0.00	0.03	0.01
m/z 231																					
C_{26} / C_{28}S Triaromatic steroid	2.1	2.2	2.1	2.1	2.1	1.8	1.6	1.7	2.1	2.7	3.5	3.5	3.7	2.0	2.0	2.0	1.8	1.6	0.0	1.9	2.0
C_{27} / C_{28}S Triaromatic steroid	0.5	0.5	0.5	0.6	0.6	0.6	0.4	0.5	0.6	0.9	1.1	1.1	1.0	0.5	0.5	0.5	0.6	0.4	0.0	0.4	0.5
TA (I) (Sum of C_{20} to C_{21})	19.0	18.7	21.1	5.1	5.1	4.5	19.1	19.4	5.1	8.9	7.9	8.4	8.4	14.3	15.6	17.6	5.2	19.0	0.0	19.5	9.3
TA (II) (Sum of C_{26} to C_{28})	41.4	40.1	40.3	41.9	41.6	44.5	28.5	31.5	42.0	36.2	32.8	33.7	32.5	43.3	42.0	42.4	43.0	32.2	0.0	12.8	7.9
TA (I) / ((TA (I) + TA (II))	0.3	0.3	0.3	0.1	0.1	0.1	0.4	0.4	0.1	0.2	0.2	0.2	0.2	0.2	0.3	0.3	0.1	0.4	0.0	0.6	0.5

Note:

1. OEP 1 = (C_{21} + 6C_{23} + C_{25}) / (4C_{22} + 4C_{24})
2. OEP 2 = (C_{25} + 6C_{27} + C_{29}) / (4C_{26} + 4C_{28})
3. OEP 3 = (C_{29} + 6C_{31} + C_{33}) / (4C_{30} + 4C_{32})
4. OEP 4 = (C_{33} + 6C_{34} + C_{35}) / (4C_{34} + 4C_{36})
5. OEP 5 = (C_{35} + 6C_{37} + C_{39}) / (4C_{38} + 4C_{40})
6. Tricyclic/(tricyclic + Hopane) = (C_{20} + C_{23} + C_{24} + C_{25} + C_{26} + C_{28} + C_{29} tricyclic) / (C_{20} + C_{23} + C_{24} + C_{25} + C_{26} + C_{28} + C_{29} tricyclic) + (Ts + Tm + C_{29} hopane + C_{29}Ts diahopane + C_{30} hopane + moretane + all of the homohopane homologs)
7. % C_{31} homohopane = C_{31} 22S+22R homohopane / total homohopane homologs
8. Gammacerane Index = Gammacerane / (Gammacerane + C_{30} hopane)
9. Homohopane index = (C_{35} homohopane S+R) / (C_{35} + C_{34} + C_{33} + C_{32} + C_{31} homohopane S+R)
10. % C_{27} Steranes = (Total C_{27} steranes)/(Total C_{27}+C_{28}+C_{29} steranes)*100
11. % C_{27} Diasteranes = (Total C_{27} diasteranes)/(Total C_{27}+C_{28}+C_{29} diasteranes)*100
12. C_{27} diasterane/(Dia+Reg) steranes= C_{27} diasteranes / (C_{27} diasteranes + (C_{27} + C_{28} + C_{29}) steranes
13. C_{30}/(C_{27} - C_{30}) steranes = C_{30} / (C_{27}+C_{28}+C_{29}+C_{30}) Steranes
14. Diasterane / Sterane = C_{27} diasteranes / C_{27} Steranes

15. TPP ratio = (2 x C_{30} tetracyclic polyprenoid) / (2 x C_{30} tetracyclic polyprenoid) + (total C_{26} 27-norcholestanes)
16. % 27s = (Total C_{27} monoaromatic steroid)/(Total C_{27}+C_{28}+C_{29} monoaromatic steroids)*100
17. MA (I) = Sum of C_{21} to C_{22} monoaromatic steroid
18. MA (II) = Sum of C_{27} to C_{29} monoaromatic steroid
19. TA (I) = Sum of C_{21} to C_{22} triaromatic steroid
20. TA (II) = Sum of C_{27} to C_{29} monoaromatic steroid

Table 6. Stable carbon isotope values of oil samples

Field	ID#1	ID#2	ID#3	Wt (mg)	Amp(V) C	Wt. % C	$\delta^{13}C$ VPDB	Run
Trap Spring	LA02	Saturate	Oil	0.259	1.683	84.11	-30.07	8
	LA03	Saturate	Oil	0.210	1.438	88.20	-29.66	9
	LA04	Saturate	Oil	0.229	1.522	86.15	-30.13	10
	LA13	Saturate	Oil	0.170	1.095	82.79	-30.21	22
	LA14	Saturate	Oil	0.191	1.218	82.07	-30.29	23
	LA15	Saturate	Oil	0.309	1.923	80.40	-30.17	24
Grant Canyon	LA08	Saturate	Oil	0.187	1.277	88.39	-30.02	14
	LA09	Saturate	Oil	0.260	1.757	87.36	-28.26	15
Eagle Spring	LA05	Saturate	Oil	0.171	1.096	82.45	-29.80	11
	LA06	Saturate	Oil	0.180	1.122	80.51	-28.89	12
	LA07	Saturate	Oil	0.180	1.172	83.74	-29.76	13
	LA10	Saturate	Oil	0.240	1.522	81.93	-29.23	16
Ghost R	LA11	Saturate	Oil	0.286	1.913	86.93	-28.90	18
Kate Spring	LA12A	Saturate	Oil	0.171	1.078	80.99	-28.48	19
	LA12B	Saturate	Oil	0.230	0.764	42.58	-28.85	20
	LA12C	Saturate	Oil	0.160	1.111	89.01	-28.60	21
Trap Spring	LA02	Aromatic	Oil	0.205	1.304	81.82	-30.42	29
	LA03	Aromatic	Oil	0.250	1.046	53.54	-30.46	30
	LA04	Aromatic	Oil	0.249	1.716	89.10	-30.53	31
	LA13	Aromatic	Oil	0.197	1.318	86.03	-30.47	43
	LA14	Aromatic	Oil	0.252	1.693	86.87	-30.52	44
	LA15	Aromatic	Oil	0.206	1.283	80.51	-30.45	45
Grant Canyon	LA08	Aromatic	Oil	0.219	1.488	87.38	-30.14	35
	LA09	Aromatic	Oil	0.184	1.264	88.46	-29.61	36
Eagle Spring	LA05	Aromatic	Oil	0.192	1.309	87.36	-28.96	32
	LA06	Aromatic	Oil	0.310	2.110	87.40	-28.59	33
	LA07	Aromatic	Oil	0.223	1.493	86.21	-28.99	34
	LA10	Aromatic	Oil	0.240	1.593	85.81	-28.82	38
Ghost R	LA11	Aromatic	Oil	0.201	1.379	88.88	-28.75	39
Kate Spring	LA12A	Aromatic	Oil	0.180	1.190	84.52	-28.61	40
	LA12B	Aromatic	Oil	0.245	1.615	85.23	-28.83	41
	LA12C	Aromatic	Oil	0.182	1.203	85.57	-28.81	42

Notes:
Notes as defined in Table III.

Table 7. Diamondoids concentration of oil samples

Diamondoids compounds	Oil Samples													
	TS			ES			GC		ES	GR	KS			TS
	LA-02	LA-03	LA-04	LA-05	LA-06	LA-07	LA-08	LA-09	LA-10	LA-11	LA-12A	LA-12B	LA-12C	LA-13
D3 1-Methyladamantane (I.S.)	33.9	36.7	47.4	55.5	35.7	29.0	26.3	46.4	43.8	32.1	37.5	51.0	46.0	34.9
1-Methyladamantane	9.2	1.4	5.3	3.6	1.2	2.6	15.2	17.6	9.3	14.8	15.3	25.8	21.0	13.1
2-Methyladamantane	10.0	0.4	1.2	0.9	0.8	1.9	0.7	-	5.0	8.8	7.8	11.7	9.7	10.7
1-Ethyladamantane	10.3	0.3	0.7	0.9	0.7	0.7	1.3	-	2.2	5.0	5.5	8.8	5.4	8.0
2-Ethyladamantane	21.9	0.9	1.4	2.2	1.2	1.7	0.1	-	4.5	6.8	6.9	10.1	7.7	15.7
Adamantane	2.5	0.2	0.3	0.6	0.4	1.4	0.4	0.4	4.1	4.6	4.2	7.3	6.0	3.2
D4 Adamantane (I.S.)	20.4	22.1	28.5	33.4	21.5	17.4	15.8	27.9	26.3	19.3	22.5	30.6	27.6	21.0
1,3-Dimethyladamantane	10.3	0.5	1.2	1.4	0.8	2.6	4.1	0.5	6.8	10.5	11.8	20.0	14.9	14.5
1,4-Dimethyladamantane (1)	13.3	0.7	1.5	1.4	0.9	1.9	2.4	0.3	5.1	8.5	8.8	13.6	9.9	15.2
1,4-Dimethyladamantane (2)	12.2	0.6	1.4	1.3	0.8	1.7	2.1	0.2	4.5	8.0	8.1	11.9	8.8	13.4
1,2-Dimethyladamantane	16.3	1.0	2.0	1.8	1.2	1.9	3.2	0.3	5.2	10.2	11.2	16.1	11.5	17.2
4-Methyldiamantane	12.6	0.4	0.9	0.9	1.6	0.8	1.7	0.8	1.4	1.6	2.3	3.7	3.3	3.7
D3 1-Methyldiamantane (I.S.)	4.2	4.5	5.8	6.8	4.4	3.5	3.2	5.7	5.4	3.9	4.6	6.2	5.6	4.3
1-Methyldiamantane	8.7	0.3	0.4	0.3	0.5	0.2	1.6	2.3	0.6	1.0	1.6	2.1	1.8	2.3
3-Methyldiamantane	6.7	0.3	0.5	0.4	0.6	0.3	0.9	0.6	0.5	0.6	0.8	1.3	1.1	1.7
1-Ethyldiamantane	0.7	0.1	0.1	0.1	0.1	0.0	0.3	0.4	0.1	0.1	0.1	0.2	0.1	0.2
D5-Ethyldiamantane	3.0	3.2	4.2	4.9	3.1	2.5	2.3	4.1	3.8	2.8	3.3	4.5	4.0	3.1
2-Ethyldiamantane	1.0	0.1	0.1	0.1	0.1	0.0	0.2	0.4	0.1	0.1	0.1	0.1	0.1	0.3
Diamantane	2.8	0.5	0.8	1.3	1.7	1.2	1.1	0.1	1.8	1.9	2.6	4.7	3.5	2.2

D4 Diamantane (I.S.)	2.7	2.9	3.8	4.5	2.9	2.3	2.1	3.7	3.5	2.6	3.0	4.1	3.7	2.8
Hopane	670.6	129.4	210.1	354.1	417.9	291.1	162.7	183.9	298.8	319.3	403.5	318.3	290.6	274.4
4,9-Dimethyldiamantane	3.9	0.2	0.3	0.3	0.5	0.3	0.8	0.5	0.4	0.4	0.6	1.0	0.9	1.2
1,4+2,4-Dimethyldiamantane	5.1	0.2	0.4	0.3	0.6	0.3	1.3	0.9	0.4	0.5	0.7	1.2	1.1	1.4
4,8-Dimethyldiamantane	8.0	0.3	0.6	0.5	0.9	0.5	1.8	1.3	0.7	0.8	1.1	1.9	1.6	2.1
3,4-Dimethyldiamantane	8.0	0.3	0.7	0.5	0.8	0.4	1.4	1.2	0.6	0.7	1.0	1.5	1.3	2.0
Cholane (I.S.)	13.6	14.7	19.0	22.2	14.3	11.6	10.5	18.6	17.5	12.8	15.0	20.4	18.4	14.0
C_{29} ααα 20R Sterane	130.8	21.8	34.2	104.4	128.3	74.6	32.3	24.6	81.1	68.6	78.7	55.8	53.7	65.3
9-Methyltriamantane	18.5	1.3	3.4	1.2	2.8	1.1	5.8	2.7	2.3	1.8	2.0	2.7	2.4	3.6
Triamantane	12.2	0.8	2.0	1.1	1.9	0.8	5.1	2.1	1.2	1.1	1.4	2.0	1.8	3.0
D4 Triamantane	2.0	2.1	2.7	3.2	2.1	1.7	1.5	2.7	2.5	1.8	2.2	2.9	2.6	2.0
Tetramantane-1	1.2	0.1	0.3	0.2	0.3	0.1	0.7	0.6	0.3	0.2	0.3	0.2	0.2	0.3
Tetramantane-2	0.7	0.1	0.1	0.1	0.3	0.1	0.4	0.3	0.2	0.1	0.2	0.2	0.2	0.2
Tetramantane-3	0.3	0.0	0.0	0.0	0.1	0.0	0.2	0.1	0.0	0.0	0.0	0.0	0.0	0.1

Note:

Diamondois concentration in ppm.

I.S. : Internal standard

: Parameters used for cross plot of diamondoids vs stigmastane (Figure 17).

BIBLIOGRAPHY

Anna, L. O., Roberts, L. N., and Potter, C. J., 2007, Geologic assessment of undiscovered oil and gas in the Paleozoic-Tertiary composite total petroleum system of the Eastern Great Basin, Nevada and Utah: U.S. Geological Survey Digital Data Series DDS-69-L, v. 2, 50 p.

Bortz, L. C., and Murray, D. K., 1979, Eagle Springs oil field, Nye County, Nevada: American Association of Petroleum Geologists Bulletin, v. 62, p. 881.

Claypool, G. E., Fouch. T. D., and Poole, F. G., 1979, Chemical correlation of oils and source rocks in Railroad Valley, Nevada: Geological Society of America Abstract with Programs, v. 11, p. 403.

Cook, H.E., and Corboy, J.J., 2004, Great Basin Paleozoic carbonate platform – Facies , facies transition, depositional models, platform architecture, sequence stratigraphy, and predictive mineral host models: U. S. Geological Survey Open-File Report 2004-1078, 129 p.

Conlan, L. M., 1995, Geochemical analysis of crude oil from Railroad Valley, Nye County, Nevada [M.Sc. thesis]: Long Beach, California State University, 332 p.

Dahl, J. E., Moldowan, J. M., Peters, K. E., Claypool, G. E., Rooney, M. A., Michael, G. E., Mello, M. R., and Kohnen, M. L., 1999, Diamondoid hydrocarbon as indicators of natural oil cracking: Nature, v. 399, p. 54-57.

DeCelles, P.G., 2004, Late Jurassic to Eocene evolution of the Cordilleran thrust belt and foreland basin system, western USA: American Journal of Science, v. 304, p.105-168.

Dickinson, W. R., 2006, Geotectonic evolution of the Great Basin: Geosphere, v. 2, p.353-386.

Dolly, E. D., 1979, Geologic techniques used in Trap Spring field discovery, Railroad Valley, Nye County, Nevada, *in* G. W. Newman and H.D. Goode., eds., Basin and Range Symposium: Rocky Mountain Association Geologists and Utah Geological Association, Guidebook, p. 469-476.

Druschke, P., Hanson, A. D., Wells, M. L., Rasbury, T., Stockli, D. F., and Gehrels, G., 2009, Synconvergent surface-breaking normal faults of Late Cretaceous age within the Sevier hinterland, east-central Nevada: Geology, v. 37, p. 447-450, doi: 10.1130/G25546A.1

Duey, H. D., 1979, Trap Spring oil field, Nye County, Nevada, *in* G. W. Newman and Goode. H. D., eds., Basin and Range Symposium: Rocky Mountain Association Geologists and Utah Geological Association, Guidebook, p. 469-476.

Foster, N. H., 1979, Geomorphic exploration used in discovery of Trap Spring oil field, Nye County, Nevada: American Association of Petroleum Geologists Bulletin, v. 62, p. 884.

French, D. E., and Freeman, K. J., 1979, Tertiary volcanic stratigraphy and reservoir characteristics of Trap Spring field, Nye County, Nevada, *in* G. W. Newman and H.D. Goode, eds., Basin and Range Symposium: Rocky Mountain Association Geologists and Utah Geological Association, Guidebook, p. 450-469.

French, D. E., 1983, Origin of oil in Railroad Valley, Nye County, Nevada: The Wyoming Geological Association Earth Science Bulletin, v. 16, p. 9-21.

French, D. E., 1995, Member of the Chainman Shale of Illipah Anticline; regional implications, *in* M. W. Hansen., J. P. Walker., J. H. Trexler., J. A. Mitchell., A. E. Saucier., D. E. French, eds., Mississippian source rocks in the Antler Basin of Nevada and associated structural and stratigraphic traps; Eureka, Elko, Nye, and White Pine counties, Nevada, p. 61-64.

Garside, L. J., Hess, R. H., Fleming, K. L., and Weimer, B. S., 1988, Oil and gas development in Nevada: Nevada Bureau of Mines and Geology Bulletin 104, p. 136.

Gilmore, T.J., 1990, Stratigraphy and depositional environments of the Lower Mississippian Joana Limestone in southern White Pine and northern Lincoln Counties, Nevada: The Mountain Geologist, v. 27, p. 69–76.

Greene, T. J., Zinniker, D., Moldowan, J. M., Keming, C., and Aiguo, S., 2004, Controls of oil family distribution and composition in nonmarine petroleum systems: A case study from the Turpan-Hami basin, northwestern China: American Association of Petroleum Geologists Bulletin, v. 88, p. 447-481.

Gutschick, R.C., Sandberg, C.A, and Sando, W.J., 1980, Mississippian shelf margin and carbonate platform from Montana to Nevada, *in* Fouch, T.D., and Magathan, E., eds., Paleozoic paleogeography of West Central United States, Rocky Mountain Paleogeography Symposium 1: SEPM (Society for Sedimentary Geology), Rocky Mountain Section, p. 111–128.

Hanson, A. D., Ritts, B. D., Zinniker, D., Moldowan, J. M., and Biffi, U., 2001, Upper Oligocene lacustrine source rocks and petroleum systems of the northern Qaidam basin, northwest China: American Association of Petroleum Geologists Bulletin, v. 85, p. 601-619.

Holba, A. G., Dzou, L. I. P., and Masterson, W. D., 1998, Application of 24-norcholestanes for constraining source age of petroleum: Organic Geochemistry, v. 29, p. 1269-1283.

Holba, A. G., Tagelaar. E., Ellis, L., Singletary, M. S., and Albrecht, P., 2000, Tetracyclic polyprenoids: indicators of freshwater (lacustrine) algae input: Geology, v. 28, p. 251-254.

JMP, 1995, Statistical discovery software, version 3.1: SAS Institute, Inc., 580 p.

Katz, B. J., 1995, Factors controlling the development of lacustrine petroleum source rocks – an update, *in* Huc, A. Y., ed., Paleogeography, paleoclimate, and source Rock: Tulsa, American Association of Petroleum Geologists, p. 61-70.

LaPointe, D., D., Price, J., G., and Hess, R., H., 2007. Assessment of the potential for carbon dioxide sequestration with enhanced oil recovery in Nevada: Nevada Bureau of Mines and Geology Open-File Report 2007-07, 24 p.

Levy, M., and Christie-Blick, N., 1991, Tectonic subsidence of the early Paleozoic passive continental margin in eastern California and southern Nevada: Geological Society of America Bulletin, v.103, p.1590-1606.

Moldowan, J. M., Dahl, J., Huizinga, J., Fago, F. J., Hickey, L. J., Peakman, T. M., and Taylor, D. W., 1994, The molecular fossil record of oleanane and its relation to angiospermae: Science, v. 265, p. 768-771.

Moldowan, J. M., Dahl, J., Jacobson, S. R., Huizinga, B. J., Fago, F. J., Shetty, R., Watt, D. S., and Peters, K. E., 1996, Chemostratigraphic reconstruction of biofacies: molecular evidence linking cyst-forming dinoflagellates with pre-Triassic ancestors: Geology, v. 24, p. 159-162.

Moldowan, J. M., Seifert, W. K., and Gallegos, E. J., 1985, Relationship between petroleum composition and depositional environment of petroleum source rocks: American Association of Petroleum Geologists Bulletin, v. 69, p. 1255-1268.

Mullarkey, J. C., Wendlandt, R. F., Clayton, J. L., and Daws, T. A., 1991, Petroleum source rock evaluations of the Cretaceous Newark Canyon Formation in north-central Nevada: American Association of Petroleum Geologists Bulletin, v. 75, p. 642.

Newman, G. W., 1979, Late Cretaceous (?)-Eocene faulting in the central Basin and Range, *in* G. W. Newman and H.D. Goode., eds., Basin and Range Symposium: Rocky Mountain Association Geologists and Utah Geological Association, Guidebook, p. 440-450.

Nolan, T. B., Merriam, C. W., and Williams, J. S., 1956, The stratigraphic section in the vicinity of Eureka, Nevada: U.S. Geological Survey Professional Paper 276, 77 p.

Palmer, S. E., 1984, Hydrocarbon source potential of organic facies of the lacustrine Elko Formation (Eocene/Oligocene), northeast Nevada, *in* Woodward, J., Meissner, F. F., and Clayton, J. L., eds., Hydrocarbon source rocks of the Greater Rocky Mountain region: Rocky Mountain Association of Geologists, Denver, Colorado, p. 497–511.

Peters, K. E., 1986, Guidelines for evaluating petroleum source rock using programmed pyrolysis: American Association of Petroleum Geologists Bulletin, v. 70, p. 318 - 329.

Peters, K. E., and Cassa, M. R., 1994, Applied source rock geochemistry: *in* Magoon, L. B., and Dow. W. G., ed., The Petroleum system – from source to trap: American Association of Petroleum Geologist, p. 93-120.

Peters, K. E., and Moldowan. J. M., 1993, The biomarker guide. Interpreting molecular fossils in petroleum and ancient sediments: Englewood Cliffs, Prentice Hall, 363 p.

Peters, K. E., Walters. C. C., and Moldowan. J. M., 2007, The biomarker guide 2nd edition volume 2. Biomarker and isotopes in petroleum exploration and earth history: New York, Cambridge University Press, 1155 p.

Picard, M. D., 1960, On the origin of oil, Eagle Spring field, Nye County, Nevada, *in* Boettcher J. W., and Sloan, W. W. Jr., eds., Guidebook to the Geology of East Central Nevada: Intermountain Association of Geologist and Eastern Nevada Geological Society, Guidebook, p. 237-244.

Poole, F. G., Claypool, G. E., and Fouch, T. D., 1983, Major episodes of petroleum generation in part of the northern Great Basin: Geothermal Resource Council Special Report 13, p. 207-213.

Poole, F. G., Fouch, T. D., and Claypool, G. E., 1979, Evidence for two major cycles of petroleum generation in Mississippian Chainman Shale of east-central Nevada: American Association of Petroleum Geologists Bulletin, v. 63, p. 838.

Poole, F. G., and Claypool, G. E., 1984, Petroleum source-rock potential and crude-oil correlation in the Great Basin, *in* Woodward, J., Meissner, F. F., and Clayton, J. L., eds., Hydrocarbon source rock of the Greater Rocky Mountain region: Denver, Rocky Mountain Association of Geologists, p. 179-231.

Sandberg, C. A., and Poole, F. G., 1975, Petroleum source beds in Pilot Shale of eastern Great Basin—Oil and gas session I: Rocky Mountain section meeting, American Association of Petroleum Geologists: U.S. Geological Survey Open-File Report, 75–371, 11 p.

Silberling, N. J., 1991, Allochthonous terranes of western Nevada: Current status, *in* Raines, G. L., ed., Geology and ore deposits of the Great Basin: Reno, Geological Society of Nevada, p. 101-102.

Sinninghe Damste, J. S., Kenig, F., and Koopmans, M. P., 1995, Evidence for gammacerane as an indicator of water-column stratification: Geochimica et Cosmochimica Acta, v. 59, p. 1895-1900.

Smith, J. F., Jr., and Ketner, K. B., 1976, Stratigraphy of post Paleozoic rocks and summary of resources in the Carlin-Pinon Range area, Nevada: U.S. Geological Survey Professional Paper 867–B, 48 p.

Tasch, P., 1980, Paleobiology of the invertebrates: data retrieval from the fossil record: New York, John Wiley and Sons, 946 p.

Taylor, W. J., Bartley, J. M., Martin, M. W., Geissman, J.W., Walker, J. D., Armstrong, P.A., and Fryxell, J. E., 2000, Relations between hinterland and foreland

shortening, Sevier orogeny, central North American Cordillera: Tectonics, v. 19, p. 1124-1143.

Venkatesan, M. I., and Dahl. J., 1989, Organic geochemical evidence for global fires at the Cretaceous/Tertiary boundary; Nature, v. 338, p. 57-60.

Volkman, J. K., Allen, D. I., Stevenson, P. L., Burton, H. R., 1986, Bacterial and algal hydrocarbons in sediments from a saline Antarctic lake, Ace Lake: Organic Geochemistry, v. 10, p. 671-681.

Volkman, J. K., Banks, M. R., Denwer, K., and Aquino Neto, F. R., 1989, Biomarker composition and depositional setting of *Tasmanite* oil shale from northern Tasmania, Australia: Abstract of 14th International Meeting on Organic Geochemistry.

Walker, C. T., Francis, R. D., Dennis, J. G., and Lumsden, W. W., 1992, Cenozoic attenuation detachment faulting: a possible control on oil and gas accumulation in east-central Nevada: American Association of Petroleum Geologists Bulletin, v. 76, p. 1665-1686.

Wernicke, B., Axen, G. J., and Snow, K. J., 1988, Basin and Range extensional tectonics at the latitude of Las Vegas, Nevada: Geological Society of America Bulletin, v. 100, p. 1738 – 1757.

Winfrey, W. M., Jr., 1960, Stratigraphy, correlation, and oil potential of the Sheep Pass Formation, east-central Nevada: Intermountain Association of Petroleum Geologists, Eleventh Annual Field Conference Guidebook, p. 125-133.

VITA

Graduate College
University of Nevada, Las Vegas

LaOde Ahdyar

Degrees:
Bachelor of Science, Geology, 2008
Padjadjaran University, Indonesia

Special Honors and Awards: University of Nevada Las Vegas Imperial Barrel Award Team 2011. Third Place Rocky Mountain Section of American Association of Petroleum Geologists

Thesis title: Molecular Organic Geochemistry of the Oil and Source Rocks in Railroad Valley, Eastern Great Basin, Nevada, United States.

Thesis Examination Committee:
Chairperson, Andrew D. Hanson, Ph. D.
Committee Member, Rodney V. Metcalf, Ph. D.
Committee Member, Stephen M. Rowland, Ph. D.
Graduate Faculty Representative, Daniel B. Thompson, Ph. D